# Probabilistic, Rule-Based Modeling of Deltaic Networks and Stratigraphy

**A THESIS**

**SUBMITTED TO THE FACULTY OF**
**UNIVERSITY OF MINNESOTA**
**BY**

**Dan Cazanacli**

**IN PARTIAL FULFILLMENT OF THE REQUIREMENTS**
**FOR THE DEGREE OF**
**DOCTOR OF PHILOSOPHY**

**Advisor: Professor Chris Paola**

**Co-advisor: Professor Vaughan R. Voller**

**September, 2021**

## Acknowledgements

A number of people have helped in launching and shaping up this research. I am particularly indebted to Alessandro Cantelli, Matt Wolinsky, and Zoltan Sylvester for helping shape the initial ideas and the first model algorithm, to Arvind Singh for his instrumental help in assessing the mobility of the experimental channels, to John Swenson, Doug Edmonds, and Andy Wickert for their feedback and ideas and, last but not least, to the St. Anthony Fall Laboratory (SAFL) personnel, Chris Ellis and Jim Mullin in particular, for their help with setting up and running the experiments discussed here.

## Dedication

To my professors from the University of Bucharest, University of Illinois at Chicago, and University of Minnesota. To those who taught me science and the science of how to think about problems, how to investigate, how to filter what is important, how to synthesize, and how to keep an open mind about the endless interdependencies that exist in nature.

## Contents

## List of Tables

## List of Figures

# Chapter 1. Introduction

The main goal of this research is to develop simplified models that can reproduce deltaic distributary networks and deltaic stratigraphy at channel scale resolution. Through such simple models we aim to better understand the geometric arrangements of the natural deltaic channels and their deposits.

In addition to the scientific interest, given the unique role of deltas in the context of global warming, understanding the complex and diverse patterns of distributary channels found in natural deltas has also a practical motivation. The loss of land and habitat due to sea level rise dominates the ongoing conversation on climate change and, catastrophic events such as hurricane Katrina that impacted New Orleans and the Gulf Coast in 2005, increase public's awareness of the vulnerability of coastal regions including many of the large deltas around the world.

Deltaic regions represent invaluable ecosystems and vibrant places for economic activities and human habitat. Day et al. (2019) noted that *"because of the ecological richness, deltas support the highest value of ecosystem values and goods in the world"*. A large fraction of coastal wetlands are situated within the deltaic regions. Apart from their unique ecological value these wetlands host some of the larges fisheries in the world (Day et al., 2019) and represent a buffer against storms and hurricanes (Day et al., 2007). Deltas are also densely populated places with an estimated half billion people living in deltaic regions (Syvitski and Saito, 2007; Woodroffe et al., 2006). Major cities situated within or in the proximity of the deltaic regions are vital harbors and centers of commerce (Blackburn et al., 2019). Defined by elevations near the sea level and low gradients, deltas are at risk not only because of the sea level rise but also because of the natural compaction of fresh sediments amplified by human activities, primarily through the extraction of water or hydrocarbons (Syvitski et al., 2009).

Yet despite their vulnerability, in the face of sea level rising threat, deltas represent the one of the best hopes for preserving and building new natural land. By one account, in spite of the sea level rise, on aggregate deltas may be actually expanding, adding land surface (Nienhuis et al., 2020). This assessment is based on a global estimate of sediment fluxes which for many deltas, primarily large river dominated ones, is thought to have increased. This net increase in sediment flux is attributed to an increase in land erosion due to human activities, mainly deforestation. On aggregate, the enhanced erosion may exceed the global sediment reduction due to damming. But this "optimistic" outcome of

net land expansion is not shared by everyone. Giosan et al. (2014) highlight the lack of long term sustainability, particularly with respect to the larger deltas and argue for a paradigm shift in channel management, from traditional confinement through dams and dikes to adding new deltaic channels and breaching the existing ones to create crevasses and internal mini-deltas in order to divert and spread more sediment over the delta plain in a way that mimics the natural process. Similar ideas have been discussed elsewhere mainly with a focus on the iconic Mississippi Delta (e.g., Kim et al., 2009; Paola et al., 2011) whose fate is under threat due to the sea level rise coupled with sediment starvation. Thus, better understanding the geometric arrangement of the natural deltaic distributaries has practical relevance.

### 1.1 Modeling Distributary Networks

The first part of this three-part research is covered in **Chapter 2** and explores whether, instead of a deterministic approach based on explicit physical equations, a simplified rule-based model can render realistically looking geometric arrangement of deltaic channels, particularly the river dominated ones. It should be noted that globally, while representing a relatively small fraction of all deltas, river dominated deltas represent the majority of larger deltas (Nienhuis, 2020). More importantly, river deltas are the gateways for the bulk of terrestrial sediment delivered to the oceans, approximately 85% (Milliman and Farnworth, 2011), of which approximately 30% are retained within the deltaic domain (Syvitski and Saito, 2007; Kim et al., 2009). A study by Caldwell et al. (2019) on a large global data set of deltas finds that river dominated deltas are more likely to form and grow new land, whereas waves and tides tend to inhibit delta formation at river mouth and limit delta expansion.

While we have a good knowledge of the factors controlling the growth of the subaerial portion of deltas, understanding the diverse and complex nature of internal channel arrangements remains elusive. For example, from Syvitski's (2006) study on a set of 55 deltas we know that delta surface correlates with the size of the drainage area and that the collective width of the channels tends to correlate to the maximum monthly discharge. Yet the same study highlights the variability of deltaic geometries concluding that *"no two deltas are the same"*. Methodical exploration of deltaic networks geometry by Edmonds et al. (2011) leads to a similar conclusion, that *"it seems unlikely that deltas worldwide will exhibit strong internal similarity, beyond the possible fractal nature of the channel network"*.

The introduction part of Chapter 2 discusses how deltas are defined by wide variability in terms of size, shape, number of individual, channels, sinuosity, branches length, distribution of bifurcation nodes and outlets, just to name the most obvious geometric descriptors. Relatively few trends exist, trends that are not universal but rather applicable to a subset of deltas. These facts lend support to a rule-based modeling approach. The approach developed in Chapter 2 relies on a random walk piecewise method of extending the deltaic channels in small increments (steps) coupled with a bifurcation probability, applied to all leading channels at each growth step. Through this simple algorithm the distributary channels, reduced to a skeletal centerline representation, can grow indefinitely and the execution can be terminated either once a number of growth steps or once a number of terminal channels has been reached. We found that to predictably render outcomes that match the field observation the input terms and probability distributions need to be constrained within relatively narrow ranges.

Our goal was not to faithfully reproduce a particular delta style but to show how the same algorithm can generate various arrangements that, probabilistically, cover the spectrum of values seen in a multitude of deltas. Despite the lack of explicit physical relationships the model outcome compares well against field deltas by several metrics: reach lengths distribution, relative (i.e., apex to shoreline) location of bifurcation nodes, dispersion of the outlets, and the overall delta shape expressed as width over length. These similarities are possible partly through the design of the rules that implicitly capture some of physical aspects and partly through the conditioning of certain geometric aspects observed in the field, such as the typical variation of the bifurcation angles or channel sinuosity. This simple rule-based network generating model has some practical advantages over gridded numerical models. It is not only computationally inexpensive but also easy to implement as it requires no special parametrization, grid discretization, boundary conditions, or iteration schemes.

In summary, the probabilistic model introduced in Chapter 2 offers a fast and simple recipe for generating distributary networks and represents a useful instrument to explore and understand the complex geometric variability of deltaic networks.

### 1.2 Understanding Channel Dynamics

The second major goal of this research is to develop a simpler method to reproduce deltaic stratigraphy. We do so by taking advantage the simple and swift nature of the network model developed in Chapter 2. However, to go from static networks to three dimensional

deposit architecture we need to better understand how deltas evolve, particularly what is the probable dynamic of the channel networks over time. Towards this goal, in **Chapter 3** we investigate the dynamics of two very distinct deltaic experiments conducted in the same facility, a square shape tank with 5-meter sides where water and sediment (walnut shells) were introduced at steady rates at one corner built a deltaic deposit with an approximate shape of a quarter circle. The first of these two deltaic experiments, was conducted with coarser (1 mm) sediment and showed a dominant upstream channel that moves laterally continuously but at uneven rates. Extended periods of back and forth small moves are separated by short bursts of rapid migration. The main channel swept the entire deltaic domain migrating without sudden channel relocation or episodes of flow reconfiguration and relatively fast relocation along a new distinct path. This dynamic is somewhat unexpected given that the aggrading systems tend to experience such marked flow relocation episodes referred to as avulsions. The experiment demonstrates that channels with higher lateral migration rates are less likely to avulse, a concept discussed initially by Mohrig et al. (2000) and expanded by Jerolmack and Mohrig (2007).

The second experiment used finer (0.25 mm) sediment delivered at a lower rate and exhibited a very different dynamic: the dominant channel moved laterally relatively slow, at rates that were one order of magnitude lower than in the first experiment. Furthermore, the main channel remained confined within a narrow sector for extended intervals of time that were separated by shorter periods of flow spreading into multiple channels (i.e., avulsion) upon which a main, dominant channel re-emerged in a different location.

The markedly different dynamic in the two experiments is driven by the sediment flux and size. We argue that it is the second experiment that encapsulates the morphodynamic of a deltaic system whereas the first experiment is representative for the fluvial region upstream of the delta. The two experiments mirror two regions of the Mississippi River, the alluvial plain where the lateral migration rates are high and the river forms tight meanders and a much less dynamic and avulsion prone deltaic region. These two regions are separated by a zone of sediment sorting and deposition (primarily of coarse fraction) where the river enters the backwater zone and the transport capacity decreases.

### 1.3 Deltaic Stratigraphy

**Chapter 4** introduces a novel method of modeling deltaic stratigraphy at channel solving resolution. Deciphering the details of stratigraphy has practical implications as the deltaic deposits are host to some of the most important hydrocarbon reserves (Broussard, 1975).

Direct forward numerical modeling of long term delta evolution poses significant challenges that are detailed in the introduction part of Chapter 4. We propose an alternative approach, based on a large data set of networks derived from the algorithm introduced in Chapter 2. The networks are first converted to topographic surfaces through few simple but reasonable assumptions: a random partition of the discharge into two fractions at each bifurcation, a simple hydraulic relationship to relate the channel width ($W$) to discharge ($Q$), using an average literature exponent (i.e., $W \sim Q^{45}$), a constant ($W$) to depth ($D$), aspect ratio of 30 (also a literature average), and an exponential decay of levee height away from the channel bank.

At the crux of our stratigraphic model is approximating the continuous evolution of a delta with a succession (i.e., stacking) of discrete topographic surfaces. The model resembles object modeling techniques and is well suited for deltas which are characterized by stochastic processes such as avulsion and channel bifurcation. One major challenge is how to decide the network selection for the stratigraphic construction and their stacking order. Stratigraphic evidence suggests that prolonged episodes defined by incremental evolution alternate with shorter episodes corresponding to flow relocation (i.e., major avulsions), similar to the dynamic of the second experiment mentioned above and discussed in detail in Chapter 3. To capture this pattern we first adopt a method of assessing the similarity between all networks in the database, upon which we develop a simple set of rules to guide the stacking succession. In essence, extended periods of incremental evolution are captured through thicker sets of similar networks, separated by thinner sets of semi-randomly stacked networks corresponding to shorter periods of flow reconfiguration (i.e. avulsions). The model introduced here as a proof of concept requires a significant initial effort in building the database of networks. Its execution, however, is fast and straightforward allowing for exploration of spatial stratigraphic arrangements.

**Chapter 5** provides a summary discussion on the probabilistic nature of geometry of the deltaic networks, in support of stochastic, rule-based modeling techniques developed here. We conclude with a series of directions for future work to add complexity and specificity to these techniques.

# Chapter 2. A Rule-Based Model for Generating Deltaic Channel Networks

Dan Cazanacli[1,2], Chris Paola[1,2], Vaughan R. Voller[2,3]
[1]Dept. of Earth and Environmental Sciences, [2]St. Anthony Falls Laboratory, [3]Dept. of Civil, Environmental, and Geo-Engineering, University of Minnesota, Minneapolis, MN, USA

**Abstract**

Modeling distributary channel networks poses unique challenges due to complexity and limited understanding of the main genetic processes responsible for channel branching and network evolution (avulsion and bifurcation). Growing interest in reproducing plan deltaic networks has resulted in models that resort on simplified equations and/or rules, rather than analytical modeling of the water and sediment routing. Here, we explore to what extent a model based on a minimal set of rules can replicate the channel arrangements representative of field deltas. The proposed model is based on a partly correlated random walk algorithm for generating individual branches coupled with a bifurcation probability applied to each growing branch. Channels, reduced to a non-dimensional skeletonized representation, are generated piecewise, with centerline direction deflections sampled from a normal distribution. Each deflection is partly correlated with the previous one. A directional bias term controls the steering and separation of the growing channels. Lastly, a key ingredient is a bifurcation probability value that controls whether a channel continues to grow or it bifurcates. Systematic and heuristic exploration of the input indicates that if probability distributions and the proportions between terms are properly constrained the model can predictably generate realistically looking networks which, by several metrics (reach lengths distribution, relative location of bifurcation nodes, dispersion of the outlets, and overall delta shape) are comparable to a number of natural distributary networks. The rules implicitly capture some of the physical aspects which partly offsets the lack of explicit physical equations.

## 2.1 Introduction

Deltas have special economic, social, and environmental importance. Ancient deltaic deposits have been recognized to host some of the world's most important oil and gas reserves (e.g., Broussard, 1975) and many large deltas are desirable places to build and

live, an estimated half billion people living around coastal deltas (Syvitski and Saito, 2007). Deltas display tremendous morphological variation reflected in the overall size and shape, the number of individual distributary channels and bifurcation nodes, the proportion of land to water, or the patterns formed by channel and islands in case of denser networks. Shoreline shapes also show a high degree of variation, in large part due to wave and/or tidal influence. But even if we remove the deltas with considerable tidal and/or wave influence from consideration, it is still difficult to predict how particular genetic processes can account for the variability among river dominated deltas. Incoming discharge and sediment type, vegetation, climate, or basin geometry are chief factors accounting for this variation (Postma, 1995) and, longer term, sea level fluctuations and tectonics play an increasing role.

Setting aside those models that focus mainly on alluvial fans or fan deltas (e.g., Sun et al, 2002; Rietz et al., 2010), there are relatively few attempts to model low gradient deltas at a level that can render networks and individual channels in detail. Discussing the category of “channel resolving” delta models, Paola et al. (2011) distinguish between flow solving and sediment transport numerical models and reduced complexity models that replace the full expression of shallow water and sediment transport equations with simplified expressions and/or rules. The former category is perhaps best exemplified by Delft3D, a high-resolution, computationally intensive model suited for engineering application as well as geomorphologic exploration. Examples of geomorphologic investigation based on Delft3D and fuller description of the model are found in Edmonds and Slingerland (2007, 2009) or Geleynse et al. (2010, 2011). Seybold et al. (2007, 2009) introduced a reduced complexity model based on simplified water and sediment routing formulae. The model reproduces various plan morphologies that seem to approximate well specific natural deltas, particular attention being given to the Mississippi bird-foot delta type. More recently, a more sophisticated reduced-complexity model series that combines abstract physics based rules with directed random walk transport was developed by Liang et al. (2014a, 2014b). The proposed set of rules is intermediate in complexity between the Seybold et al. model and Delft3D. The model captures a range of physical processes that operate at different space and time scales (e.g., bifurcation, avulsion, channel migration, lobe switching).

Here we adopt a different approach to simplification, focusing on the geometry of the channel networks. We explore what minimal set of network generating rules can succeed in rendering realistic geometric representations of a wide spectrum of deltaic networks but

primarily river dominated ones. The rule driven distributary network model presented here is inspired by 2D fractal tree growth patterns. The proposed network growth method does not operate on a grid and does not represent elevation explicitly. The goal is to develop a model for network configurations that can provide the core of a suite of models to create many realizations of delta geometry rapidly. Rather than attempt to devise routing schemes for flow and sediment from which the channel network emerges naturally, as the delta models mentioned above do, we instead study network generation algorithms that are based on simple geometric rules which include random variables sampled from imposed distributions of the simplest forms (i.e., uniform and Gaussian). By including random terms we deliberately seek to explore the variability. There is an obvious danger in this approach: the results could be seen as a purely heuristic approach to draw networks with no mechanistic constraint. There is a sense in which this criticism is correct: the model we propose really is a set of summary geometric rules and not an explicit representation of the mechanics. However, by carefully conditioning the rules, we succeed in keeping the model connected to reality and compare the resulting synthetic networks with natural examples that are representative for a wide spectrum of the modern river dominated deltas.

Our central goal is not to reproduce networks that faithfully resemble a particular delta example (i.e., generate “look alike”) but rather to test to what extent a minimal set of rules can replicate the channel network configuration of field deltas in a stochastic sense. The development of a generic rule based model is both helped and hampered by the aforementioned variability and lack of universal consistent geometric relationships and topologic properties. The model we introduce here renders geometric arrangements that are quantifiably similar to many deltaic channel networks, yet replicating particular deltas in a predictable manner is challenging without additional rules.

Syvitski (2006) provides an extensive investigation of potential correlation between various geometric aspects of deltas and their associated influx (water and sediment) parameters. Regression analyses using a set of 55 major deltas from the world reveal relatively few correlations: on average, the area of a delta is proportional to the water discharge while the gradient of the delta plain is proportional to the volume of sediment influx. Also, the total number of channels and the total cumulative width of the distributary channels seem to correlate well with the maximum monthly discharge, a trend confirmed and amended by Syvitski and Saito (2007). These are important scaling relationships that connect the size of the water and sediment input to the size of deltas in terms of area,

gradient or number of channels. But if we remove the scale from consideration, none of these correlations tell us something specific about the internal topologic properties of the deltaic networks.

The lack of universal internal geometric arrangements in delta networks stands in contrast with the tributary networks that are self-organized and display quasi-universal scale-invariability (Rodriquez-Iturbe and Rinaldo, 2001). Tributary networks are also defined by universal topological rules known as Horton's laws (Horton, 1945) which postulate that the number of streams decreases exponentially with a stream order whereas stream length and drainage areas increase exponentially with the stream order. It should be noted though, that Kirchner (1993) showed that these properties are a topologic trait of most binary tree networks and thus, the presence of Horton's laws is a weak indicator of a genetic process. To the best of our knowledge, no such strong and universal relationships were identified for deltaic, distributary networks.

Edmonds and Slingerland (2007) examined the mechanism of mouth bar formation and found that for some river dominated deltas, the channel depth, width, and the channel length between successive bifurcations, referred to as bifurcation length, decrease systematically downstream, with the bifurcation order. The bifurcation length decrease with bifurcation order is an important topologic trend; however, it is not universal. For the selected deltas this trend appears to exist only for bifurcation lengths measured along the dominant channels, not for the delta as a whole. If bifurcation length were to decrease systematically across the entire delta plain, one would expect distributary networks to exhibit stronger scale invariant properties, similar to tributary networks. Fagherazzi et al. (1999) and Rinaldo et al. (1999a, 1999b) suggest the opposite: that delta networks show little scale invariance.

Jerolmack and Swenson (2007) investigate the distribution of channel lengths, noting a break in scale attributable to a key genetic process, avulsion, which they argue creates a small number of long channels while bifurcation at the mouth results in many more, but smaller channels. The latter roughly follow a power trend and with lengths varying from one to ten times the width of the main trunk channel.

Investigating a set of four deltas (Mossy, Wax Lake, one numerical, and one experimental delta), all of which can be considered non-cohesive, river dominated systems, Edmonds et al. (2011) found, in their own words, "a mix of similarity and intrinsic variability". The deltas show fractal characteristics and similar fractal exponents but not scale invariance when other metrics such as the size of the inter-distributary islands or

distance to the nearest edge are considered. Notably, the authors concluded that “it seems unlikely that deltas worldwide will exhibit strong internal similarity, beyond the possible fractal nature of the channel network”.

This remark is strengthened by other studies that emphasize the morphologic variability and the lack of similar geometric patterns. For example, Syvitski et al. (2012) highlight the variation of the shape of active delta plains. Olariu and Bhattacharya (2006) underscore the variation in number of terminal channels among river dominated deltas as well as irregular distribution of the terminal channel outlets (i.e., delta mouths). Syvitski (2005), pointing out the degree of variation in large (50 to 55 deltas) data set, remarked that "no two deltas are the same".

The goal of this study is straightforward: to find a minimal set of rules by which to construct delta networks that match observations. We believe that natural deltas include a fundamental stochastic component so our models are partly stochastic. The model we propose is useful in practice for quickly generating large numbers of realizations of delta channel patterns (for example, for analyzing subsurface reservoirs) and also as a way of quantifying delta network geometry. For comparison with field observations we later propose a series of metrics.

### 2.2 Model Description

We employ a schematic representation of the deltas networks consisting solely of channel centerlines with no width or depth expression. From a geomorphologic perspective this is indeed a simplification given that typical subaerial modern deltas are defined by one or few dominant channels that carry most of the flow and sediment plus, often, many more minor channels. In the long term, as deltas evolve the flow partition across deltaic channels may change, minor distributaries can become major flow routes (Jerolmack and Paola, 2007) and channels of all sizes can at some point become inactive. Our focus here is on the major channels.

Each network realization originates from a short stem channel of unit length that bifurcates into two branches. The network emerges through successive bifurcations of each leading branch. The first bifurcation node represents the delta apex, defined as the place where the flow branching begins. In its simplest form the model realizations involve growing individual branches through addition of short channel segments (piecewise). At each step a new unit length segment is added to each growing branch based on a simple set of rules. Each new segment introduces a change in direction (i.e., angle deflection)

which is partly correlated to the deflection of previous segment. The amount of deflection, $\Delta\theta$ is drawn from a normal distribution of zero mean and a relatively small (less than 5°) standard deviation. A key parameter of the model is the bifurcation probability. At each time step each leading branch within the network has a given probability to bifurcate into two daughter branches. If bifurcation is not realized, the branch keeps growing. As the network becomes denser, growing branches "collide" with other branches, forming confluences.

***Network Generation***

In the interest of clarity we first discuss the network generation assuming straight channels, unencumbered by channel planform shape. Let us imagine a regular binary tree process in which segments of equal unit length bifurcate symmetrically and at a constant angle into two segments at each step. Regardless of the bifurcation angle, these assumptions yield a regular network where branches intersect each other (i.e., channel confluences) after three orders of bifurcation (Figure 1A). If we seek to avoid a regular geometric pattern, which would be unusual in natural deltas, one option is to allow for some random variation in the bifurcation angle around a mean value and let the angle bisector vary relative to the direction of parent branch so that the bifurcations are no longer symmetrical. Figure 1B illustrates this concept, bifurcation angles being sampled from a normal distribution with a mean of 45° and a standard deviation value of 5°. Variation in bifurcation angles renders geometric arrangements that are no longer axisymmetric but the networks retain a high degree of homogeneity due to the constant length of growth segments. In Figure 1B, all segments have a fixed length of one unit, except those intercepted by other reaches to form a confluence. Next, we can extend and vary the length of branches by threading together multiple unit length segments using a bifurcation probability value that controls whether a branch continue to grow or divides into two daughter branches. The simplest way to accomplish this is to employ a single bifurcation probability value for all growing branches and a uniform probability distribution. Figure 1C depicts networks with unequal reaches generated by using a bifurcation probability of 0.1 (i.e., on average each growing branch splits into two branches at every 10 steps). If the segment lengths are constant the network area increases exponentially at each step. Through successive bifurcations the networks can grow indefinitely, generating more branches and increasingly wider networks. The growing edge would eventually curve back

and encircle the point of origin (Figure 1D), after which the network would continue to grow ad infinitum in all directions.

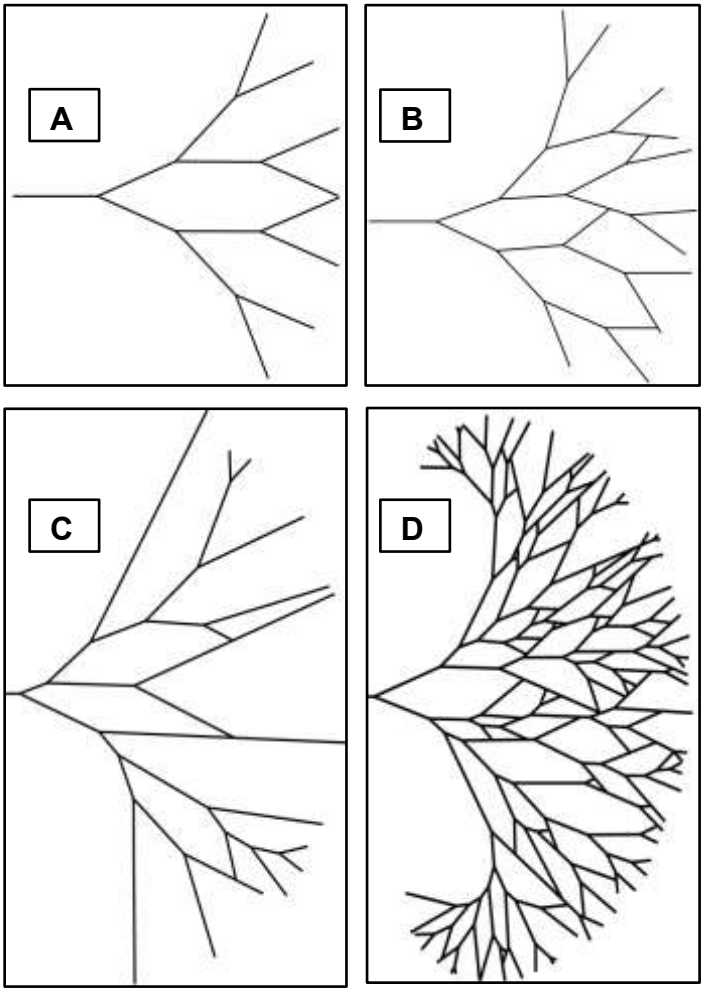


**Figure 1. Network construct progression: A - Symmetrical binary tree network with constant bifurcation angles and equal length branches. B – Bifurcation angles vary according to a normal distribution. C – At each growth step each leading branch has a 0.1 chance to bifurcate resulting in reaches with varying length. D – With no additional rules, network grows to infinity in all directions.**

Since our goal is to compare final model outcomes to real deltas, as discussed later in the paper, we are interested in generating networks with a moderate number of branches. Furthermore, we are interested in the final outcome and the network growth mechanism described above is not intended to replicate a field delta evolution.

***Channel Planform***

Thus far the channels have been considered perfectly straight, giving the resulting networks an unnatural "stiff" look (Figure 1). A simple way to generate irregular trajectories is to allow for a small change in direction between successive segments comprising each branch. For small, constant unit size segments, the angular deflections are an approximation of the local curvature. With each new added segment deflections can be sampled from a normal distribution with a mean of zero and a small standard deviation value.

$$\Delta\theta_i = \boldsymbol{N}(0,\ \sigma_\theta^2) \qquad (1)$$

Figure 2A shows the examples of channel centerlines generated using $\sigma_\theta^2$ values of 1, 2, and 4°. As expected, lager values translate in more sinuous trajectories.

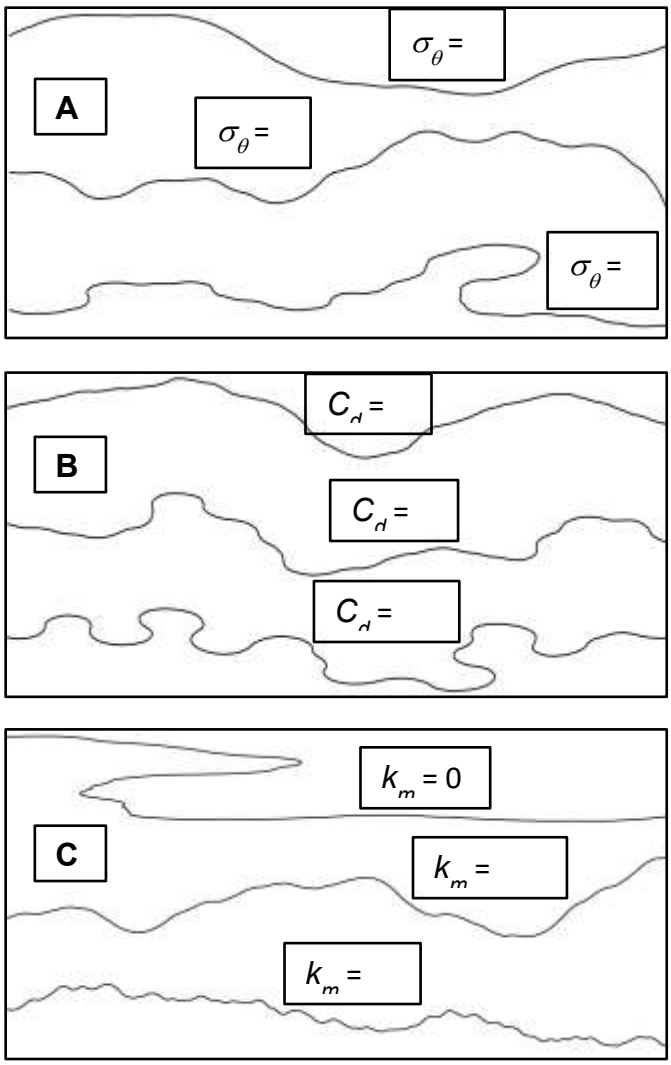


**Figure 2. Impact of three key parameters (italics) on channel planforms. A – Deflection (angular change in direction) between successive unit segments, $\Delta\theta$, is sampled from a normal distribution with a mean of zero and a choice for *standard deviations* $\sigma_\theta$. Larger values of $\sigma_\theta$ trigger more pronounced change in channel trajectory, back turning and possible crossover. B – Directions (signs) of successive deflections are correlated through $C_d$ - *the probability of correlation*. Lower values of $C_d$ produce random walk trajectories while higher values generate persistent curvatures (correlated random walk). C – *Directional bias term,* $k_m$ is the weight fraction assigned to a dominant flow direction (left to right) when computing direction of each segment. Without this bias term ($k_m$=0) there is no directional stability. Small $k_m$ values ensure directional stability while larger value tend to overcorrect the direction yielding zigzagging trajectories.**

The use of piecewise gaussian random walk methods to describe river planforms has a long history (Schelling, 1951; Thakur and Scheidegger, 1968; Ferguson, 1976). The centerlines generated by random walk lack curvature persistence a common trait of real river channels. Furthermore, the approach also lacks directional stability, meaning that the path could curve back and occasionally crosses itself forming loops.

The directional stability aspect was addressed by Surkan and van Kahn (1969) as well as Thakur and Scheidegger (1970) who proposed modified random walk algorithms that considered a dominant direction, or bias. Both methods restrict the variation of deflections when the local channel direction is close to the dominant direction but allow for wider variations as the channels strays away from the dominant direction, thus increasing the chance of realignment. Ferguson (1976) proposed a second order autoregressive method that provides both directional stability and curvature trend persistence as a way to model irregular meanders. Each deflection

is the sum of a term that is slightly smaller in magnitude than the previous deflection and a perturbation term sampled from a random distribution.

It has been shown that recursive methods used to generate river centerlines may, on aggregate, approximate the distribution of the centerline directions but do not capture other more subtle details of the centerline shapes (Mariethoz et al., 2013). Howard and Hemberg (1991) showed that channel planform generated using a meandering model such as the one proposed by Howard and Knutson (1984) are distinct from natural rivers meanders when the comparison includes higher order moments of the direction-angle probability distribution function (PDF) such as the skewness and kurtosis, and terms like asymmetry of individual meander loops. Mariethoz et al. (2013) have shown that a better way to successfully generate centerlines that are stochastically equivalent to those of natural channels is to use a filtering procedure that relies on direct sampling from a field example. Our goal, however, is not to recreate look alike of a particular channel style or to perfect individual planform shapes. Furthermore, there are reasons to suspect that deltaic channels are less likely to form regular meandering patterns, because of their limited length and because their trajectories are shaped by processes other than lateral migration (Limaye et al., 2021). Edmonds and Slingerland (2009) showed that sometimes channel bends result from a “failed” bifurcation at the mouth while Ashton et al. (2013) showed that wave activity and longshore sediment transport actively define the direction of channel as delta grows. Some delta distributaries originating from a local avulsion are relatively young and their centerlines are likely to be defined by the topography and roughness of the terrain, rather than a self-forming meandering process (Lazarus and Constantine, 2013). Finally, recent studies have shown a direct connection between the bedload and channel migration rates (Wickert et al, 2013; Constantine et al, 2014). Many deltas, however, lose much of their coarse sediment at the transition into backwater zone which contributes to a loss in lateral mobility (e.g., Fernandes et al, 2016). Cohesion due finer sediment material and dense vegetation in some cases may also inhibit the lateral mobility. Therefore, deltaic channels are less likely to develop regular meander bends.

With these considerations in mind we aim to generate reasonable channel patterns using a simple method that can approximate the low-order geometries of a wide variety of deltaic channel planforms. In addition of sampling the angular deflections from a normal distribution with mean of zero, our proposed recursive method correlates successive deflections and includes the effect of a dominant, main flow direction.

Successive deflections are correlated via a correlation factor, $C_d$ which takes numerical values between 0 and 1 and defines the probability of correlation between successive deflections. In physical terms, $C_d$ describes how persistently a channel bends in one direction before turns to the other direction (i.e., before the curvature changes sign). As a first approximation, we consider successive deflections to be correlated in sign only. For $C_d = 1$:

$$\Delta\theta_i = abs[\mathbf{N}(0, \sigma_\theta^2) \times \Delta\theta_{i-1}] / \Delta\theta_{i-1} \quad (2)$$

For $0 < C_d < 1$, at each step we sample a variable $u_i$ from a random uniform distribution ***U(0, 1)***. The angle deflection is then computed using either Equation 1 or 2 as follows:

$\Delta\theta_i = \mathbf{N}(0, \sigma_\theta^2)$, *if* $u_i > C_d$

$\Delta\theta_i = abs[\mathbf{N}(0, \sigma_\theta^2) \times \Delta\theta_{i-1}] / \Delta\theta_{i-1}$, *if* $u_i < C_d$

For $C_d$ values larger than about 0.8 to 0.9 the results are quasi-periodic regular meanders while for smaller $C_d$ values the resulting trajectories appear quasi-random. This is reflected in Figure 2B that shows three centerlines generated with $C_d$ values of 0.5, 0.9, and 0.99. A smoother curvature variation can be obtained by strengthening the correlating, not only the sign but also the magnitude of successive deflections:

$$\Delta\theta_i' = C_d \Delta\theta_{i-1} + (1-C_d) \Delta\theta_i \quad (3)$$

The effect of having a preferred direction of flow is explicitly captured through:

$$\theta_i = (1-k_m)(\theta_{i-1} + \Delta\theta_i) + k_m\theta_m \quad (4)$$

Where the term $k_m$ is a small number (i.e., less than 0.01) representing the weight given to the mean direction of flow or, in physical terms, the dominant gradient. The direction of each new segment computed through equations 1, 2, or 3 is "diluted" by the dominant flow direction.

For simplicity, if the mean direction of flow is assumed to be from left to right or in the direction of X-axis, $\theta_m$ and the last term in equation (4) becomes zero.

Without correlation between successive deflections (i.e. $C_d = 0$), only equations (1) and (4) apply and the deflections follow a pattern that is referred to as "biased Gaussian random walk".

The algorithm operates as follows: an initial deflection value, $\Delta\theta_i$ computed from equations (1) or (2) is inserted in equation (4) in order to compute a new direction (angle) $\theta_i$ upon which $\Delta\theta_i$ is recomputed as:

$$\Delta\theta_i = \theta_{i-1} - \theta_i \quad (5)$$

The magnitude of corrected deflections, $\Delta\theta_i$, in Equation (5) are smaller than initially computed using Equation (2) due to the correction term $k_m$ which, albeit small in magnitude (~$10^{-3}$ to $10^{-2}$), is essential in providing directional stability. Smaller values could lead to full back turning while larger values tend to overcorrect the direction resulting in zigzagged trajectories (Figure 2C).

### 2.3 Results

Thus far we presented (1) a concept of generating binary tree networks using approximate channel bifurcation angles sampled from a Gaussian distribution with a mean that is representative for natural deltas and a low bifurcation probability value sampled from a uniform distribution and (2) an algorithm that generates random to quasi regular planforms of varied sinuosities. One might think that using these very simple geometric processes easily reproduce deltaic networks and that perhaps almost any combination of parameters would generate a network that looks more or less as a skeletonized representation of a delta. In fact that is not the case, and further parameter conditioning is necessary.

Figure 3 shows nine outcomes generated using random values sampled from a uniform distribution within the range of 1 to 4° for $\sigma_\theta$, 0.6 to 1 for $C_d$. and 0.001 to 0.01 for $k_m$. The bifurcation angle was set at 48° with standard deviation value of 2.5°. The bifurcation probability was set at 0.01 and each network was allowed to evolve for 150 steps. In Figures 3A, 3B, and 3C, one of the three parameters was set at the top of the range to illustrate the effect of: A - large direction deflections (random trajectories); B - large correlation in deflection angles (unnaturally curved channels); C - direction correction (channels converging towards a main direction). In Figures 3D through 3I, however, the parameters were selected at random from the ranges listed above. Despite the fact that these ranges are rather small, many of these networks do not realistically look like deltaic networks while some do (Figures 3E, 3I) but just by chance.

#### *Model Optimization*

Model exploration, heuristically and systematically examining the effect of each term and combination of terms, showed that tightening the parameter range can generate more realistic outcomes. Specifically, $C_d$ values within the 0.8 to 0.9 range and $\sigma_\theta$ values the 2 to 2.5° range appear to generate networks that more predictably resemble natural deltas.

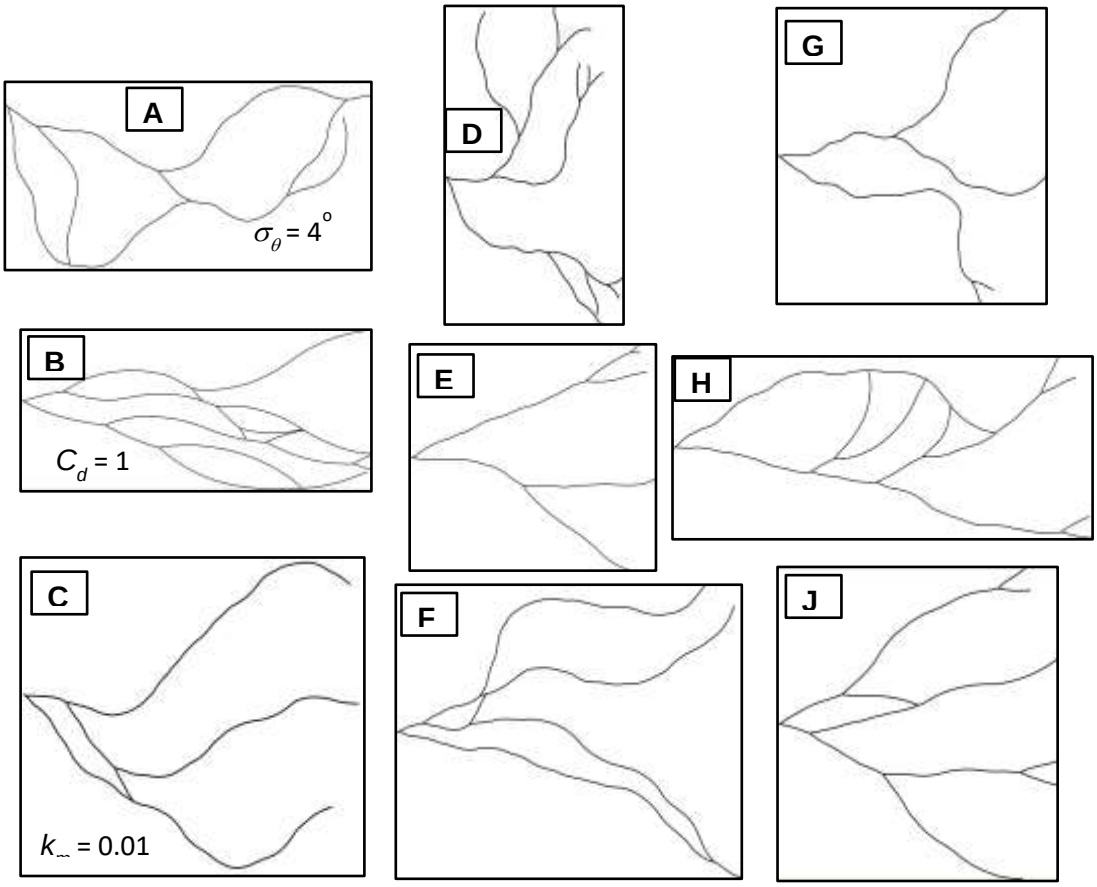


**Figure 3. Networks generated using arbitrary values for three key parameters, sampled from the following ranges: 1° to 4° for $\sigma_\theta$, 0.6 to 1 for $C_d$. and 0.001 to 0.01 for $k_m$. In A, B, and C the largest value within range was selected to highlight the distorting effect of large values in $\sigma_\theta$, $C_d$, and $k_m$, respectively. In D-I, all values were taken at random from the range. All networks were allowed to evolve for 150 growth steps and employed a constant bifurcation probability of 0.01, and bifurcation angles with a mean of 48° and a standard deviation of 2.5°.**

Furthermore, an essential ingredient is to prescribe a relationship between the weight given to the mean flow direction, $k_m$ and the standard deviation of angle deflection, $\sigma_\theta$. In principle $k_m$ and $\sigma_\theta$ can be varied independently. However, because resulting sinuosity decreases with increasing $k_m$ and increases with increasing $\sigma_\theta$ it makes sense to relate these two parameters, perhaps through a simple linear relationship like:

$$k_m = \lambda \, \sigma_\theta \qquad (6)$$

Where $\lambda$ is a proportionality constant on the order of $10^{-3}$. Additionally, it is useful to split the dominant direction weight $k_m$ into two parts, one representing the mean flow direction of the delta (left to right in our projection) and one representing the flow direction of each

individual channel defined as the direction at the place of channel inception (i.e., bifurcation).

Although we do not focus specifically on confluences, a few remarks are necessary given that confluences make distributary networks topologically distinct from the tributary ones. Compared to the field deltas considered later in this study, the model tends to over-predict the number of confluences due to the fact that there is no explicit elevation. In natural deltas the trajectories of newly formed channels are at least in part controlled by the surrounding topography. Levees, subaerial or subaqueous, preclude frequent confluences and new channels tend to follow existing troughs (Shaw et al., 2013). In our algorithm the channels are defined by random walks and their trajectories are more likely to cross each other. One way to reduce the number of confluences is to develop more complex rules that would steer channels away from each other. To keep the model as general as possible, a simpler way is to "prune" some of the branches that form confluences. This could reflect, for example, the abandonment of crevasse channels which thus fail to integrate in the network. Another form of channel "pruning" emerges from numerical modeling by Edmonds and Slingerland (2009) showing that occasionally after a bifurcation at mouth bar is initiated one of the resulting branches is abandoned. The "pruning" routine does not eliminate all confluences. Of each pair of "twin" channels originating at a bifurcation node, if both "collide" into other channels, only one is removed from the network while the other one is kept thus, preserving fewer confluences, at par with the observations of natural deltas.

One other aspect we need to clarify is the choice of 48° as the mean value for the bifurcation angle. Coffey and Shaw (2017) showed that, similar to tributary networks, the bifurcation angle in distributary networks appears to be a function of diffusive groundwater flow which would result in a theoretical value of 72°. The authors documented a mean value of 70.4° for a set of 10 field deltas and 68.3° for experimental deltas. The key aspect, however, is that these values were measured right at the point of channel (centerline) separation. Within a short distance (approximately two channel widths) downstream of the split the resulting two channels pull closer together and the bifurcation angles narrow, typically to approximately 55° to 48° trending towards the lower value further downstream. Instead of mimicking this bifurcation angle narrowing process through a set of additional rules, in order to keep the model as simple and general as possible, we opted for a lower central value 48° deliberately sacrificing a subtle localized geometric aspect but without

impacting the larger scale network geometry as given by the trajectory of the channels and not particularly sensitive to the exact angle at bifurcation.

With these adjustments, we generated another set of realizations using the following constant parameter values: 2° for $\sigma_\theta$ (standard deviation in direction deflection); 0.8 for $C_d$ (correlation between successive deflections in channel direction); and 0.004 for $k_m$ (weight assigned to a preferential flow direction) which, based on Equation (6) renders the term $\lambda$ equal to 0.002. This value of $\lambda$ results in sinuosities that approximate well the sinuosity range of many natural deltaic channels. As before, the mean and standard deviation values of the bifurcation angles were taken as at 48° and 2.5°, respectively, the probability of bifurcation was 0.01 for all branches at each step and the networks were let to evolve for 150 steps. The nine network samples showed in Figure 4 differ from one another in terms of shape, sinuosity, number of bifurcations (and implicitly number of channels and outlets) as well as the spatial arrangements of the bifurcation nodes (and implicitly the lengths of individual reaches). More importantly, unlike the networks if Figure 3, the outcomes in Figure 4 appear, at least visually, plausible representation of skeletonized field deltas.

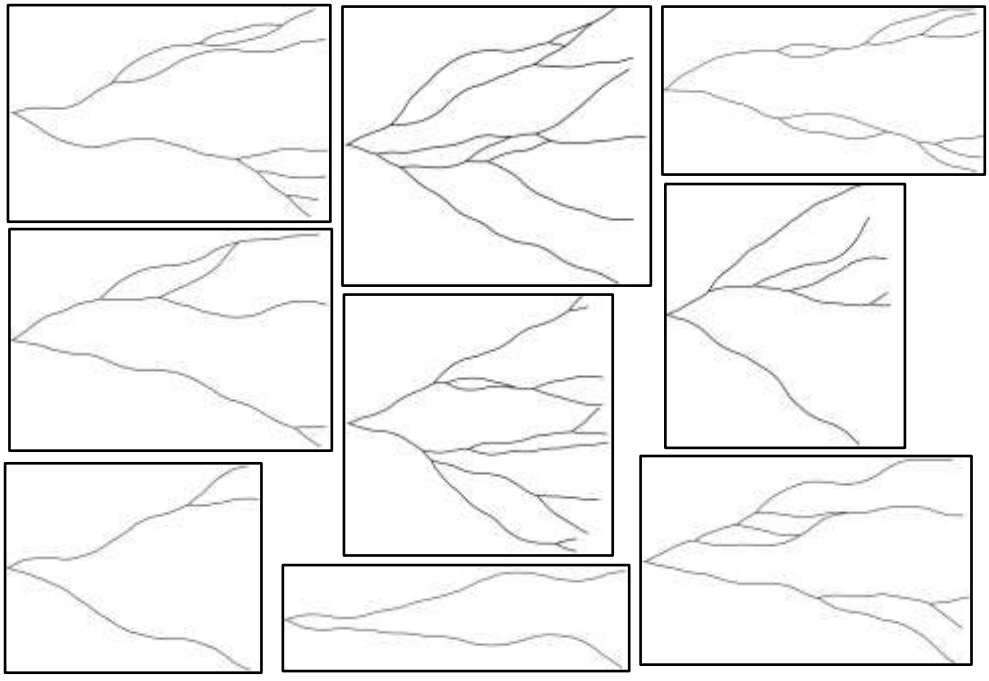

**Figure 4. Examples of networks generated using fixed, optimized values for: Standard deviation of centerline deflections, $\sigma_\theta$ = 2°. Probability of correlation between the signs of successive deflections, $C_d$ = 0.8. Weight assigned to dominant flow direction, $k_m$ = 0.004.**

## 2.4 Comparison to Natural Distributary Networks

### *Field Deltas*

To compare the potential of proposed rules to replicate field deltas we selected a subset of seven predominantly fluvial deltas: Atrato, the northern-most active part of Danube Delta, Don, Mississippi, Mossy, Lower Parana, and Wax Lake Delta. Apart from avoiding strong wave or tidal influence, we sought to capture systems with a moderate number of outlets, leaving out deltas with too few channels or too many channels such as Nile or Lena, respectively. This was done because networks with very few, say 2 to 4, channels offer little basis for comparison aside from planform shape. Unconfined deltas with a large number of channels such as Lena or Volga with over 200 terminal channels each, though many not identifiable through conventional imagery (Olariu and Bhattacharya, 2006), present a uniform, quasi-homogenous distribution of channels. As deltas widens and many new channels form, all regions become channel occupied, a trend also observed in our more extended runs. In these cases, the model may match the reality but in that it populates with channels, quasi-homogeneously, all the available space.

Considerable variability exist among these seven deltas in terms of geographic location, size, shape, discharge, sediment volume and type, channels sinuosity and spatial distribution. The image processing is depicted in Figure 5. Using satellite images from USGS Earth Explorer we applied a color range selection criterion followed by manual "clean up", to identify each major channel that can be tracked continuously over its entire length and has a width of at least 3 pixels. We obtained simplified binary images where

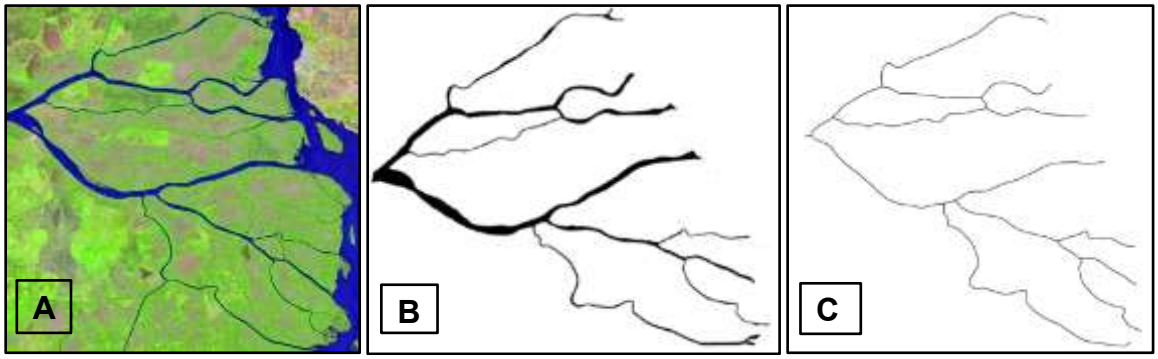


**Figure 5. Skeletonizing field deltas: A - Identifying the wet regions (blue) through image processing. B - Black and white representation after slight rotation and removal of basin, small backwater lakes, and man-made channels. C - Skeletal image of the channels.**

black represents the "wet" channelized areas and white represents the inter-channel "dry" areas. Imperfections stemming from the quality of the data or leaving out small distributaries do not affect the overall geometry of the deltaic networks. To obtain a tree-like representation of the channel network, we cropped out the basin area, lakes, and

marshy areas between the channels, man-made channels, and everything outside the two most distant natural lateral channels. Deltas often have complex shapes and tracing the limits of the deltaic region is not straightforward. In some cases included in this set (e.g., Danube, Parana) two or three major branches form upstream but then rejoin into a single channel before spreading laterally in multiple distributaries farther downstream. In such cases we cropped out the upstream part and chose the apex as the point downstream of which the flow region of the active delta irreversibly widens forming multiple distributaries. Next, we skeletonized each network, transforming the black and white image by reducing the full width channels to centerlines. Skeletonizing certain deltas that exhibit intricate, braided patterns or multiple varied width channels (e.g. Brahmaputra) may require a more complex algorithm. The deltas listed above do not present such intricacies and going from full width channels to centerlines is straightforward. Figure 6 shows the seven skeletonized delta networks that were also rotated such that the averaged flow direction is towards right, to enable a direct comparison to the model outcomes.

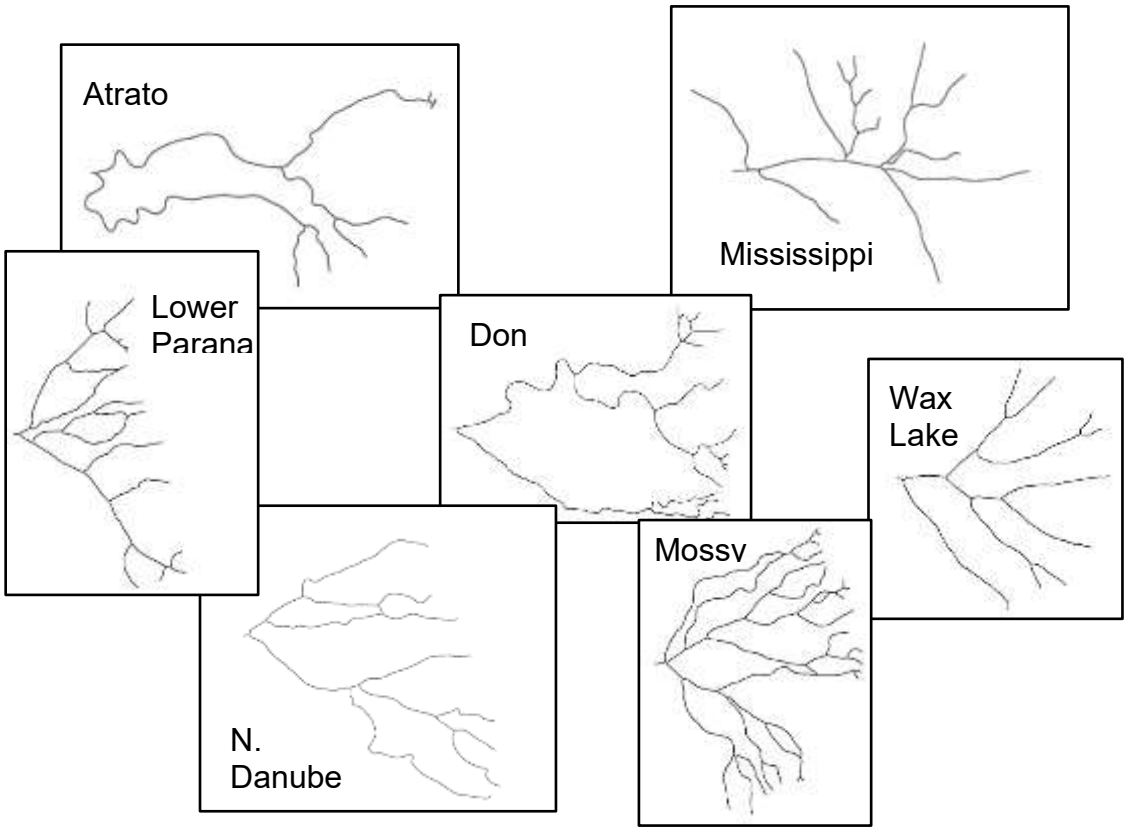


**Figure 6. Skeletonized and rotated field networks.**

***Metrics for Comparison***

Given the variety of the field delta in our set and of the deltas in general, the comparison with the proposed outcomes is not aimed at explore geometric identities. Instead we aim to establish whether a spectrum of properties such as nodal distributions or geometric proportions of field deltas are captured by the model. Rather than reducing the delta distributaries patterns to abstract networks, (i.e. a collection of nodes and links) as commonly done in network analysis (Newman, 2010), we retain the full topology, seeking metrics that can be related to important geomorphologic aspects. We considered the geometry defined by the overall delta shape and nodal distribution within the network, mostly bifurcations as well as the distribution of the nodes at the extremities of the network, that is, the delta outlets (i.e., channel mouths).

The question of what to measure and compare is not trivial. For example, given the skeletonized and non-dimensional aspects of the proposed approach, the metrics relating to scale are obviously not suitable for comparison. These metrics include individual channel dimensions (e.g. width, depth) that are not captured in the centerline representation as well the overall delta size. As a side note, because the proposed algorithm is non-dimensional each outcome can be scaled to match the size of a field delta.

Other parameters, such as the mean bifurcation angle, are not suitable for an objective comparison because their values were chosen to approximate the field observation. Another parameter that falls in this category is the channel sinuosity. In an averaged sense the sinuosity can be conditioned such that the sinuosity of the generated centerlines matches the sinuosity of channels in the delta set. Overall, the sinuosity of the reaches in the selected deltaic systems is consistently low, with very few values exceeding 1.2. Part of the explanation is that we considered individual reaches (i.e., bifurcation to bifurcation or to outlet) many of which are relatively short. Furthermore, the sinuosity, measured on the pixelated, skeletonized representation of the distributary network, is subject to some degree of error. Though sinuosity of deltaic channels is not universally low, other river deltas distributaries have been documented to have low sinuosity (e.g., Volga – Overeem et al., 2003). Another consideration is that sinuosity arises from channel bar deposition leading to meandering. Large, low gradient deltaic channels, however, tend to abandon much of the coarse bedload at the upstream portion of the backwater zone, thus losing their mobility and sinuosity implicitly (Nittrouer et al, 2012; Fernandes et al, 2016). To match the observed field delta sinuosity we generated large sets of individual reaches

(i.e., 200 reaches in each set) using different discrete values of $\lambda$ which in turn sets the directional stability parameter, $k_m$, via Equation 6. The results show that if $\lambda$ is on the order of $10^{-3}$ the distribution of modeled reach sinuosity approximates well the field values, the closest match being a $\lambda$ value of 0.002. If $\lambda$ is one order of magnitude higher or lower, the sinuosity is under or over predicted, respectively.

The network examples in Figure 4 were generated using a fixed number of steps. This approach, however, leads to outcomes where the number of bifurcations, and implicitly the channels and outlets can vary greatly. To perform an adequate comparison we take advantage of the fact that the model networks can grow indefinitely and terminate the execution once the average number of outlets matches that of the field deltas we try to replicate. Thus, we generated a larger set of networks (25) by terminating the execution when the network resulted in 11 growing channels, the typical and the average number of channel outlets in the field data set. Nine example of networks are illustrated on Figure 7.

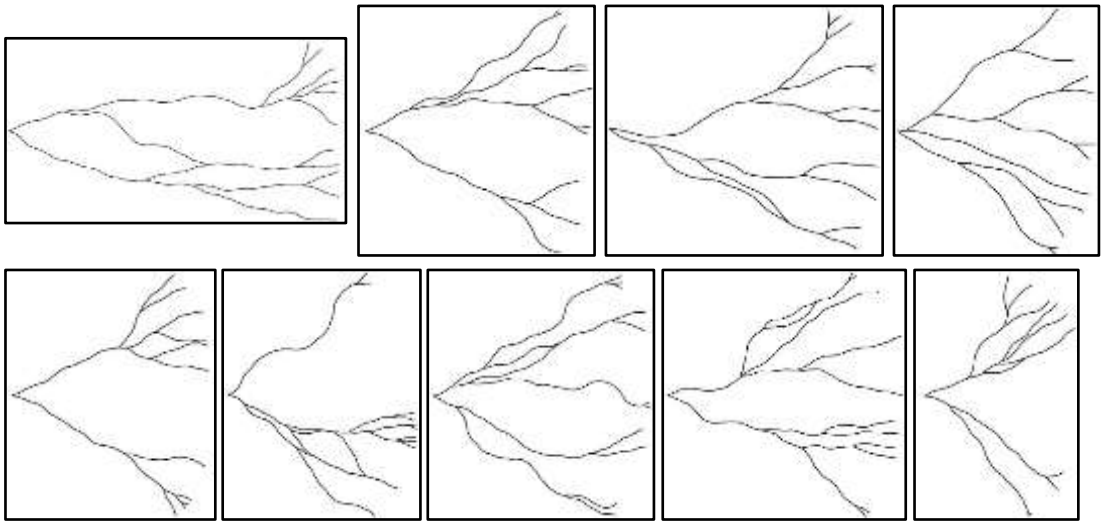

**Figure 7. Networks generated using the same parameters as in Figure 4 except that instead of a fixed number of growth steps the code execution was terminated when the number of growing channels (outlets) reached 11 (the average number of outlets for the field delta set).**

With these considerations in mind (i.e., excluding scaling dimensions and bifurcation angle while constraining the average sinuosity and the number of channels) we identified four simple metrics that can be employed to compare the model outcome against the properties of the field deltas: (a) distribution of individual reach lengths; (b) upstream to downstream (apex to shoreline) distribution of internal nodes (i.e., bifurcations); (c) dispersion of the terminal nodes expressed as the coefficient of variation of distances between adjacent outlets; and (d) the overall shape as defined by width to length ratio of the entire delta.

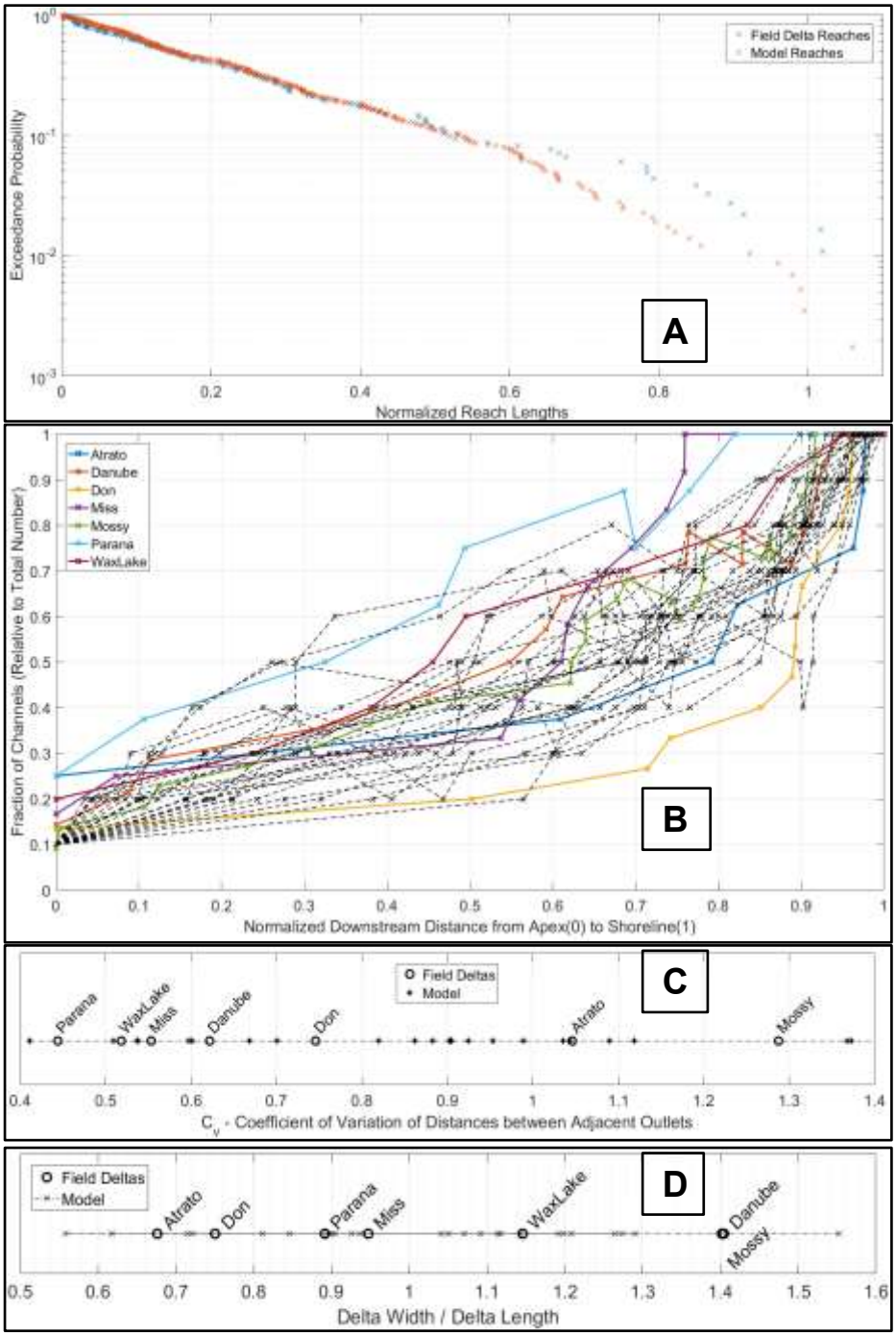


**Figure 8. Comparison between field networks and model generated networks: A – Distribution of individual reach lengths (normalized by delta length). B – Increase in number of channels (expressed as a fraction of the number of terminal channels) along normalized downstream distance (0 at apex / 1 at shoreline). C – Dispersion of outlets expressed as Coefficient of Variation ($C_v$) of the distances between adjacent outlets. D – Delta Width over Delta Length.**

### *Distribution of Reach Lengths*

For both field and model, within each network all reach lengths were normalized by the average length of delta taken as the distance between apex and shoreline. Figure 8A shows the distribution of all reach lengths, field deltas and model, expressed the probability of exceedance. For reach lengths up to about 0.6 of the overall delta length, that is, the vast majority of reaches, there is a nearly perfect overlap between field examples and model outcomes. The few longest reaches appear to be slightly more probable in the field data set which includes few long, non-bifurcating branches that are longer than the distance between apex and shoreline, whereas the model construct allows for simultaneous uniform extension of all growing channels.

### *Distribution of Bifurcation Nodes*

The distribution of the bifurcation nodes from the apex downstream reflects how the number of channels increases from two to the number of channels reaching the shoreline (i.e., the number of outlets). Each bifurcation increases the number of channels by 1. Conversely, each confluence decreases the number of channels by 1. To consistently assess the how the number of channel changes from the apex to the shoreline for deltas of various sizes and shapes we used a normalized, dimensionless coordinate system in which the distance at apex is set as 0 while the distance at the shoreline is set as 1. We also tracked the number of channels between the apex and shoreline as a fraction of the number of terminal channels (Figure 8B). For the field deltas the results show a good amount of variation. In the case of the Don and Atrato deltas most channels form close to the shoreline, while in the case of Lower Parana and Wax Lake deltas the distribution in channel number is more uniform. Like the field deltas, the model outcomes do not follow a particular trend but rather display a wide spectrum of channel number increase trends that, remarkably, fall within the trends of field deltas (Figure 8B).

### *Dispersion of the Outlets*

While some deltas tend to have outlets that are more or less uniformly distributed along the shoreline (e.g. Wax Lake Delta) others exhibit one or more clusters of outlets closely spaced together (e.g. Mossy Delta). Visually, the same seems to be true for model outcomes. A simple test of dispersion of the terminal nodes is the coefficient of variation of all distances between adjacent outlets, $C_V$. Since the model does not explicitly render a shoreline, we measured the Euclidian distances for both field delta set and model set.

Figure 8C shows that the model values of $C_v$ range roughly between 0.4 and 1.4 encompassing the $C_v$ values for the field deltas ranging between 0.43 and 1.29.

***Width to Length Ratio***

Finally, we compared the length to width ratio of field deltas against the networks generated by the algorithm. The length of each delta was measured between the apex and most distant outlet, and the width was measured between the most lateral outlets. The values for the model outcome range roughly between 0.55 and 1.55 and encompass the values for the field delta which range between 0.68 and 1.41. A broader range for the model networks is to be expected, with smaller values occurring as the networks may occasionally become elongated due to multiple "failures" of "timely" bifurcation or, conversely, the width to length ratio values may fall on the large side when the bifurcations occur "soon" resulting in resulting in relatively short networks.

**2.5 Discussion**

Figure 8A indicates that the reach lengths in both sets closely approximate an exponential distribution. The exponential distribution of lengths in the model is not surprising but rather an elegant result stemming from the simplicity of the model that employs a unique bifurcation probability at each step for all growing branches. Given that the bifurcations occur randomly based on a single threshold value applied to a uniform distribution (i.e., a Poisson process), the time interval (steps) between bifurcation events follows an exponential distribution.

The model does not consistently replicate the scaling relationships documented by Edmonds and Slingerland (2007), relating the bifurcation length to the bifurcation order. These are indeed important aspects but not universal and, even for the field cases that were considered predicated, such trends appear to be valid along the main, dominant active channel, not for the entire delta. On aggregate, the generated networks do not follow a consistent trend in terms of upstream to downstream reach lengths distribution. And neither do the field distributary networks. Figure 8B shows significant variation in the increase in number of channels. This differs from the delta growth mechanism proposed by Edmonds and Slingerland (2007) and further investigated by Jerolmack and Swenson (2007) which suggests that, if bifurcation due to sediment deposition at the mouth bar is the dominant channel forming process, as the bifurcation length progressively decreases downstream with the bifurcation order, the number of channels should increase

exponentially. However, as Jerolmack and Swenson (2007) pointed out, other processes, such as avulsion, would not produce this spatial signature. Furthermore, other factors can obscure the expected downstream increase in bifurcation numbers. Channel abandonment or the fact that mouth bars form in active regions of a delta and not all regions are active simultaneously, are two possible explanations. Although the model construction may appear to simulate delta growth through bifurcation at the mouth bar we do not assign a specific genetic mechanism to our algorithm. The outcomes include channel trajectories that hint at avulsion, near the apex (regional avulsion), or further downstream (local avulsion) as a potential formative process.

The model outcomes are similar to the field deltas in other topological aspects. As seen in Figures 8C and 8D, the dispersion of outlets and the overall width to length ratio of generated deltas shows significant variability yet the numerical range of these metrics encompasses the range corresponding to the field analogues, without clustering around a certain delta type and without values that are far outside the observed field range.

The fact that the same exact algorithm can render networks that on aggregate are comparable to a wide spectrum of natural distributary networks suggests that this simplified approach can be used as an effective alternative to numerical modeling of distributary networks. It also invites an essential question: How can such a simple stochastic construction that does not employ any physical equations capture multiple quantitative aspects that define the natural deltas (particularly river dominated ones) whose evolution is driven by complex physical laws governing the fluid flow and fluid sediment interaction (transport, deposition, erosion)?

First, certain physical aspects are in fact embedded in the model, just not explicitly. For example, the rules governing the trajectory of individual channels emulate the flow inertia of natural channels rendering persistent curvature trends and generating quasi-periodically alternating bends while retaining a certain amount of planform irregularity. Also, the directional bias term can be seen as a proxy for the delta gradient and gravity induced flow (direction). Coupled with the directions taken by each newly formed branch at bifurcation nodes, this term results in spatial ramification of the branches in all downstream directions, even though the model has no knowledge of topography.

Secondly, other aspects of natural deltas were translated more directly into the model. Because the model is non-dimensional and networks can grow indefinitely, the channel density can be set directly by stopping the execution when a desired channel number has been reached. The choice of bifurcation angle not only mimics the field observed range

but also constrains the overall shape of the networks. Also, the average channel sinuosity has been conditioned through the relationship between parameters in Equation 6 to approximate the typical sinuosity of natural deltaic channels.

Thirdly, both the model and field channel arrangements are emergent outcomes. In the case of river dominated deltas, distributary channels evolve and multiply to distribute the sediment originating from a single major channel to an increasingly broader delta front. Long term, this sediment redistribution can be viewed as a dispersion processes characterized by internal randomness. Through the use of random terms the model describes the same kind same spatial dispersion, even though there is no physical quantity. It just reproduces the transfer structure.

We can also turn around the question as to why a model with no explicit physical equations can generate networks similar to those shaped by complex physical processes and ask instead what can the model tell us about deltaic processes? What can we infer from the fact that a certain blend of parameters yield networks that compare well against field deltas while others do not? We note, for example, that model centerlines are characterized by low sinuosities and curvature persistency but no regular meanders, an outcome that stems from sampling the deflection angles from a population with $\sigma_\theta \sim 2^o$ and using a correlation between successive deflections, $C_d \sim 0.8$. Figures 2A-B show that much smaller values would result in nearly straight channels and random trajectories, respectively. Larger $\sigma_\theta$ values yield tortuous channels which are more likely to develop in upland landscapes, shaped perhaps in part by a rough irregular terrain topography (Lazarus and Constantine, 2013). Deltaic channels follow a straighter path to the shoreline and coevolve with more even, low elevation topography of the newly created land. $C_d$ values near 1 yield regular meanders common in upper alluvial river sections but not that common in deltaic region (e.g., Mississippi) likely due depletion of coarse bed material and increasingly cohesive overbank sediment. With respect to the network internal geometry we see that the nodal arrangement, upstream to downstream, is somewhat random (Figure 8B) which suggests that, although a mechanism for an exponential downstream increase in bifurcations has been proposed and tested for some deltas, other deltaic processes (regional avulsion, local avulsion, channel abandonment) are responsible for creating (or destroying) bifurcations making the nodal arrangement highly variable. We also see that the dispersion of the outlets is neither too regular, nor excessively variable (Figure 8C).

One important strength of this rule based geometric approach is the simplicity of implementation. The computational scheme employs only of a handful of rules and randomly varied terms. It involves no parametrization, no grid, no boundary conditions, no special starting setup, and no smoothing or convoluted iteration schemes. By contrast, numerical models aimed at solving long term morphological evolution of large deltaic domains at fine resolution (i.e. channel solving) are extremely complex at many levels, not just computationally. The relationships governing the flow of water and sediment are inherently complex and, in the case of deltas, the transition from fluvial domain to the marine one and additional forcing factors (e.g. wave regime) add to this complexity. In nature, complexity also arises from many other factors such as variable hydrologic regime or the sediment properties as well as heterogeneity of materials which makes it difficult to quantify certain aspects (e.g., bank erosion, flow around vegetation). Furthermore, channel origination processes in the deltaic domain, bifurcations or avulsions primarily, are difficult to frame analytically. Channel bifurcation geometry and stability are sensitive to small perturbation (e.g., Edmonds and Slingerland, 2008) while timing and location of an avulsion involves some degree of uncertainty (which makes a random based approach attractive). Thus, although a deterministic approach is anchored in physical equations, the extraordinary complexity of the input and analytical framework forces simplifying assumptions (e.g. constant discharge or bank erodibility, simple sediment distributions, etc.). The role of a powerful numerical model like Delft 3D is not to predict the detailed long term evolution of a complex deltaic system but to make more generalized long morphodynamic predictions (e.g. Caldwell and Edmonds, 2014). We should add that even for simpler problems a detailed numerical approach does not necessarily lend to optimal predictability. A good example is the work of Posner and Duan (2012) on predicting meandering trajectories, showing that, given the heterogeneity in bank erodibility, a stochastic approach (Monte Carlo simulation) is more suitable than a solely deterministic approach.

While this non-dimensional approach is no substitute for a complete model it is an efficient approach of generating network configurations that are morphologically representative of many deltaic networks. Through adequate scaling, flow partition rules, and hydraulic geometry relationships relating the discharge to channel dimensions the model can be transposed in simplified three-dimensional construction. A gradient can be applied to the network domain to capture the downstream slope while a smoothed line connecting the outlets can serve as a simplified representation of the shoreline. Because

all leading branches grow continuously, the delta area increases exponentially with each growth step. However, we can assign a mass expression to the networks, for conservation purposes, and convert the growth steps into time units knowing that, under constant sediment supply, the delta area increases linearly with time (Wolinsky et al. 2010), so the length scales increase as $t^{1/2}$. Taking advantage of the speed of execution, a large set of networks that are comparable to one another can be stacked vertically to simulate stratigraphy representative for cohesive deltas (Hoyal and Sheets, 2009), a line of work that is currently undertaken in a separate paper.

As stated from the onset, our goal here was confined to exploring whether a simple geometric model can render a variety of network geometries that, on aggregate, are representative of the deltaic networks. The algorithm presented above can be used as such to generate deltas with variable number of channels (few vs many) by terminating the execution of the code at a desired level of channel saturation. Alternatively, the code can be refined to reflect a certain deltaic morphology. For example, the overall delta shape (i.e., wide vs narrow) can be prescribed via a smaller or larger value assigned to the main direction of flow, respectively. Channel sinuosity can be altered via the terms in Equation 6. If one seeks to reproduce a more systematic downstream decrease in reach length the bifurcation probability can be modified towards this purpose. However, any attempt to recreate a particular deltaic morphology would require careful parameter exploration, different constraints, and additional rules.

Our intent was not to capture the details of a particular delta. We opted instead for the simplest, most general form, deliberately casting a wide net by using only few parameters. In this minimalistic approach we kept the number of rules and variables as low as possible and succeeded in generating networks that are similar to many, but by no means all, of the existing modern river dominated deltas. We used four random terms sampled from the simplest distributions. Bifurcation angles and the magnitude of direction deflection were taken from normal distributions (with fixed means and standard deviations), while the bifurcation probability and correlation between successive deflections were sampled from uniform distributions using constant threshold values. A fifth parameter, the weight assigned to the main direction of flow, is not independent but rather set indirectly via Equation 6 to approximate the distribution of observed channel sinuosities.

The use of random terms in this rule based approach is justified by the observed field variation in channel arrangements of deltas, primarily the river dominated ones. But evidently the deltaic networks are not entirely random. There is indeed a level of

systematic evolution and hierarchical arrangement. Channels spread out following winding trajectories that occasionally intersect each other (i.e., confluences). An increased number of prograding channels fill in the available space and, over long periods of time, deltas grow more or less uniformly in all downgradient direction. The results discussed here and compared against natural deltas in Figure 8 indicate that the parameters of the model strike the right balance between systematic and arbitrary arrangements of distributary networks.

### 2.6 Conclusions

The apparent lack of universal geometric relationships in deltaic distributary networks lends support to a modelling effort based on random variables. Starting with a goal of exploring what essential set of rules that can render channel arrangements that are similar to those find in nature (river dominated deltas in particular), we found the following:

- Irregular distributary networks emerge from a modified binary tree process, by imposing a single bifurcation probability to each growing branch and by adding some minimal variation to the bifurcation angles. Such networks, however, have perfectly straight channels and grow quasi-homogeneously in all directions.
- A simple piecewise method for channel growth addresses both these aspects. The method employs a guided normal distribution of direction shifts rendering centerlines with relatively low sinuosity and persistent curvatures, a good approximation for many deltaic channels. A small weight assigned to the main direction of flow is necessary to provide directional stability to both channels and the delta growth as a whole.
- To consistently generate networks that are visually similar to the deltaic distributaries the random terms used in the model must be selected from a narrow range. Remarkably, using fixed values of these parameters, the same algorithm (code) generates diverse geometric arrangements which, on aggregate, capture the geometric variability of many river dominated deltaic networks as tested by several metrics.

The ability of model to render networks that compare well with deltas despite lack of explicit physical equations is partly because the parameters are conditioned to reproduce certain geometric aspects (bifurcation angle, average sinuosity) and partly because other physical aspects such as flow instability forming alternating bends or delta gradient are captured implicitly, by imposing a curvature persistency or assigning a small weight to the dominant flow direction, respectively.

The model introduced here illustrates that deltaic morphologies are, to a significant degree, inherently characterized by randomness and provides insight in deciphering the structure of this randomness. Using as a combination of carefully crafted rules and random terms it offers a prescription for not only reproducing (encoding) but also for understanding (decoding) the observed natural variability of the deltaic networks.

# Chapter 3. Channel Migration Patterns in Experimental Deltas: Implication for Fluvial Morphodynamics

Dan Cazanacli[1], Chris Paola[1], Arvind Singh[2]

[1]Dept. of Earth and Environmental Sciences & St. Anthony Falls Laboratory, University of Minnesota, Minneapolis, MN

[2]Dept. of Civil, Environmental, and Construction Engineering, University of Central Florida,

*Submitted to Journal of Geophysical Research: Earth Surface (2021)*

## Abstract

Understanding channel migration is essential in interpreting long-term evolution of fluvial systems and their deposits. Using data from an experimental delta, we analyzed the kinematics of the main upstream channel and assessed the relative dominance of continuous lateral channel migration vs abrupt changes (i.e. avulsions). Detailed investigation of channel centerline location at minute intervals reveals a short-term correlation between migration rates measured at the same location and a spatial correlation that diminishes with distance between points. The most interesting observation is that the channel migrates across the entire deltaic domain without large and abrupt lateral shifts through continuous lateral migration at variable rates. Long periods of back and forth small moves are separated by short bursts of rapid lateral migration. This is somewhat surprising given that aggrading systems tend to be characterized by avulsions. Data also reveal that highly mobile rivers avulse less. We contrast these findings with another experiment conducted under similar conditions but with finer sediment supplied at a lower rate which shows drastically less lateral migration; channel kinematics is instead dominated by periodic flow reconfiguration episodes akin to avulsions, an indication that channel migration style depends on the quantity and size of sediment. The characteristics of these two experiments parallel two regions of the Mississippi River, the meandering and highly mobile alluvial plain and the less dynamic deltaic region suggesting that sediment sorting and deposition at the transition into backwater zone plays an important role in re-shaping the river planform and migration style.

### 3.1 Introduction

The stratigraphic architecture of fluvial deposits has been described as a function of channel migration patterns coupled with sediment aggradation (Allen, 1965, 1978, 1979, 1983; Leeder, 1978; Bridge and Leeder, 1979; Bridge, 1984, 1985; Mackey and Bridge, 1995). In most lowland depositional settings, rivers occupy only a fraction of their alluvial plain. Through bank erosion, point bar accretion, and cutoffs, a meandering river impacts a zone that is few times its width, referred to as the channel belt (e.g., Allen, 1978; Bridge, 1984, 1985). Over the long term, however, channels migrate laterally over the entire fluvial plain, typically several times wider than the channel belt itself.

Channel migration occurs over a wide range of length and time scales, and to some extent depends in specific style on the type of channel pattern (e.g., braided, meandering, anastomosed, tributary, distributary). Here we adopt a simplified broad approach by dividing the scales of motion into 'local', by which we mean bar-mediated short-term movement within a delimited channel belt; and 'basinal', by which we mean movement of the channel or belt on the scale of the whole alluvial plain or basin. In this frame, at the most basic level, the long term dynamics of a channel can be viewed either as a gradual and quasi continuous migration or as a relatively abrupt change in course. The latter process, referred to as avulsion, is commonly associated with depositional systems such as alluvial fans and deltas. The avulsion is generally thought of as a rapid process (e.g., Allen, 1978; Törnqvist and Bridge, 2002).

Both avulsion and gradual channel migration are important processes controlling the long term morphodynamics of alluvial systems and the stratigraphy of alluvial deposits (Jerolmack and Mohrig, 2007; Jobe et al, 2016). In particular, sand bodies associated with lateral migration are continuous and connected in the subsurface, while those associated with avulsion are potentially disjoint (Allen, 1978; Leeder, 1978; Bridge and Leeder, 1979; Mohrig et al., 2000, Michaels et al., 2010) though more recent work advances the possibility of connected multi-storey sand bodies forming as a result of clustered avulsions that re-occupy nearby channels (Chamberlin and Hajek, 2015).

Lateral migration at large scales, commonly described as sweeping (e.g., Jerolmack, 2007), implies that the flow path changes gradually, though at variable rates that depend on many parameters, chiefly the river energy relative to the bank erodibility as well as the channel curvature. Note that within-belt processes such as meander growth and cutoff are, in effect, below the spatial scale of interest to us here. The sedimentary products of gradual migration in aggrading system, fluvial meandering deposits that is, have been

abundantly described in the stratigraphic literature (e.g. Allen, 1983; Friend 1983; Miall 1985; Bridge, 1993). While there are multiple models exploring the evolution of meandering rivers (e.g. Howard, 1996; Sun et al., 2001; Camporeale et al., 2005; Motta et al., 2011; Frascati and Lanzoni, 2013) the use of such models to generate long term stratigraphy is uncommon (van de Lageweg et al., 2015).

Avulsions are driven by greater in- and near-channel deposition rates relative to sediment accumulation farther away from the channel (Bridge and Leeder, 1979), which leads to a condition termed super-elevation (Bryant et al., 1995; Heller and Paola, 1996; Mohrig et al., 2000; Slingerland and Smith, 2004). Eventually, a breach through one of banks can occur diverting the flow along a new, steeper path, ultimately resulting in a new active channel. Avulsion is considered a common if not necessary process in the formation of large scale alluvial deposits; over a time scale of millennia or greater avulsion has been assumed to be the mechanism through which sediment is dispersed across an alluvial plain (Allen, 1978; Leeder, 1978; Bridge and Leeder, 1979; Bryant et al, 1995; Heller and Paola, 2006; Jerolmack and Mohrig, 2007; Straub et al., 2009; Hajek et al., 2010; Wang et al., 2011; Chamberlin and Hajek, 2015; Hajek and Straub, 2017). While several avulsion styles exist (Slingerland and Smith, 2004), we refer to avulsion as a regional process through which a river course takes a new flow path forming a new deltaic outlet (mouth) or a new lobe, as opposed to local avulsions in which the bulk of the flow abandons the main channel in favor of new (shorter) path but rejoins the main channel further downstream (Heller and Paola, 1996).

The mechanism of avulsion is not fully understood. Many factors contribute to the likelihood and frequency of avulsions, including overall aggradation rate, differential aggradation rates, channel lengthening, bank erodibility, or sea level rise. Several studies indicate that regional avulsions characterizing large deltaic systems seem to be concentrated within the upstream half of backwater zone avulsion (Nittrouer et al., 2012; Lamb et al., 2012; Chatanantavet et al., 2012). Generally speaking, prediction of avulsion occurrence both locally and temporally is challenging and stratigraphic models typically treat avulsion as a stochastic process assuming either a random spatial distribution of the channel location and their deposits (Allen, 1998; Bridge and Leeder, 1979; Allen, 1979; Bryant et al., 1995; Heller and Paola, 1996; Mohrig et al., 2000) or including additional assumptions such as channel re-occupation (Jerolmack and Paola, 2007) or compensational stratigraphy (Straub et al., 2009).

Although avulsion has been frequently invoked in statigraphic interpretation, there are relatively few detailed descriptions of modern avulsion deposits (e.g., Mack and Leeder, 1998; Bristow, 1999; Morozova and Smith, 2000; Stouthamer and Berendsen, 2007) or ancient sequences with clear evidence of multiple avulsions (Marzo et al, 1988; Kraus, 1996; Mohrig et al, 2000; Arche and Lopez-Gomez, 2005; Hajek et al., 2012; Chamberlin and Hajek, 2015). Since the initial work of Allen (1978, 1979), Leeder (1978), and Bridge and Leeder (1979) stratigraphic modeling based on avulsion as a driving process has been rather prolific (e.g. Mackey and Bridge, 1995; Heller and Paola, 1996; Törnqvuist and Bridge, 2002; Jerolmack and Paola, 2007; Hajek et al., 2010; Hajek and Wolinsky, 2012, Chamberlin et al., 2015).

To distinguish rivers that migrate laterally at sustained rates and tend to avulse infrequently from the less dynamic rivers with highly cohesive banks that tend to avulse more, Jerolmack and Mohrig (2007) introduced a non-dimensional mobility number *M*, $M = \frac{V_c}{B} \times \frac{H}{V_a}$, representing the ratio between avulsion time scale and the lateral migration time scale, where the former is defined as the ratio between channel depth, *H* and aggradation rate, $V_a$, and the latter as the ratio between channel width, *B*, and migration rate, $V_c$, Jerolmack and Mohrig show that systems with large *M* (i.e., *M* >>1) experience only infrequent avulsions.

In this paper, we analyze a deltaic experiment focusing on the dynamics of the main channel located upstream of the distributary (flow diverging) zone. Using high-resolution images, we examine the lateral channel migration rates and patterns in space and time to analyze the overall channel kinematics and the relative importance of gradual lateral migration over avulsion. In particular, we try to determine whether significant basin-wide aggradation (i.e., in excess of typical channel depth) can occur without abrupt flow path changes (i.e., avulsion).

### 3.2 Experiment Description

The experiments reported here were conducted at the St. Anthony Fall Laboratory with the aim of exploring the evolution of the full deltaic system and provided a rich data set that allowed for a detailed investigation of the kinematics of the main stem channel. The experiments were performed in the “Delta Basin” tank, a square tank devised for clastic deposition experiments with 5 m sides and 0.6 m deep (Figure 9A). Water and sediment were fed from one corner using a calibrated computer controlled valve and a screw-type

powder feeder, respectively, forming a deltaic deposit with the approximate shape of a quarter circle, bounded by the sides of the tank (fixed boundaries) and an evolving (prograding) shoreline.

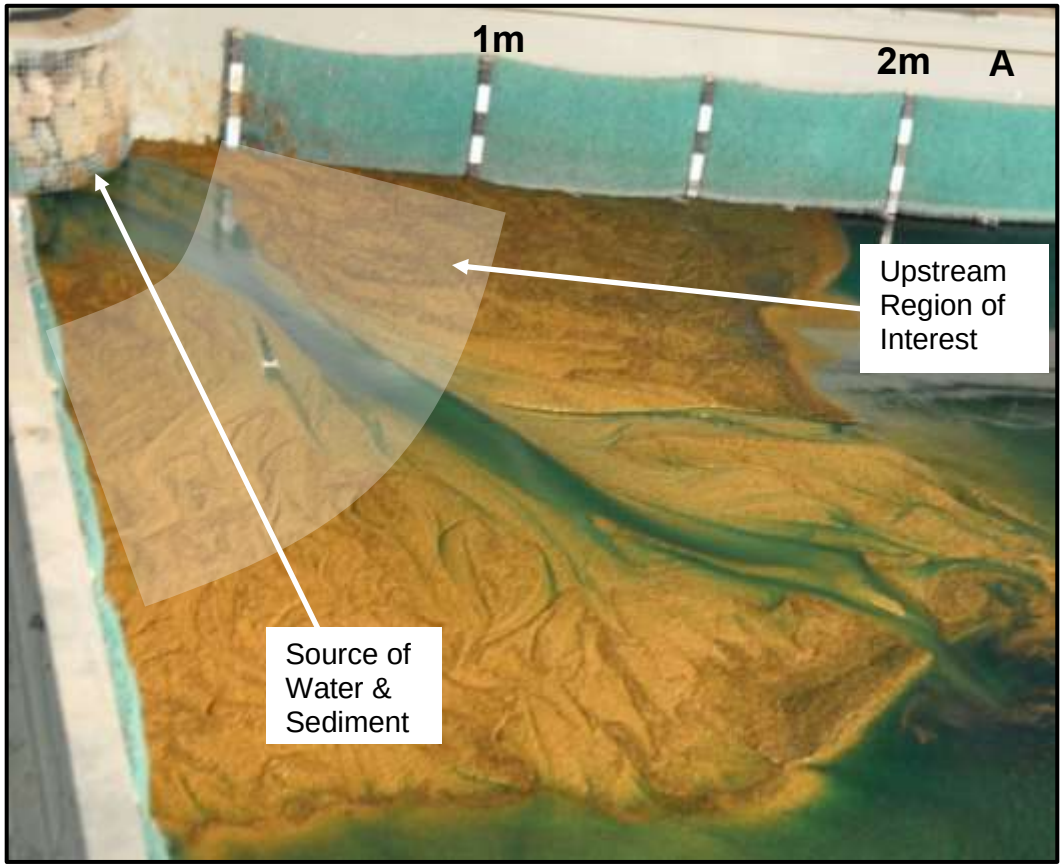


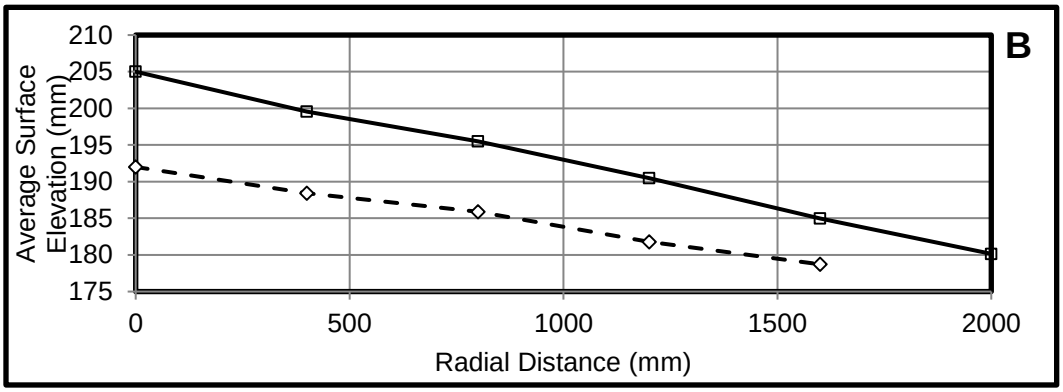


**Figure 9. A - Experimental basin overview showing the upstream region of interest used in data analysis along with main channel formed. B - Averaged cross-shore deposit surface before (dashed line) and after (solid line) the 5-hour stage referred to as Experiment-1.**

The basin was filled with 0.18 m of water at the onset of the experiment. The water discharge was continuously monitored with a flow meter and the sediment discharge was manually checked every few hours to ensure rate consistency. The water level in the basin was monitored using an ultrasonic probe and was kept constant by a movable weir at the outflow location. Water and sediment were mixed in a funnel and discharged as a homogenized mix at the corner of the tank via a pebble crib (Figure 9A). A blue color dye tracer was also added (dripped into the funnel through a small pump) to highlight the structure of the flow. In the dry state, the specific gravity of the shells was approximately 0.9 g/cm$^3$. When placed in contact with water, much of the porous structure of the shell grains quickly fills up yielding an average specific gravity of approximately 1.3 g/cm$^3$. With an overall lower density, the walnut shell formed a deposit surface with a lower slope compared with surface deposit from silica sediment.

The main experiment discussed here was part of broader experiment series consisting of several stages with various water and sediment supply rates. As expected, based on observations made during prior experiments, a large water to sediment ratio led to laterally spread flow (i.e., sheet flow) whereas a lower water to sediment ratio led to more coherent, channelized flow. Here we focus on a five-hour interval during which the water to sediment ratio was at its lowest and allowed for identification of channelized flow in the upstream part of the deposit. During this five hour stage we referred to as Experiment-1 the subaerial deltaic deposit prograded from an averaged radial distance (i.e., distance between source corner and shoreline) of 1.9 m to approximately 2.4 m (Figure 9B).

The sediment in Experiment-1 consisted of walnut shells with a median diameter ($D_{50}$) of 1 mm and a narrow grain size range of 0.59 to 1.41 mm. The inflow rates for water and sediment were kept constant at 200 mL/s and 4 mL/s, respectively. For comparison purposes we later reference a second experiment (Experiment-2) conducted in the same tank, also under steady conditions but a median grain size of 0.25 mm and water and sediment discharges of 32 mL/s and 1.6 mL/s, respectively (Table 1).

### 3.3 Data Collection and Processing

High resolution overhead images were taken 1 minute apart and used to document the structure of the flow. Although multiple channels radiating from the inflow corner were present at various times, in the upstream area the images indicate the dominance of one channel that captured the majority of the flow. This upstream main channel was reliably tracked to a distance of approximately 1 m from the corner, downstream of which the flow

tends to fan out as sheet flow or multiple (two or three) wider and shallower channels. The width of the main channel varies in time and space but on average it is about 90 mm everywhere within the region of interest, upstream and downstream alike. Our focus here is on the dynamics of this main channel, which is relatively coherent and can be tracked during the entire experimental time, i.e. in each of the 300 images collected 1 min apart, given its dark blue color tones.

Taking advantage of the color contrast, the deeper main channel in the upstream region was isolated using a range of red, green, blue, light intensity and saturation values. The edges of dark blue tones corresponding to the main channel were first identified in each image. Subsequently, the secondary, smaller flow areas and the areas of stagnant water were removed. A raw centerline was generated by locating the midpoints between the edges (banks) of the channel and was subsequently smoothed using a fifth order Savitski-Golay filter (Savitski and Golay, 1964). Thus, the channel position at each minute is represented by a curved line, that is, its centerline. The centerlines vary in shape from nearly straight to slightly curved, reflecting the fact that channels are characterized by relatively low sinuosity. Figure 10A shows the centerline position at every 5 minutes.

The radial distance over which we collected data, measured from the corner of the tank, is from 0.45 m to 1.05 m (Figure 9A). Upstream of this range the position of the channel is tied to the source point and does not have a truly independent dynamic while downstream of this range the channel cannot be reliably isolated in the images as the flow widens and separates into multiple paths. In principle, the angular position can vary from 0 to 90°, as the flow moves from one side of the tank to the other. However, the observed range is more limited, from approximately 17 to 84° in part because, although the channel bank occasionally touches one side of the tank, the position of the centerline itself is always several degrees away from the side (Figure 10A).

We also captured the topography of the deposit using a high precision (i.e., 0.2 mm vertical accuracy) laser scanner that collected elevation data on a dense (2 mm cells) rectangular grid. Because the laser method does not perform well over water, the scanning was done periodically, when the inflow was paused. Thus, the surface of the deposit was scanned before and after the five hour stage discussed here. We used these detailed topographic measurements to determine the deposit thickness and estimate the dimensions of the main channel.

During the 5 hour stage, the delta experienced both seaward extension (progradation) and vertical growth (aggradation). On average, the thickness of the deposit in the region

of interest was approximately 10 mm (Figure 10A), with slightly more accumulation upstream (~11 mm) than downstream (~9 mm). Divided over 300 minutes, this translated into accumulation rates varying from 0.037 mm/min upstream to 0.030 mm/min downstream.

The surface scans also reveal the shape of the main channel as seen in a circular cross-section taken at 0.75 m distance from the apex, the middle of the region of interest (Figure 10A). Both before and after surfaces suggest that the maximum channel depth is approximately 6 mm (Figure 10B).

### 3.4 Results

Throughout the 5-hour stage discussed here the flow zone appeared to be moving continuously but not uniformly in time or in space. Based on visual inspection of 300 overhead images corresponding to the five hour stage, we can make the following qualitative observations: (1) the main channel "sweeps" most of the surface from one side of the tank to the other, but not uniformly. Longer episodes of flow within a relatively narrow sector are separated by shorter episodes of sustained lateral migration; (2) although the main flow sweeps much of delta surface moving in the same general clockwise direction, the channel makes numerous smaller back and forth lateral moves at various rates; and (3) sometimes some portions of the channel move laterally more than others. To understand these observations and quantify the channel kinematics in time and space, we performed a more formal investigation using the time varied location of the centerlines as a representation of the channel location.

#### *Channel dynamics description*

Given the geometry of the experiment, it is important to define adequate metrics for analyzing channel motion. Because the source of flow is fixed at the corner of the square tank, the main channel migrates laterally more downstream than it does upstream. Thus, to compare downstream vs upstream dynamics we tracked the lateral movement of the centerline as the angular shift defined as the change in angle with time. Figure 10A indicates how each point along a centerline can be defined in polar coordinates by the angle between the point in question, apex position (corner of the tank) and the *x*-axis (side of the tank) and by the radial distance measured on a straight line from the apex to that point. We denote $\Delta\theta$, the angular change in centerline position over 1 minute (image frequency), with the associated units of degrees per minute and examine the patterns of

centerline migration in space (i.e., upstream vs downstream) and time. $\Delta\theta$ is essentially a proxy for migration rate normalized by the downstream distance to account for the geometry of the experiment. Where necessary, we convert the angular shift into actual distance (i.e., mm) and/or into number of channel widths.

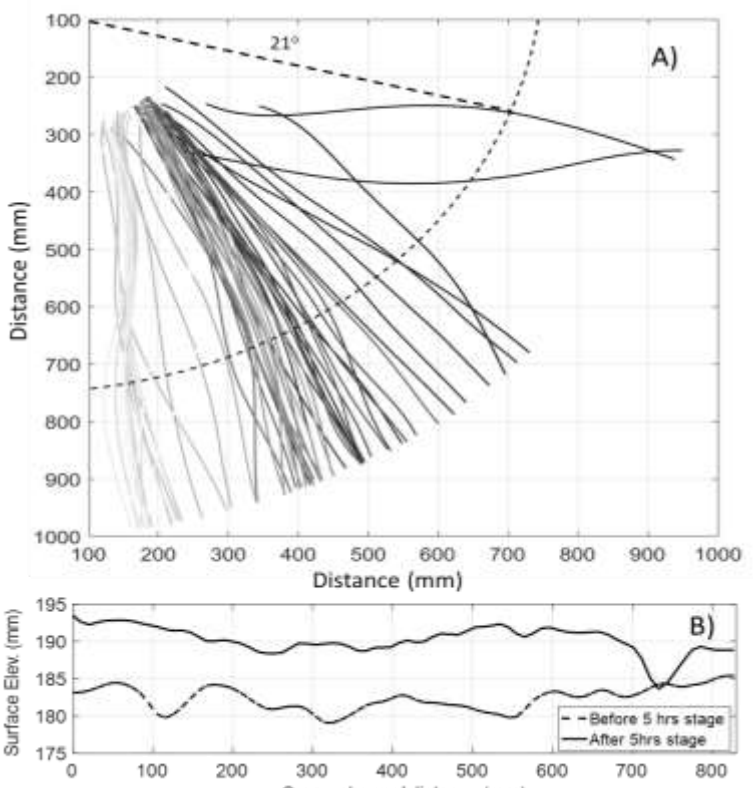


**Figure 10. A - Main channel centerline position in time (black to white) every 5 minutes. Dashed line shows how centerlines radial coordinates were defined (*R = 750 mm, θ = 21º*). B - Circular cross-section of the deposit surface before (dashed line) and after (solid line) the 5-hour stage, taken along the quarter circle (750 mm) in A.**

Tracking the centerline position in time at various locations confirms the above qualitative observations. The essential aspect is that the channel moves at irregular rates but not randomly. Figure 11A depicts the angular position in time for three radial distances, upstream (0.45 m), middle (0.75 m), and downstream (1.05 m). Periods of relative stability during which the channel "vibrates" back and forth within a narrow range alternate with periods during which the channel migrates at higher rates. More specifically, there are three long intervals (lasting tens of minutes) when the centerline moves within a narrow range of only few degrees. The typical (average) migration rate, $\Delta\theta$, within these intervals, one direction or the other, is less than 1° per minute, in most cases less than 0.5° per minute. Outside these quasi-stable intervals the centerline moves more rapidly at rates above 1° per minute. There is only one instance at the beginning of the stage where the channel moves rapidly, spanning a sector of approximately 25° in 5 minutes. Figure 11B shows the incremental angular shift between consecutive images, that is, at one minute time interval. The difference in angular shift distribution among the three locations indicates that the channel has a fairly complex

mobility, with different sections moving at different rates. Furthermore, parts of the channel (i.e., downstream vs upstream) do not always move in the same direction.

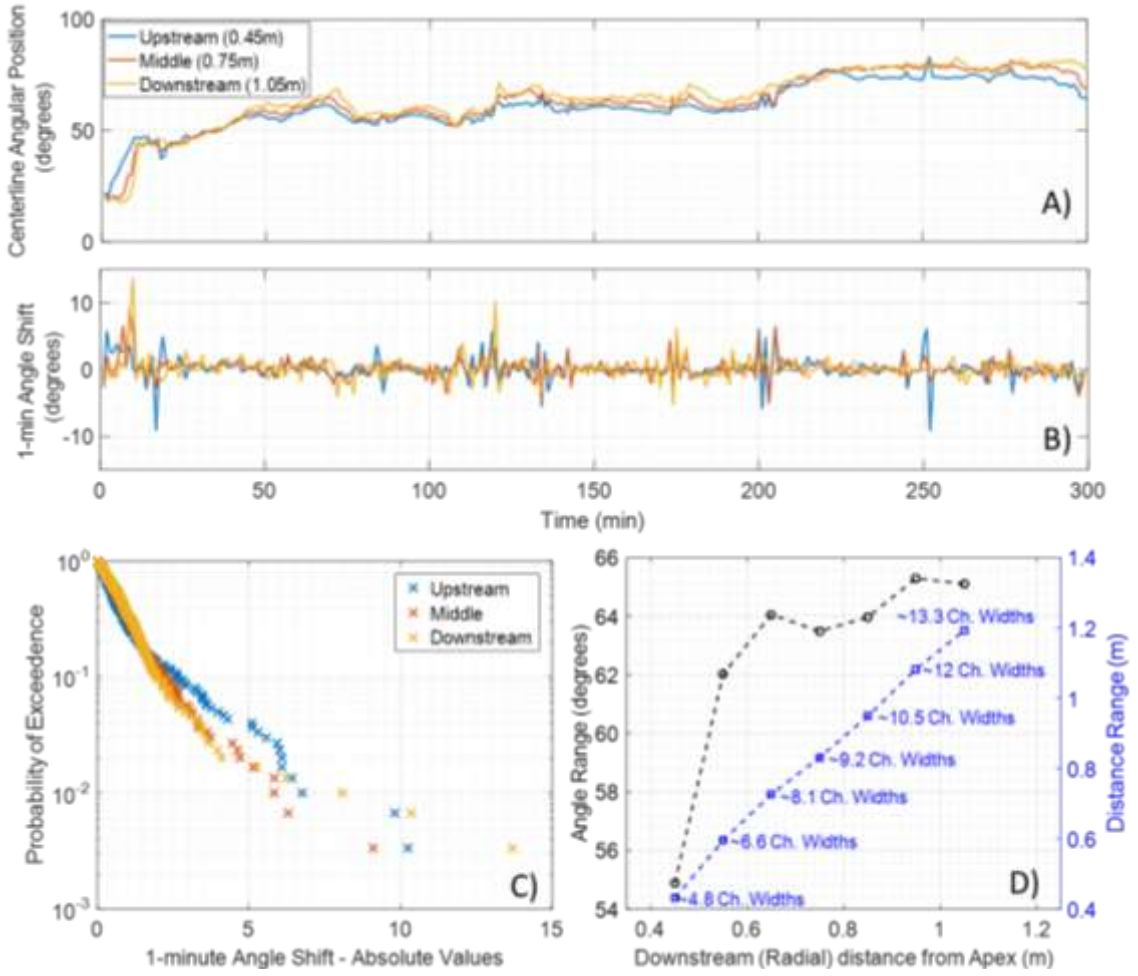


**Figure 11. A - Centerline angular position in time at three locations. B - Angular 1-minute shifts, $\Delta\theta$ at the same three locations. C - Complementary cumulative distribution of $\Delta\theta$ (absolute values) showing two regions (0 to 2º and above 2º). D - Total centerline range as a function of downstream distance given as degrees (left Y axis, black line), distance swept (right Y axis, blue line), and number of typical channel widths (blue labels).**

The investigation of the centerline location in time and space shows that the main channel migrated from one side of the tank to the other spanning a total angular range of approximately 62 to 65°. This angular range is slightly smaller in the upstream area (Figure 11C). At any given location, the centerline sweeps an arc of a circle greater than the downstream distance, that is, slightly more than one radian. Converted into a multiple of channel widths, given that the typical channel width is approximately 90 mm, the distance swept by the centerline increased quasi-linearly from 4.8 channel widths upstream to 13.3 channel widths at the downstream end of the study region (Figure 11C).

In aggregate, the *net* rate of migration, from one side of the tank to the other, averaged 0.24° per minute. However, the averaged absolute value of $\Delta\theta$ (angular shift in either direction), was approximately 1° per minute, or about four times the net average rate. The migration patterns are fairly complex showing variable rates and numerous direction switches that warrant further investigation.

The distribution of $|\Delta\theta|$, the absolute values of 1-minute angular shifts in the form of the complementary cumulative distribution function (1-$F_x$ or probability of exceedance), shows an exponential trend with a thicker (power law) tail (Figure 11D). Specifically, the values up to about 2° (the smooth part of the curve) fit an exponential trend and correspond mostly to the three periods of relative stability mentioned above. The larger values correspond to the bursts of more rapid movements with the largest value corresponding to the largest channel move at the beginning of the stage.

***Temporal and Spatial Correlations***

Given that there were three relatively long quiescent periods of little mobility and other periods of more intense activity, we explore whether there is some dynamic persistency, specifically, whether larger or smaller $\Delta\theta$ are followed by $\Delta\theta$ of comparable magnitude. Towards this goal, we look at the correlation between $\Delta\theta$ values taken over increasing intervals from one to several minutes both as signed and absolute values (Figure 12A). Note that all $\Delta\theta$ are measured 1 minute apart but the measurements, taken at the same locations, are lagged in time. Using the signed $\Delta\theta$ values, it can be seen that there is no measurable correlation (Figure 12A) which would suggest a somewhat unstructured mobility. It is also possible that the lack of correlation is in part due to frequent change in the direction of migration. In fact, for absolute values, we detect a small correlation for the 1 to 2 minutes time lag (Figure 12A), suggesting that smaller lateral moves are slightly more likely to be followed by comparably small moves and larger lateral moves likewise to be followed by larger moves, yet not necessarily in the same direction.

Next, we examined whether there are any spatial relationships between simultaneous $\Delta\theta$ values at different locations. We grouped all pairs of simultaneous $\Delta\theta$ by the radial distance between the two points. Using 61 locations spaced equally (i.e., 0.45 m to 1.05 m, every 0.1 m), we plotted the average correlation as a function of distance. Figure 12B shows that the channel locations close to one another (i.e., up to ~20 cm or approximately two channel widths) are well correlated in their dynamics but as the distance between points increases this correlation drops essentially to zero, indicating that the channel does

not move as a “stiff” object but, at least on the short-term, the downstream and upstream regions move independently.

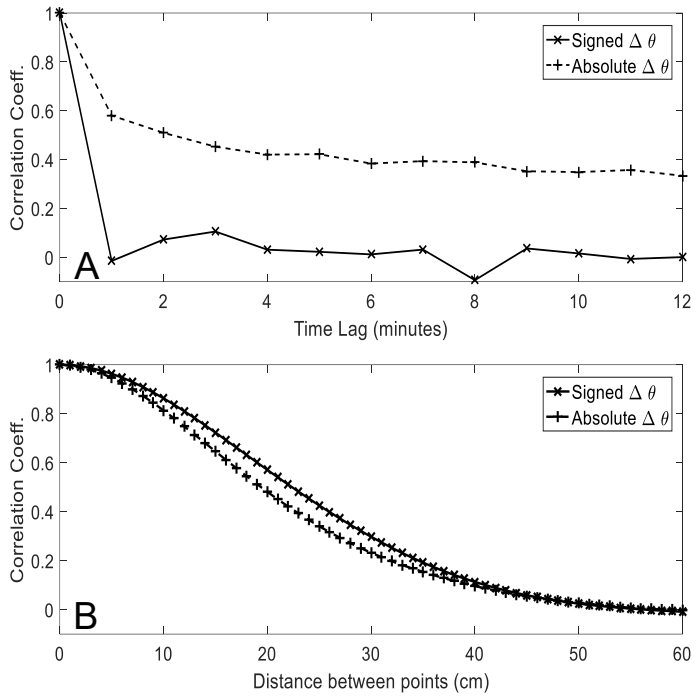


**Figure 12. A - Average temporal correlation in $\Delta\theta$ occurring at same locations, 1 to 12 minutes apart. B - Average spatial correlation of synchronous $\Delta\theta$ pairs grouped by distance between points, from 1 to 60 cm. Note that, consistently throughout the paper, $\Delta\theta$ refers to 1-minute change in angular position whereas (time) lag refers to time span between $\Delta\theta$ evaluations.**

Thus far we have examined correlations between $\Delta\theta$ at the same location lagged in time, and correlations between simultaneous $\Delta\theta$ for pairs of points as a function of distance between the points. We also look at the interdependency of these shifts in a more generalized space-time context, by pairing all 61 locations and examining the correlation in $\Delta\theta$ between each pair of points in a matrix format. Again, by definition $\Delta\theta$ always refers to angular shifts that are one minute apart. The matrix of correlations of synchronous $\Delta\theta$ shown in Figure 13A confirms, in general, that the points close to each other are well correlated (main diagonal band) in their motion, and as the distance between points increases the correlation drops to zero (corners). We can use this generalized correlation matrix representation but instead of simultaneous $\Delta\theta$ we now consider $\Delta\theta$ that are lagged in time, relative to one another. That is, $\Delta\theta$ at the second point in the pair occurred 1, 2, or 3 minutes later (i.e., lagged). Figure 13B shows the correlation of *shifts* that are one minute apart, confirming the trend in Figure 12B. It also reveals that the $\Delta\theta$ in the middle region tend to be followed one minute later by $\Delta\theta$ of comparable magnitude downstream. Figure 13C shows that a correlation in $\Delta\theta$ values that are two minutes apart exists only in the upstream region. No significant

correlation exists between $\Delta\theta$ pairs that are three (or more) minutes apart (Figure 13D), suggesting that the system has no memory beyond a two minute span.

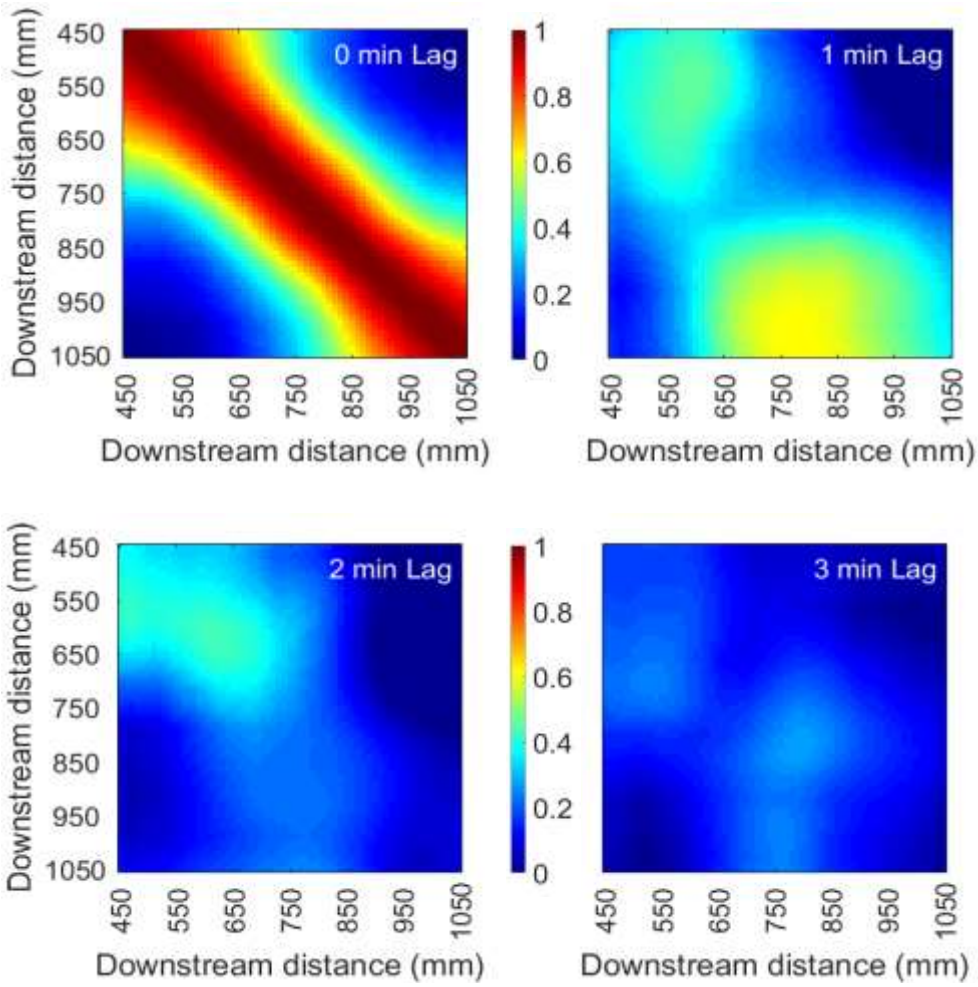


**Figure 13. Generalized spatial-temporal correlation of $\Delta\theta$ (absolute values): A - Synchronous shifts, showing a strong correlation for points closer in space (red diagonal) vanishing to zero with distance between points (blue corners). B, C, and D - $\Delta\theta$ downstream (Y-axis) occurs 1, 2, or 3 minutes later (i.e., lagged) relative to the upstream location (X-axis). Note the sharp decrease in correlation with time lag from limited correlation at 1 minute lag, to only residual correlation in upstream region at 2 minute lag, to no correlation at 3 minute lag.**

### *Structure of Flow Direction*

The $\Delta\theta$ statistics presented above reveal important lateral migration trends and spatial correlations (or lack thereof). Additional insight can be gained from a more localized data investigation by looking at the orientation of the centerline, which approximates the local flow direction. Thus, instead of centerline location changes discussed above, we explore the (flow) orientation changes. Using the same matrix of points paired as above we can examine how the changes in local flow direction over 1-minute span are correlated,

spatially and temporally. Synchronous changes in flow direction are well correlated for points closer to one another and the correlation decays as the point spacing exceeds 0.2 m or approximately two channel widths (Figure 14A). However, if we look at changes in flow direction that are lagged by one minute we observe an inverse (negative) correlation between points close to each other, suggesting that, locally, the centerline switches directions, as would be expected for sinuous channels. We also observe that the change in local direction at a given location is positively correlated with the change in local direction about 0.2 m (~2 channel widths) downstream occurring one minute later (Figure 14B, orange band) a result that can be interpreted as migration of a meander bend (Sylvester et al., 2019). These results suggest that, although the experimental main channel has a low sinuosity, its dynamics are comparable to the patterns of natural meandering rivers.

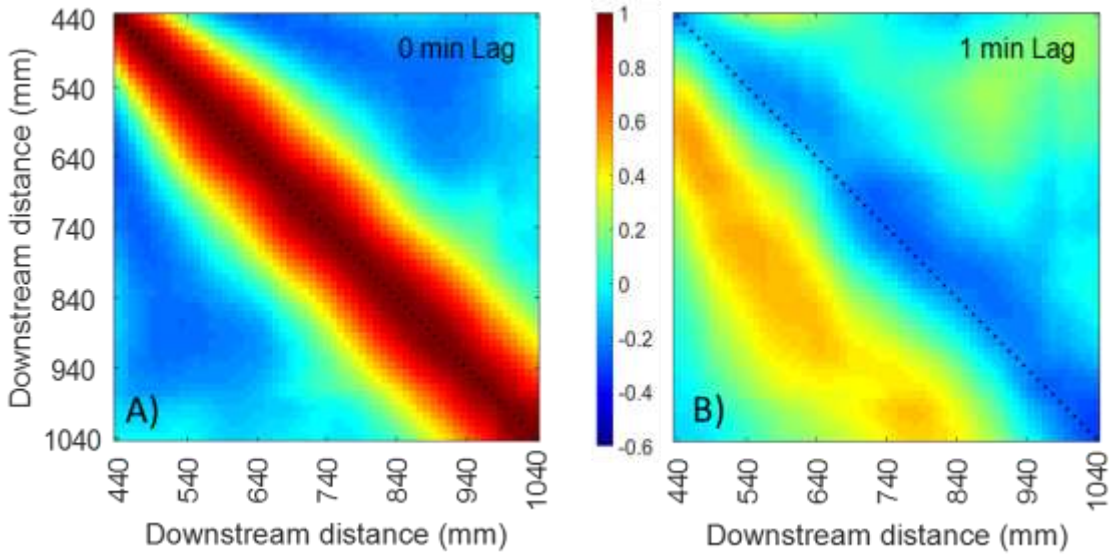


**Figure 14. Spatial-temporal correlation of changes in flow direction as defined by the local orientation of the centerline (*not* the angular position): A - Synchronous shifts in flow direction showing a strong correlation for points closer in space (diagonal) decreasing with distance between points (corners). B - Changes in flow direction lagged by 1 minute, showing: (i) negative correlation for points close to each other (diagonal) indicating that, locally, the flow alternates direction, and (ii) positive correlation between points that are about 0.2 m apart suggesting that channel bends migrate downstream.**

### *Channel Migration Style*

From Figure 10A, it can be seen that the centerline migrated from one side of the tank to the other, spanning a total radial distance of about 65°. The channel itself covered a wider sector of approximately 75° (of the 90° domain). One key question we try to address is whether the observed interspersed fast migration bursts discussed above are equivalent

to an avulsion or rather a burst of rapid yet continuous lateral migration. This distinction is not semantic: at issue is whether or not a continuous body of channel deposits is left over the trace of the channel's lateral motion.

In lateral migration the channel occupies *each point* along the path between the beginning and end points of a given lateral trajectory, whereas in avulsion the channel moves from a starting location to an end location without transitioning through the intervening lateral area. It should be noted, however, that an avulsion may also be gradual in time with the newly formed channel and the (later to be) abandoned channel coexisting for long periods (Bridge, 1984; Mack and Leeder, 1998; Kleinhans et al., 2008). The key point for our analysis is that, regardless of the time scale, avulsion is spatially abrupt, without occupation of the space between the new and previous channel paths.

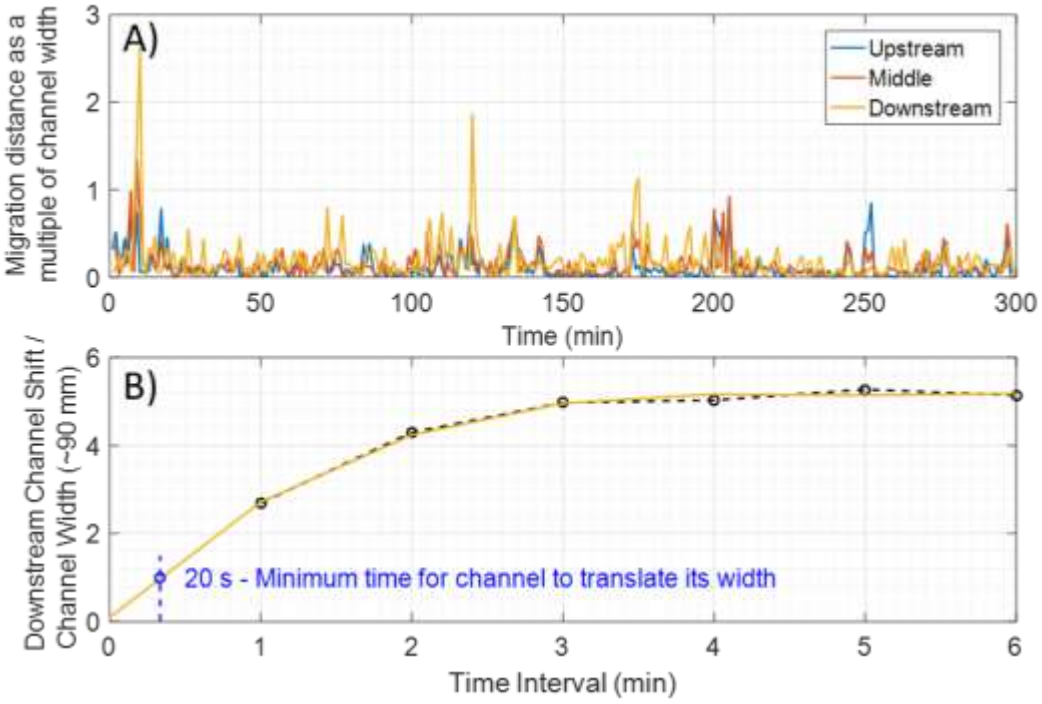


**Figure 15. A - Lateral 1-minute channel shifts (absolute values) expressed as multiple of typical channel width (90mm). Note that only in four instances has the centerline migrated more than one channel width over the course of 1 minute. B - Maximum channel migration (measured at downstream location) as a function of time interval. Data fit well a 3rd degree polynomial curve and extrapolation suggests that it takes at least 20 seconds for a channel to migrate over its width.**

Considering the three locations (upstream, middle, and downstream) and converting $\Delta\theta$ into distance shifts (i.e., mm), only four observations exceed the typical 90 mm channel width, i.e., one-channel width (Figure 15A), the three larger ones located downstream and

one in the middle. However, a shift greater than one-channel width over one minute interval does not imply that an avulsion occurred. It is possible that during the one minute time span between consecutive images the channel has migrated relatively fast yet continuously, reworking all the sediment surface between the two positions. To assess the minimum probable duration of an avulsion, we extrapolated the 1-minute data. Figure 15B shows the maximum centerline distance shift over various time intervals estimated at the downstream end, where the channel is most likely to move over a distance greater than its width. The maximum centerline migration increases non-linearly with time interval, from about 250 to 390 to 450 mm for 1, 2, and 3 minutes time intervals beyond which it remains approximately constant. The data fits well a third degree polynomial curve ($r^2$=0.99) and extrapolation suggests that the shortest migration time interval over which the centerline spans the typical channel width of 90 mm is approximately 20 seconds (Figure 15B). Given that we did not observe persistent bifurcations in the region of interest and that each image shows only one dominant stem channel we infer that, in the context of our experiment, an avulsion process had to be rather sudden. We cannot categorically rule out the avulsion based on extrapolation alone, but a close inspection of the sediment surface in each image indicates that only the largest shift near the very beginning of the 5-hour stage may correspond to an avulsion that took place in the downstream portion in our region of interest. In other words, for most, possibly the entire duration of the experiment, the channel dynamics was defined by continuous rather than discontinuous lateral migration.

***Comparison with a less dynamic channel experiment***

The fact that main channel swept most of the available domain without large jumps from one location to the other is remarkable, considering that the entire domain experienced aggradation in excess of the typical channel depth. We attribute this exceptional channel mobility to a relatively large rate of coarse sediment input. To verify this hypothesis, we compared the data presented above with data from another deltaic experiment performed in the same experimental tank, also under steady conditions and the same corner inflow setup but with finer sediment material delivered at a lower rate (see Table 1).

For this second experiment (Experiment-2), we focus on a 13.5 hour stage during which a main channel was present in the upstream region for extended periods of time, i.e. tens of minutes or more. The flow shows very different dynamics compared to that of Experiment-1. The main channel in Experiment-2 had much less lateral mobility. Furthermore, five times during the 13.5 hours, the flow switched from one single dominant

channel to a multichannel flow (two channels of comparable size and/or several smaller, anastomosed channels) after which most of the flow coalesced again into one dominant and stable channel located in a significantly different location. Figure 16 depicts location of the channel at five different times. These episodes of flow reconfiguration are discontinuous laterally and hence qualify as avulsions.

**Table 1. Experimental conditions and extracted channel characteristics:**

| | Units | Experiment-1: (Laterally Dynamic) | Experiment-2: (Stable Channel) |
|---|---|---|---|
| **Duration** | **min** | **300** | **810** |
| **Sediment Discharge - $Q_s$** | **mL/s** | **4** | **1.6** |
| **Median grain size – $D_{50}$** | **mm** | **1** | **0.25** |
| **Water Discharge - $Q_w$** | **mL/s** | **200** | **32** |
| **Number of Avulsions episodes** | | **none (see text)** | **5** |
| **Avulsions time – $T_a$** | **min** | **>285 (see text)** | **87/ 91/118/52/367** |
| **Angular domain between avulsions** | **degrees** | **~60** | **~10-15** |
| **Average angular channel shift rate $\lvert\Delta\theta\rvert$** | **deg./min** | **1** | **0.1** |
| **Average channel shift rate downstream** | **mm/min** | **18** | **1.8** |
| **Typical channel depth – $H$** | **mm** | **6** | **4** |
| **Average channel width – $W$** | **mm** | **90** | **80** |
| **Total Aggradation** | **mm** | **10** | **10** |
| **Aggradation rate** | **mm/min** | **0.033** | **0.013** |
| **Mobility Number – $M$** | | **36** | **7** |

The differences between the main, laterally dynamic Experiment-1 discussed above and the “stable” Experiment-2 are summarized in Table 1. Experiment-2 was conducted with finer sediment delivered at a lower rate of 1.6 mL/s (compared to 4 mL/s in Experiment-1). The key observation is that the main channel in Experiment-2 was remarkably stable, migrating laterally very little and very slowly, at average rates of less than 0.1° per minute, one order of magnitude less than the channel in Experiment-1. Between the avulsion episodes, the main channel spanned an angular area ranging from about 10° to at most 14° (Figure 16). On average, the time span between avulsions was 143 minutes but the intervals (i.e., avulsion times, $T_a$) are irregular (Table 1). Remarkably, between the last two avulsions the main channel remained “stuck” within a 10° range for over 6 hours, more than the entire duration of the dynamic Experiment-1 during which the channel spanned a sector of circle of about 75°. The total aggradation in the upstream

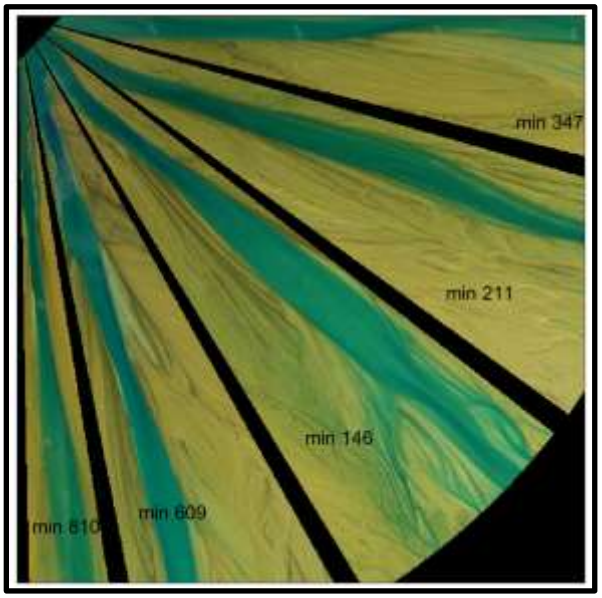


**Figure 16. Composite image showing typical locations of the main channel in the comparison Experiment-2. Labels indicate time of channel position in minutes. In Experiment-2 the main channel remained stable, confined within a narrow sector, for extend periods of time. It changed its location five times, through brief episodes of flow divergence, upon which main channel re-emerged in a significantly different location.**

region over 13.5 hours was approximately 10 mm, as the deposit thickness in the main experiment (Experiment-1) that lasted only 5 hours.

In summary, this comparison Experiment-2 shows a substantially different channel dynamic, one in which the channel migrates laterally within a narrow band for extended amounts of time, separated by short episodes of flow reconfiguration characterized by flow divergence over a wider area (a "finding phase"), after which the flow coalesces again into one channel but in a distinctly different location.

### 3.5 Discussion

Avulsion has been inextricably associated with depositional systems, in-channel and near channel (i.e., levee) aggradation being a necessary condition for avulsion to take place (i.e., via levee breaching). However, whether avulsion must occur wherever active fluvial deposition takes place is not evident. The data from our main experiment suggest that a very dynamic channel could aggrade and distribute sediment across an entire alluvial plain through lateral migration only, that is, without avulsing. One obvious criticism is that natural rivers in depositional settings, are flanked by levees which are a morphological expression of the differential deposition rate between near channel zone and the more distal floodplain area. Natural levees enable the river bed to aggrade more rapidly relative to the floodplain thus creating conditions that favor an avulsion via levee breaching. In support of the relevance of our experimental channel to natural rivers, we offer the following arguments: (a) levees though not well developed, are present in our experiment based on cross-sections from the scanned topographic surfaces (Figure 10A); further discussion of

experimental levees made under similar conditions can be found in Ganti et al. (2016. (b) Even without levees, the channel is still a confining conduit, and avulsions are still expected to occur due to bed aggradation driven by subsidence and/or channel extension at the shore line; and (c) in natural systems, if the lateral migration rates are high relative to the rate of levee growth, an active meandering river may continually erode its levees as it wanders laterally (Jobe et al., 2016).

To be clear, we do not suggest that avulsion is not essential in defining the long term evolution of major fluvial systems and the stratigraphic record. In fact, as aggradation total approaches the channel depth, only a highly dynamic fluvial system with significant bedload may resemble the dynamics of our experiment and continue to "avoid" avulsion. Such rivers are likely to be characterized by a high sediment discharge, particularly bedload, as the connection between channel mobility and (bed) sediment flux has been well documented through both experimental (Wickert et al., 2013) and field (Constantine et al., 2014) data. Wickert et al. (2013) estimated channel migration from 9 experiments performed under variable conditions (i.e., aggradation rates, water to sediment ratio, grain size, or presence of vegetation in two of the experiments that generated braided networks) showed a proportional relation between the channel mobility rate and the downstream sediment flux (sediment discharge divided by the cross-section area of the flow) over a range of scales.

Mohrig et al. (2000) and Jerolmack and Mohrig (2007) proposed that the avulsion time scale is linked to the deposition rate and that, for single thread rivers, the avulsion time scale is equal to the average channel depth divided by the aggradation rate *of the channel bed*. However, this connection does not readily predict the number of avulsions over the wider alluvial plain which may aggrade through multiple avulsions as the channel belt migrates periodically from one location to another. Alternatively, as the data from our experiment suggest, the active channel can sweep a wide area without avulsing. Using the data of the experiments, we computed a value of Jerolmack and Mohrig's mobility number $M$ of 36 for the main Experiment-1, a reflection of the high lateral mobility. By contrast, the mobility number $M$ in Experiment-2 was 7. The data set of Jerolmack and Mohrig contains only one natural system with $M$ above 36, the alluvial plain of the Lower Mississippi with an estimated $M$ value of 395, meaning that this portion of the Mississippi River is extremely mobile and not likely to experience avulsions. Certainly, other rivers have large lateral migration rates (Constantine et al., 2014) but many do not. The $M = 395$ value was derived based on a channel depth of 30 m, an average long term aggradation

rate of 4 mm/year and average lateral migration rate of 50 m/yr which is not uncommon for reaches near and upstream of Old River Control Structure (Hudson and Kessel, 2000), located approximately 500 km upstream of the Head of Passes. Measured rates of lateral migration along the Mississippi River also show that the lateral channel mobility decreases significantly downstream. The average lateral migration rate decreases by full order of magnitude from over 50 m/yr to approximately 5 m/yr over a distance of approximately 200 km downstream of the Old River Control Structure and, as it approaches the delta region downstream of New Orleans, the typical lateral migration rate decreases further to approximately 1 m/yr or less. The value of the mobility parameter *M* drops accordingly to about 10 (Jerolmack, 2009).

The abrupt decrease in lateral mobility downstream of the Old River Control Structure corresponds to the transition into backwater zone. Jerolmack (2009) suggested that the sediment deposition in this region is responsible for a transition in channel pattern from meandering to straight and avulsion prone, attributing the decrease in channel mobility to sediment fining resulting in more cohesive banks.

Several studies based on one-dimensional hydraulic analysis indicate that the avulsion is likely to occur in the upstream portion of the backwater zone. Nittrouer et al. (2012), Lamb et al. (2012), and Chatanantavet et al. (2012) determined analytically that in the upstream portion of the backwater zone, a reduction in surface slope and transport capacity favors channel bed aggradation, thus increasing the chance of avulsion, while in the downstream portion occasional high discharge events translate into a steeper, drawdown water surface profile (type M2) which causes periodic channel scouring and deepening, making the avulsion unlikely. A variable flow regime seems essential in explaining the scaling between avulsion length and backwater zone. Experimental data from Ganti et al. (2016) and further analysis by Chadwick et al. (2019) show that under constant discharge this scaling is not present.

Without minimizing the importance of the complex and variable hydraulic regime in the backwater zone, based on our findings we suggest that the abrupt drop in channel mobility due to sediment deposition at the backwater zone transition is critical in defining the preferential location of avulsion nodes and the change in alluvial style. In effect, the contrast between the two zones of the Mississippi River, upstream and downstream of the backwater zone, mirrors the contrast between our two experiments in which no backwater effect was present. As the Mississippi River enters the backwater zone it loses much of

the coarser bed load. USACE grain size measurements compiled by Nittrouer et al. (2012) (their Figure 6) reflect a downstream exponential decay in the median grain size with numerous samples upstream of the Old River Control Structure within the coarse sand range but no such samples further downstream. At the transition into the backwater zone, the deposition of the coarse sediment likely maintains and possibly enhances the lateral channel migration due to the formation of bars. The largest rates of bank migration rates documented by Hudson and Kessel (2000) are in fact clustered within this transition zone, approximately 500 to 700 km upstream of the Head of Passes. The sediment is stored across the channel belt which, upstream of the Old River Control Structure, is approximately 10 to 20 km wide (Fernandes et al., 2016), much wider than the channel itself. A relatively short distance downstream, however, as the channel loses much of the coarse sediment it also loses its lateral mobility. This also enables levees to develop which, in conjunction with channel bed aggradation, create conditions that favor avulsion.

### 3.6 Conclusions

A deltaic experiment conducted under constant discharge and sea level provided a rich data set of flow kinematics in the upstream region characterized by one dominant and highly mobile channel. The most interesting observation is that this main channel moved across the experimental domain through lateral migration without relocation akin to an avulsion process. Over the course of 5 hours the centerline moved from one side of the experimental tank to the other following complex patterns with long periods of back and forth small moves punctuated by short bursts of rapid lateral migration. This is somewhat unexpected, given that the system experienced aggradation in excess of one full channel depth, that is, sufficient to trigger an avulsion. The idea that highly mobile, non-avulsive channels has been advanced before (Jerolmack and Mohrig, 2007) but not tested experimentally.

Using the changes in centerline position over one minute intervals ($\Delta\theta$) as a proxy for normalized migration rate, we documented the following quantitative kinematic aspects:

- A limited correlation exists between lateral migration rates estimated at successive moments at the same locations. Specifically, large or small centerline shifts seem to be followed by comparable shifts but not necessarily in the same direction.
- Synchronous channel migration rates at locations situated close to each other are strongly correlated but the correlation vanishes quasi-linearly with the distance between locations.

- At any given location, successive (i.e., one minute apart) changes in flow directions are inversely correlated. A good direct correlation exists between flow direction changes at a location and flow direction change downstream, one minute later.

We link the channel mobility to sediment rate and size by comparing the findings from the main experiment against a second deltaic experiment conducted with finer sediment size and lower sediment influx that shows limited lateral mobility and periodic channel relocations through abrupt flow reconfiguration equivalent to avulsions. The channel kinematics in the two experiments parallel two adjacent but morphologically different regions of the Mississippi River: the lower alluvial plain defined by high lateral mobility and sinuosity and the backwater zone characterized by much lower lateral mobility and periodic channel relocation. Our experimental findings suggest that one key reason why the transition into backwater zone reshapes the fluvial morphodynamics is the loss of coarse sediment and lateral mobility implicitly which, in conjunction with bed aggradation, makes the upstream portion of the backwater zone prone to periodic avulsions.

**Data Availability Statement**

The data used in this paper is available online (https://doi.org/10.5281/zenodo.5219070).

# Chapter 4. Synthetic Modeling of Deltaic Stratigraphy through Guided Stacking of Channel Networks

Dan Cazanacli[1,2], Chris Paola[1,2], Vaughan R. Voller[2,3]

[1]Dept. of Earth and Environmental Sciences, [2]St. Anthony Falls Laboratory, [3]Dept. of Civil, Environmental, and Geo-Engineering, University of Minnesota, Minneapolis, MN, USA

## Abstract

Forward modeling of deltaic stratigraphy at channel solving resolution poses significant challenges given the difficulties in modeling multiple channels that are part a coherent network. In this paper we introduce an alternative approach in the spirit of object based modeling but with important connections to the physical process. This approach is well suited for subaerial deltas which are characterized by stochastic processes such as avulsion and channel bifurcation that are difficult to implement numerically. Stratigraphic sequences are realized through superposition of topographic surfaces sampled from a large ($10^4$) database of distributary networks that are topologically similar to field deltas. We developed a metric to define similarity between networks (pairwise) and use vertical arrangements of similar simple topographic surfaces to approximate the incremental evolution of distributary systems. Evidence suggests that prolonged episodes defined by incremental network changes alternate with shorter episodes corresponding to flow relocation (i.e., major avulsions) and reconfiguration of the network. To better capture this pattern stratigraphically we investigated the dynamic of a deltaic experiment that reflects key field observations and developed a set of minimalist rules to guide the stacking succession. We contrast the results, referred to as guided stacking sequences, against two hypothetical types of sequences: one with randomly stacked networks and one in which successive networks are as similar as possible. The model, presented here as a proof of concept, requires a significant initial effort in building the database. However, the execution is straightforward allowing for fast exploration of spatial stratigraphic arrangements resulting from various assumptions.

## 4.1 Introduction

Modeling deltaic stratigraphy at channel resolution remains challenging despite progress in several key areas including better understanding of deltaic processes, increasingly complex basin scale models, and advances in numerical morphodynamic models or simplified equivalents, i.e., reduced complexity models. While dip section, 2D stratigraphic models (also referred to as laterally averaged or cross-shore models) have become more sophisticated, adding details in the third dimension at channel resolution remains difficult. The 2D models render the long term arrangement of the deposits by solving the partition of sediment between top-delta, delta front and pro-delta (deep) regions. If the complex aspects of buoyant plumes of fine sediment are omitted and other simplified assumptions are made, this partition can be solved analytically to include sea level variations, incision, and complex shoreline advance and retreat patterns (e.g., Swenson, 2005; Kim et al., 2006, Parker et al., 2008). The need to capture other complex aspects such as (differential) subsidence, compaction, variable basin geometry or multiple facies requires a more elaborate numerical program like DELTASIM (Hoogendoorn et al., 2008).

An intermediary step towards a more detailed, channel solving stratigraphy are those models that capture the 3D shape of deposit sets, typically the quasi-conical foreset deposits. Earlier examples assume that a dominant deltaic channel moves randomly in a radial pattern to distribute the sediment quasi-uniformly at the shoreline (Ritchie et al., 1999, 2004; Overeem et al., 2011). Other models crudely solve the flow and sediment routing starting with an irregular topography and routing the flow dispersively (cf. Hajek and Wolinsky, 2012 - flow distributed to all lower neighboring cells, not just to one cell as done in the steepest descent method) which yields bifurcations and avulsions (Karssenberg and Bridge, 2008; Dalman and Weltje, 2008). Dionsios, a diffusive model (Granjeon, 2014; Harris et al., 2016), uses a coarse (i.e., much larger than typical channel width) horizontal grid but a finer vertical discretization to explores basin scale stratigraphy under variable eustatic level. Falivene et al. (2019) presented a more complex basin scale diffusion model that combines the elements of dispersive flow and sediment routing, variable eustatic level, and a simplified facies distribution (sand proportion).

These 3D models employ a grid size larger than typical channel width and do not capture the channel geometry but rather establish major flow and sediment routes connecting the terrestrial domain to the delta front, an approach that may be adequate when the bulk of accumulation occurs at the delta front forming thick foreset deposits. However, as Edmonds et al. (2011) showed, for many deltas the bulk of the deposition

occurs in the subaerial deltaic region. These top-set dominated deltas tend to be low slope deltas with relatively shallow receiving basins. Their internal structure is defined by network planform, thus, solving the channel details is important.

Analytical solvers for water and sediment routing that employ shallow water equations and sediment transport relationships typically operate with small time steps and small grid size and are impractical for long term, large scale simulations. Alternative options include numerical models that operate with longer time steps or acceleration schemes. Sophisticated morphodynamic models like Delft 3D (e.g., Geleynse et al., 2010; Hillen et al., 2014), NAYS2DH (e.g., Schuurman et al., 2016), CAESAR-Lisflood (Coulthard et al., 2013), or HSTAR (Nicholas, 2013) are aimed mostly at short term exploration (though van de Lageweg et al. 2016 have used NAYS2DH to explore millennial depositional patterns in a meandering belt). Of these, only Delft 3D has been designed for the deltaic domain. Few other models that can render deltaic channels come from the reduced complexity spectrum. The models by Seybold et al. (2007, 2009) are focused on planform morphology whereas DeltaRCM (Liang et al., 2014; Liang et al., 2016) can also capture the deposit accumulation. Delft3D has not been used to explore long term stratigraphic architecture but rather specific, meso-scale aspects such as the effect of hydraulic forcing (river flow, tides, or waves) on delta evolution (Geleynse et al., 2011, Hillen et al. 2014), the impact of sediment properties (i.e., cohesion, sand fraction) on the deltaic morphology (Edmonds and Slingerland, 2009; Caldwell et al., 2014; Burpee et al., 2015) or impact of discharge on the channel network configuration (Edmonds et al., 2010). Similarly, DeltaRCM has been used to explore changes in deltaic planform and deposit accumulation under varied sea level (Liang et al., 2016). Both DeltaRCM and Delft3D operate on fixed Cartesian grids and render deltaic morphology at channel scale resolution. Rendering realistic channel planforms, however, remains challenging in part because the bank erosion is assessed through simplified sediment partition schemes that do not capture the channel curvature details and could also inhibit channel migration (Nicholas, 2013).

Although in principle it may possible to improve the resolution of these models and, with ever increasing computational power, extend a computer run to simulate tens of thousands of years of deltaic evolution, a detailed dynamic simulation of a complex system on the finest grid possible is not necessarily the proper recipe for capturing the stratigraphic details of interest (Paola 2000). While there are well established equations for channel flow and sediment transport, there is unsolvable uncertainty due to the variable nature of the input drivers (e.g., basin configuration, climate, hydraulic regime, sea level)

and the heterogeneity of sediment deposits. Additionally, other aspects such as cohesion or the vegetation flow interaction, both important for planform morphology, are difficult to quantify.

Given these considerations we turn our attention towards an alternative, more direct approach. Broadly speaking alluvial architecture models fall into two categories, process imitating and structure imitating (for a comprehensive discussion see Coulthard and Van De Wiel, 2012). The stratigraphic models mentioned above are based on some form of forward model process and belong to the former category. Structure imitating models tend to circumvent the dynamic approach. Most are object based models (e.g., Omre, 1992; Jones and Larue, 1997; Deutsch and Tran; 2002) and involve filling the subsurface volume by randomly placing discrete idealized depositional units (e.g., channel, point bar, overbank deposits) based on some global stochastic rules (e.g., proportion of facies, net to gross ratio). The evolution of object based models has been driven by practical goals: to quantifying the connectivity of porous space for fluid (water, oil or gas) extraction. The key advantage is that object based can be easily conditioned to fit existing data, a task that is difficult to achieve with forward models. At the same time, due to their stochastic nature, object based models are largely decoupled from the geologic process which calls into question whether such models can realistically approximate the geometry and distribution of natural facies types (Bridge, 2008). To mitigate this aspect some models, termed event based models, employ a hybrid approach, placing the objects in a way that also mimics basic dynamic processes, such as channel lateral migration (e.g., Pyrcz et al., 2009).

The modeling method introduced in this paper is also a hybrid one with several particularities. It is a kinematic construction that instead of objects relies on vertical stacking of topographic surfaces corresponding to subaerial deltas. Through vertical staking of distributary networks, or rather the topographic surfaces associated with these networks, we aim to capture the long term progression of an evolving delta by assembling the probable spatial arrangement of the deltaic deposits, viewed simply as channel fill and floodplain sheet like deposits. The aggradation rate is defined implicitly as the space between successive surfaces. We argue that superimposing surfaces that are geometrically similar is an adequate way to capture successive moments in the evolution of aggradational subaerial deltas.

The topographic surfaces are derived from a database of deltaic networks generated using a rule based model, detailed in a companion paper and presented succinctly here. Several metrics for comparison indicate that the network realizations are similar to the natural distributary networks. The surface stacking rules are crafted based on the dynamic of a deltaic experiment that exhibits many of the essential characteristics of natural systems. These two aspects, the networks realizations and stacking rules guided by an experiment that represents a good field analogue, provide indirect but strong connections to the geologic process.

The paper is structured as follows: In Section 2 we describe how we assembled the database of networks, how we converted the centerline networks to three dimensional topographic surfaces, and introduce a method for assessing the similarity between networks. In Section 3 we present the arguments in favor of our model approach, discuss stacking order considerations, and introduce a deltaic experiment whose dynamic serves as a guide for building the stacking sequence. Method implementation, results, and implications are presented in Section 4. As customary, a discussion section precedes the ending conclusions.

### 4.2 Database of Topographic Surfaces

#### *Network Set*

The stratigraphic simulation introduced here relies on a large set ($10^4$) of deltaic networks that were generated using an algorithm for distributary networks described in detail in a companion paper. The algorithm combines a piecewise method of extending individual channels with a discrete probability of bifurcation applied uniformly to each growing channel. All networks originate from a short stem channel. At each step, each channel is extended by one small segment of unit length. The direction of each newly added segment relative to the previous segment (i.e., the angular deflection) is sampled from a normal distribution with a mean of zero and a standard deviation of 2°. Additionally, to render centerline curvature persistency common to natural channels, we impose a degree of correlation between successive deflections, namely a clockwise or counterclockwise deflection has approximately 80% chance to be followed by a deflection in the same direction. These numerical choices for channel growth yield a sinuosity range which, on aggregate, matches the range of many natural deltaic channels. Each channel grows one

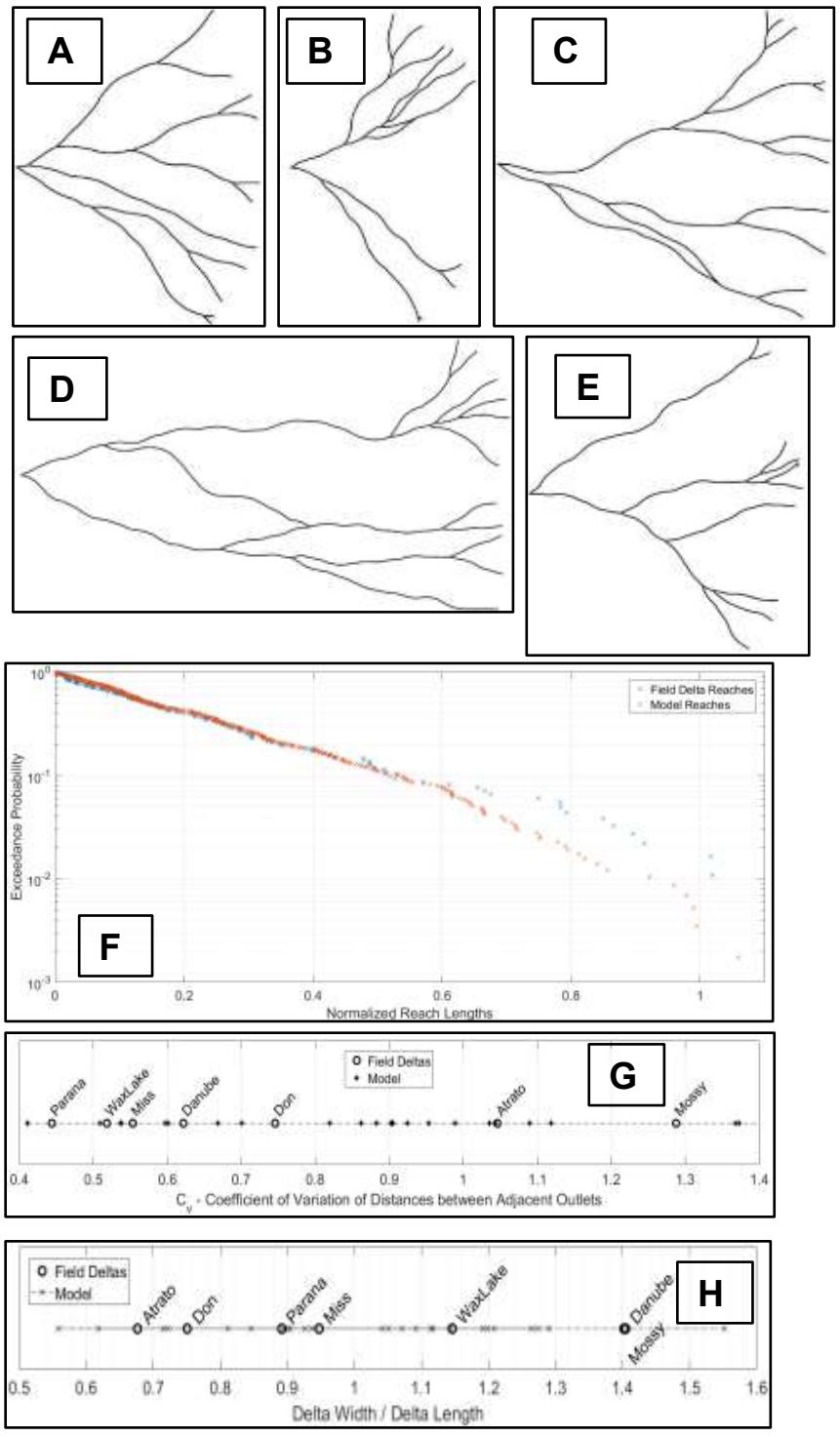


**Figure 17. A-E: Examples of complex deltaic networks generated using the same generic algorithm (see text). F-H: Comparison between a set of 40 realization and several river dominated field deltas in terms of: distribution of individual branches lengths (F), dispersion of distances between adjacent outlets (G), and delta shape aspect, width over length, (H).**

piece at each step and, to form networks, at each step each channel has a small, uniform probability (i.e. ~1%) of splitting into two channels forming a bifurcation with an average angle of 48° and standard deviation of approximately 5°. It should be noted that Coffey and Shaw (2017) documented that the average bifurcation angle at the point of channel separation is 70.4°, close to a theoretical value of 72°. However, a short distance downstream of about two channel widths the resulting channels “pull closer together” resulting in an opening angle of about 48° to 55° or slightly smaller if measured further downstream.

This algorithm generates dimensionless networks in which the channels are represented by their centerlines with no elevation, slope, cross section size or shape expression. Although the algorithm suggests a delta growth process, we do not assign a specific genetic mechanism to this method and are instead preoccupied with the final topologic results. Due to the random nature of generating mechanism, even though we employ only four parameters sampled from the simplest distributions (i.e., uniform and normal) the same code executed multiple times generates a wide variety of geometric outcomes as illustrated in Figure 17. This variety, however, appears to be a trait of many field deltas as well. We compared the results against a set of river dominated deltas that were skeletonized and reduced to their dimensionless topological representation. The model results compare well against the set of natural deltas in terms of several key geometric features: (a) distribution of lengths of individual branches normalized by delta length; (b) distribution of bifurcation nodes between apex and shoreline; (c) dispersion of the distances between outlets (i.e., delta mouths) quantified as the coefficient of variation of distances between adjacent outlets, and, (d) delta shape described simply as width over length (Figure 17).

The network generation mechanism described above can run for an arbitrary number of steps to form networks of only a few channels or much denser networks with dozens of channels or more. Our goal here is to introduce a geometric model for generating synthetic stratigraphy in a simple form, as proof of concept. Thus, we generate a network database in a form that is relatively simple, unencumbered by the complexity of aggregating and comparing networks that vary significantly in size or channel density. With this in mind we generated a set of $10^4$ simple networks averaging approximately four terminal channels (Figure 10). Furthermore, all networks originate from the same point and the size of the domain is kept constant.

***Topographic Surfaces***

To explore stratigraphic arrangements of deltaic deposits we need to convert the dimensionless, skeletal networks into networks with a physical, three dimensional representation. We do so without introducing explicit physical units but by using relative dimensions that, on average, approximate the proportions found in nature. We go from centerlines to three dimensional channels assuming a constant channel width (*W*) to depth (*d*) aspect ratio of 30, justified in part on hydraulic geometry empirical relationships in which depth and width are a power function of the discharge (*Q*). While regression equations show a power law relationship between width and depth in which the aspect ratio increases with the size of the river (Bridge and Mackey, 1993; Konsoer et al, 2013), for most channels in the depth range of several meters, the aspect ratio is in the neighborhood of 30. Furthermore, empirical relationships for deltaic channels developed by Andren (1994) show a narrow *W/d* range of ~28 to 30 over a wide range of discharge values. Other empirical equations that, in addition to discharge, take into account slope and median bedload grain size point to a similar aspect ratio range (Julien and Wargadalam, 1995; Lee and Julien, 2006) and the median values of width and depth for preserved fluvial channels compiled by Jobe et al (2016) are approximately 300 m and 11 m. In addition to the aspect ratio, the channel geometry is approximated through a common parabolic cross-section shape. We assumed a simple generic levee shape in which the levee height adjacent to the channel is equal to 10% of the maximum channel depth and the levee height decays exponentially with distance away from the channel (e.g. Bridge and Leeder, 1979) blending into a flat floodplain surface at distance equal to five times the channel width, measured from the edge of the channel.

This generic cross-section geometry needs to be scaled to reflect the flow magnitude. Channel width can be related to the discharge using a power relationship of form $W \propto Q^{0.45}$. The exponent 0.45 is an average of several values from empirical hydraulic geometry relationships (Andren, 1994 – 0.39; Julien and Wargadalam, 1995 – 0.43; Lee and Julien, 2006 – 0.44; Konsoer et al, 2013 – 0.52). A discharge value of 1 (unit) is assumed at upstream boundary, at the apex of each network. To conserve flow we use a simple random flow partition at each bifurcation, within prescribed limits. The following formula employs a random uniform distribution and renders random flow partitions between 1:1 and 3:1:

$$Q_1/Q_0 = 0.25 + 0.5\ \mathbf{U(0, 1)};\ \text{and}\ Q_2/Q_0 = 1 - Q_1/Q_0 \quad (7)$$

Where $Q_0$, $Q_1$, and $Q_2$ denote the flows in parent channel and the two resulting channels. At macro scale we assume a constant slope of the delta surface, a simple but reasonable assumption for deltaic systems whose hydrologic regime does not change drastically over time. We should also note that the longitudinal slope or shape is well captured in the 2D models discussed above whereas here the main goal is to describe the stratigraphic architecture at channel resolution in cross-flow (strike) sections, that is, the direction *not* captured in the 2D, laterally averaged models.

***Networks Comparison***

On the premise that a series of similar channel networks drawn from a database represent successive stages in the evolution of a subaerial delta, a method of comparing and quantifying the degree of similarity between networks is needed. Given that the goal is to use successive networks as a proxy for the channel migration, highly correlated networks are those with high percentage of channel overlap. The channel width, however, is small relative to the width of the delta plain. Thus, the amount of overlap is small and prone to arbitrary results. Two channels that are close spatially may have very little to no overlap while two different channels may intersect each other multiple times and have more overlap. To circumvent this challenge we applied a Gaussian smoothing to the network

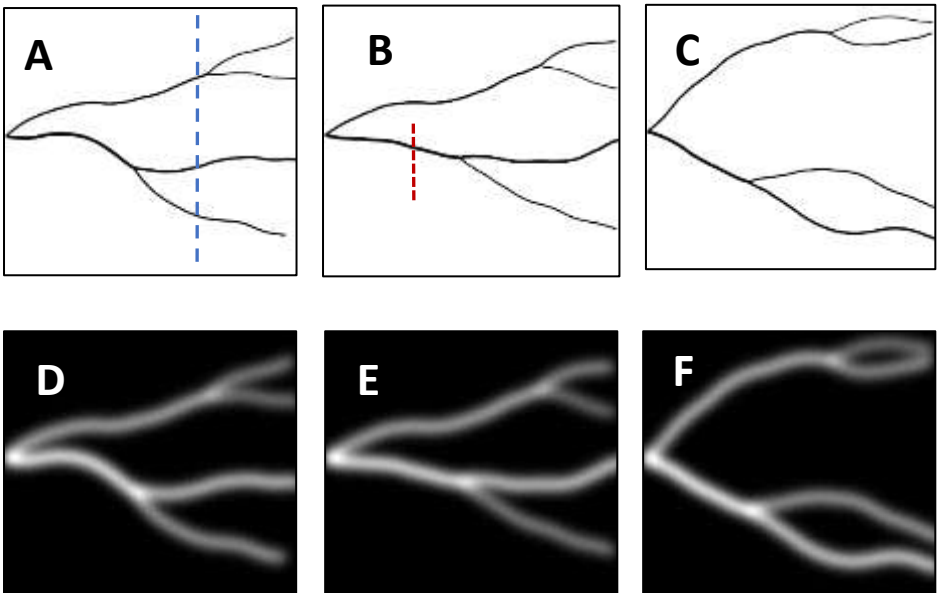


**Figure 18. A-C: Examples of networks from the database used in this study. B. is the network that is most similar to A., whereas C. is the least similar to A. D-F: same three networks "blurred" via a Gaussian diffusion filter to enable comparison via cosine similarity (see text). Colors were inverted for better visualization. Blue and red dashed lines represent cross-section locations for Figures 21 and 24, respectively.**

images to create a set of blurred images. Three examples based on the same networks depicted in Figures 18A-C are shown in Figures 18D-F with reversed colors for better visualization. White represents the channel and the gray scale represents distance away from the actual channel. Wider channels translate into wider white-to-gray bands. We compare these blurred images pairwise via cosine similarity, that is, the dot product of two high dimension vectors, each dimension being a pixel value (i.e., 0 to 255 – black to white).

By comparing all networks pairwise we obtain a symmetrical $10^4$ x $10^4$ matrix in which values closer to 1 correspond of highly correlated images while values closer to 0 correspond to uncorrelated images. Using the network in Figure 18D as reference, Figure 18E depicts the network that is most similar to it, while Figure 18F depicts the network that is least similar to it. The main attributes of the similarity matrix are summarized in Figure 19 where the colored lines illustrate the idea that some networks are, on aggregate, more similar to the rest of set than others. Nonetheless, the similarity between any given network and another one that is most similar to it is relative high (gray line), above 0.92 in most cases. Overall, the cosine similarity for all distinct pairs ranges approximately from 0.09 to 0.98. Values closer to zero are unlikely given that, by design, all networks originate in the same place from a short stem channel. Higher values are possible but with a considerably larger set that would render pairs of nearly identical networks.

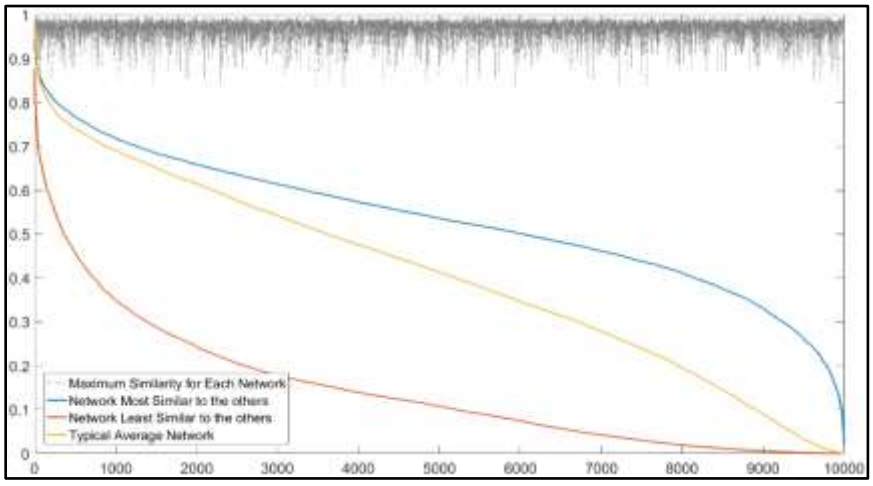


**Figure 19. Synopsis of similarity values (i.e., dot product – see text) between pairs of networks in the database. Top gray line shows the similarity between each network and its closest equivalent. Thick lines show similarities between three particular networks and all other networks in the database, sorted in descending order. Blue/Red are the networks that, on aggregate, are the most/least similar to the other networks in the data base. Yellow is a typical, average network.**

While more sophisticated statistical techniques for comparing networks may exist, this simple estimate of similarity using the dot product can robustly assess the overall spatial displacement between two networks placing the emphasis on the average channel position and less on the details of planform trajectory which in the case of natural channels shifts continuously.

### 4.3 Surfaces Stacking Model - Description

#### *General Arguments*

At the crux of our approach is the use vertical arrangements of fixed surfaces to replace the evolution of channel networks in order to generate stratigraphic packages. We argue that a database of networks that is sufficiently large can capture, in an approximate sense, nearly all the configurations that a deltaic system (i.e., few channels) can take. Thus, an episode of continuous evolution of a deltaic system can be approximated through a vertical succession of surfaces in which every added surface is geometrically similar to the previous one. In a way this modeling method is reminiscent of an old movie making technique from late 19$^{th}$ century in which the perception of continuous motion (i.e., a running horse) is rendered through mechanical spinning of a wheel with a set of still drawings on its perimeter. In this precursor of animated gifs each drawing is most similar to the adjacent ones. Likewise, in our approach, episodes of incremental continuous evolution are captured by stacking networks in an order that is based on a measure of similarity. The essential difference, however, is that we do not pick the sequence of networks to create a pre-defined "movie", i.e., a pre-defined scenario for the evolution of a deltaic system. Instead, we sample the networks stochastically (based on rules that are discussed further below) to generate a probable surface evolution sequence, a sequence that is not defined a priori but rather emerges from the sampling rules.

One obvious criticism is that stacking networks from a database has no direct connection to the physical process through which a network evolved dynamically. Fluvial stratigraphy, however, is dominated by lateral accretion and the rate of lateral migration is relatively high to the aggradation rate (e.g., Jobe et al, 2016). Consequently, the evolution of the channel trajectory is poorly retained in the stratigraphic record with new channel incision eroding into previous channel bars, levees, and floodplain deposits. This argument has been made previously by Sylvester et al. (2011) who showed that one single major channel with constant dimensions can build complex deposit shapes as it meanders across an aggrading plain, reworking most of the sediment. To track the channel trajectory

in time the authors used one of the first and simpler meander migration models developed by Ikeda et al. (1981). Other bank retreat single channel meandering models exists (e.g., Howard and Knutson 1984; Furbish, 1991; Sun et al, 1996) and more sophisticated migration models have been developed as well (e.g., Zolezzi and Seminara, 2001; Limaye and Lamb, 2014). To the best of our knowledge there is no analytical equivalent of such models for distributary networks. This may be in part because single channel migration models assume a freely moving centerline at the downstream end which would pose a challenge in attempting the migration of all individual branches of a delta. Another important observation is that deltaic systems do not seem to exhibit the same regular meandering patterns as rivers. Mississippi's delta region vs the upstream alluvial plain provide a good contrast. In the deltaic region the channels have a much lower lateral mobility (Hudson and Kessel, 2000), in part because of the increased cohesion. Because of these particularities and the difficulties of modeling the evolution of distributary networks, deltas are a good candidate for the surfaces stacking method introduced here.

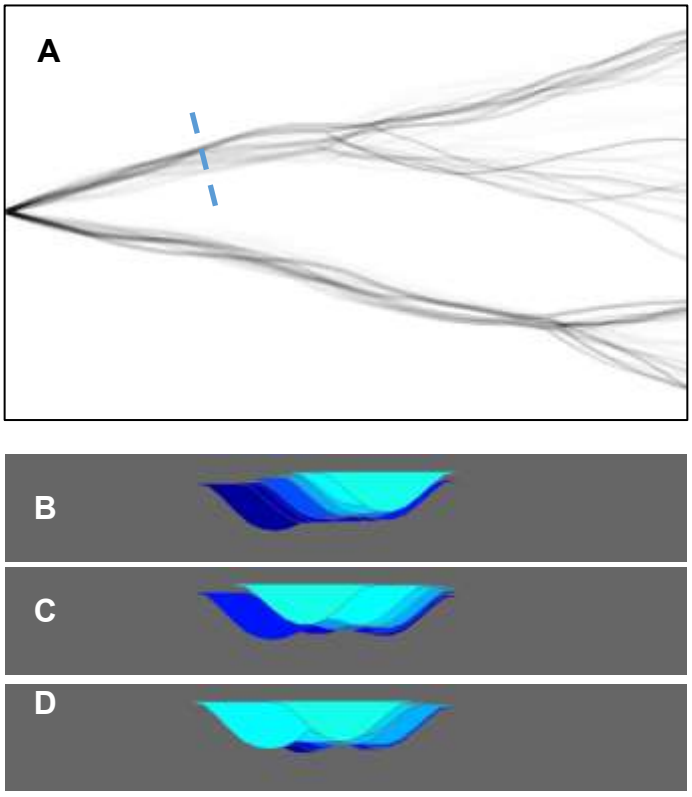


**Figure 20. A: Fifteen networks from the database that are similar to one another can be viewed as stages in evolution of an aggrading delta surface (light gray to black). B-D: channel cross-sections (V.E. x10) taken along the dashed line. Same fifteen cross-sections are stacked in random successions (dark to light shades). The cross-sections illustrate that, although the details of the channel fill body are different, when the aggradation rate is small relative to the lateral migration rate the result is qualitatively the same when viewed in the context of large scale stratigraphy.**

Furthermore, because in fluvial systems the lateral migration rate greatly exceeds the vertical accretion rate, different channel trajectories can result in a stratigraphic signatures that are qualitatively very similar. This notion is illustrated in Figure 20. Figure 20A shows a series of 15 networks that are similar to each other and can be viewed as

discrete moments in time in the evolution of the same delta. In terms of stratigraphic signature the exact order of occurrence is not crucial. This is apparent in Figures 20B-D that depict the migration of a single channel through 15 distinct positions in different order (i.e., random permutations of the same 15 positions). At a close inspection the shape of the channel fill body is indeed different but in the big picture the stratigraphic signature is essentially the same: a clustered channel deposit. In other words, at the macro scale, the timing of the short term succession is not crucial. This assumption would not be equally valid in the case of submarine channels where the ratio of vertical aggradation to lateral migration is considerably larger (Jobe et al, 2016).

***Stacking Order Considerations***

In stratigraphy, stacking patterns are a fundamental defining property of the deposits across all scales (Catuneanu, 2019). Having a large data set of deltaic surfaces and a metric for comparing the networks, the essential question is how should the networks be stacked to best approximate a plausible natural stratigraphic sequence?

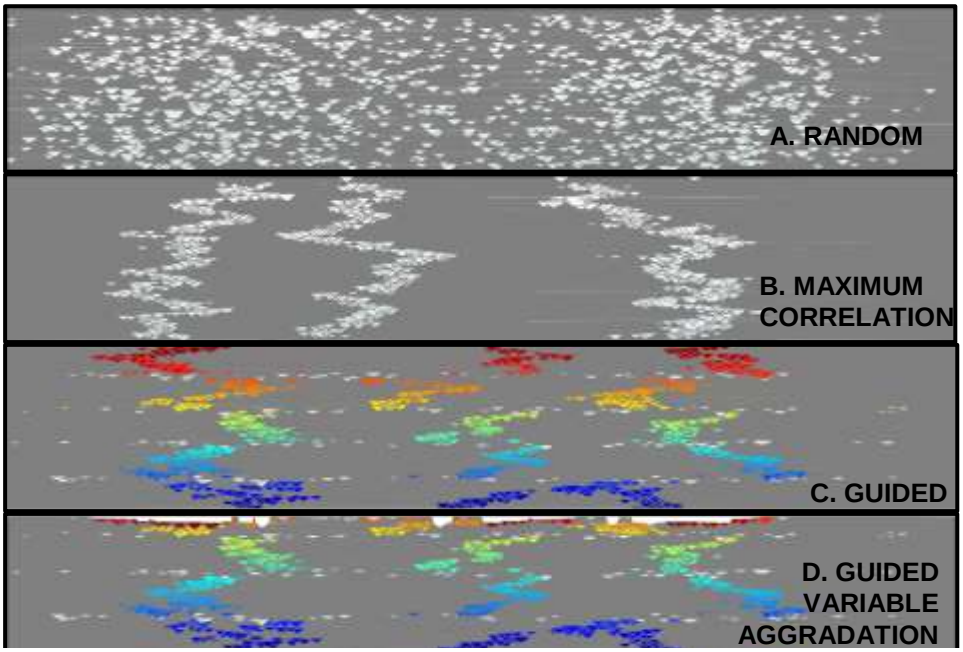


**Figure 21. Synthetic stratigraphy (V.E. x10) at a downstream location (see Figure 2A), generated by stacking networks from the data base (see text for details). A: Hypothetical random stacking. B: Hypothetical correlated stacking (each network succeeded by the network most similar to it). C-D: Guided stacking using a set of minimal rules (see text). Correlated packages are separated by thin sequences (white) corresponding to avulsion episodes. In A, B, and C the aggradation rate (i.e., vertical space between successive layers) is constant whereas in D it decreases progressively towards the top, reaching zero and turning negative (incision). C and D are comprised of the same set of networks.**

Figures 21A and 21B illustrate hypothetical end members of stratigraphic patterns obtained by stacking networks in random order versus a correlated order in which each network is followed by the most similar network in the set (excluding those previously used). The stratigraphic signature is clearly different. In Figure 21A the channel fill deposits are randomly scattered whereas in Figure 21B the channels shifted in small increments. In both cases we assumed that the entire delta surface aggraded in equal increments. Thus, the stratigraphy depicted in Figure 21 is an implicit outcome that reflects the deposition between surfaces erosion as well. As channels migrate laterally they cut into underlying surfaces. The coarse sediment (sand) is preserved as channel fill deposit (abandoned channels and channel bars) while the fine sediment is preserved as floodplain deposit (dark color).

Evidently, Figures 21A and 21B are hypothetical. Intuitively, to approximate the probable evolution of a deltaic system, packages of similar networks should be stacked together. However, such coherent sequences are likely to be disrupted by episodes of regional avulsions (e.g. Hoffmann et al., 2011) that result in reconfiguration of the deltaic domain. Avulsion has been long recognized as an essential process shaping the fluvial architecture. The frequency and style of avulsions determine the spatial distribution of sandy deposits, primarily channel-fill but also near-channel deposits (crevasse-splays and levees). Earlier avulsion models treated avulsion as a random process (Leeder, 1978; Allen, 1978) or spatially random but with frequency linked to the deposition rate (Heller and Paola, 1996). Allen (1979) pointed out that “real alluvial sand-body packings are probably neither perfectly random nor perfectly correlated” and proposed that an avulsion creates a new channel planform that avoids alluvial ridges formed along old channel belts. This idea that the bands of active deposition along active channel belts would, after a period of vertical aggradation, avulse and relocate to fill topographic lows is referred to as compensational stratigraphy. A comprehensive description of compensational stratigraphy with examples from experiments, outcrops, and subsurface exploration is provided by Straub et al. (2009) along with model simulations. Jerolmack and Paola (2007) take a different view and suggest, based on a simple gridded model, that the alluvial architecture may be defined by repeated flow switches along few established channel routes, an idea supported by field examples in which modern avulsions redirected the flow along nearby abandoned channels routes (e.g., Slingerland and Smith, 2004). Based on well data Hoffmann et al. (2011) interpreted the architecture of the Williams Fork Formation as showing both evidence of clustering at the scale of single or multi-storey

sand bodies and compensational stacking at a greater scale of hundreds of meters. The channel-fill clustering idea is supported by a growing body of evidence derived from interpretation of modern deposits (Olariu and Bhattacharya, 2006), experimental results (Sheets et al., 2007), outcrops (Hajek et al., 2010; Hampson et al., 2012; Chamberlin and Hajek; 2015; Chamberlin and Hajek; 2019), or subsurface data (Hoffmann et al., 2011).

***Guiding Experiment***

To address the question of what is the plausible stacking order, rather than creating arbitrary rules to describe the avulsion style and frequency or the channel clustering patterns, we tapped into the dynamics of a deltaic experiment in order to guide the stacking process. The experiment was conducted at St. Anthony Falls Laboratory in the Delta Basin, a square tank with 5 m sides where water, sediment, and color pigment were introduced from a corner, leading to formation of a deltaic deposit with an approximate plan surface of a quarter circle. The tank was initially filled with 0.18 m of water, a level that was kept constant throughout the experiment. The focus of our investigation is a 13-hour interval during which the shoreline extended from approximately 2.5 m to 3 m, while the surface of the deltaic deposit aggraded approximately 0.1 m. The sediment consisted of walnut shells with a relatively uniform size ($D_{50}$ = 0.25 mm) fed at a constant rate of 1.6 mL/s while the water discharge was also kept constant at 32 mL/s.

In the upstream region of the delta, for the majority of the time there was one dominant deltaic channel moving laterally back and forth within a narrow range (i.e., ~3-4 channel widths) over tens or hundreds of minutes. These relatively quiescent intervals were separated by shorter and more active periods during which the flow structure changed rapidly via single or multiple bifurcations. As these bursts of diverging flow waned, the stable style resumed with the dominant channel in different location (Figure 22A), an indication of compensation stratigraphy style. We equate these bursts of activity with regional avulsions driven by channel infill and a reduction in longitudinal slope due to local shoreline extension. Given the homogenous nature of the sediment, investigating the layer arrangements in the experiment deposit was not possible. We focused instead on the surface dynamics. Browsing through the photographs taken one minute apart allowed us to separate the quiescent intervals from the bursts of flow reconfiguration and main channel relocation. The percentage of area changed, from dry to wet or from wet to dry, in the upstream region of the delta is mapped in Figure 22B. It is important to note that the flow relocation was not instant but lasted from approximately 10 to 30 minutes during

which the flow spreads quasi randomly into multiple unstable channels to eventually coalesce into one stable dominant route. This transient period has been also documented in natural systems (e.g. Smith et al., 1989; Kleinhans et al., 2008) or experiments, by Hoyal and Sheets (2009) who refer to this interval of searching for a new flow path with a steeper gradient as “finding”.

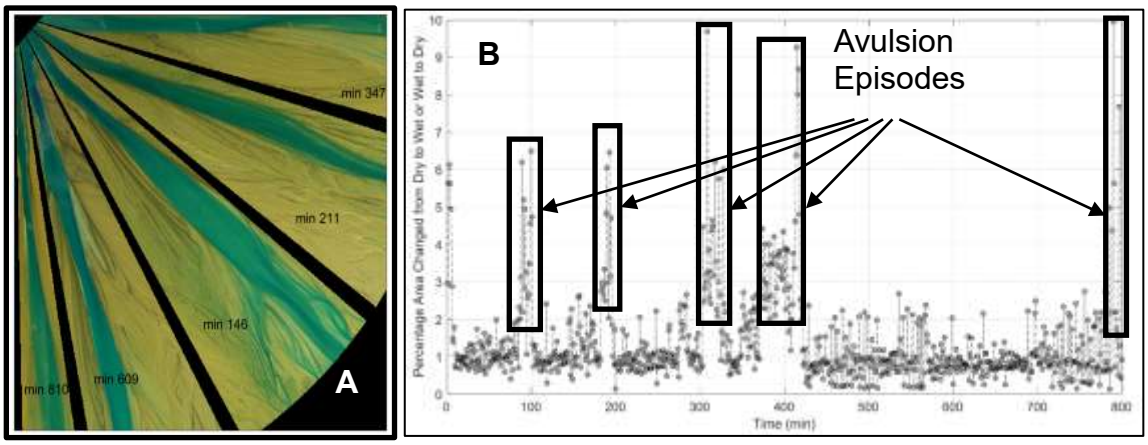


**Figure 22. A: Composite top view of a deltaic experiment illustrating that the main channels has migrated across the entire domain yet it remained confined within a relatively narrow sector (several channel widths) for extended periods of time. B: Percentage of area that changed from dry to wet (or wet to dry) during one minute intervals. Note how extended periods of relative little change were separated by shorter intervals of flow divergence and reconfiguration (i.e., avulsions). The avulsion episodes (rectangles) were identified by visually inspecting of all photographs.**

We argue that this systematic behavior of extended intervals of channel moving in small increments within a narrow sector separated by bursts of flow divergence and reconfiguration is a good approximation of how a natural system may evolve, resulting in a stratigraphic succession that is defined by both coherent packages with channel clustering and avulsion episodes resulting in relocation of the channel belt(s). Thus, the dynamics of experiment can serve as a guide for the stacking of topographic surfaces networks in an informed, guided fashion.

### 4.4 Implementation, Results, and Implications

#### *Implementation*

In order to build stratigraphic sections that we refer to as “guided stacking sequences” we employ a minimalist set of rules to render quasi-regular thicker packages separated by thinner series of dispersed channels.

(a) Denoting the current network in the stacking process as $n_i$, a simple way to build the thicker, correlated packages is to select the network above it, $n_{i+1}$, from a group of networks that are highly similar to $n_i$, say, a cosine similarity above a threshold of 0.9, essentially performing a Monte-Carlo simulation to obtain a package of highly similar networks stacked on top of each other randomly. An even simpler option is to choose the network that is most similar to $n_i$:

$$\boldsymbol{n_i} \bullet \boldsymbol{n_{i+1}} = max(\boldsymbol{n_i} \bullet \boldsymbol{n'}) \quad (8)$$

Where *n'* denotes any network in the database, except for those already used. Though it may appear that in choosing the most similar network the outcome would be predetermined resulting in identical packages for each simulation, it is sufficient to select the first network randomly to generate a different sequences. Given that only a small fraction (i.e., few percentages) of all networks in the database are used to generate stratigraphy numerous simulations can be generated using this very basic rule.

(b) To increase the chance that the channel fill deposits (colored deposits in Figure 21C) are spread across the entire domain, as a crude way to approximate compensational stacking, the bottom network in each of the thicker, correlated package was selected from a set of networks that is rather dissimilar from the top network in the previous correlated package:

$$0.2 < \boldsymbol{n_i} \bullet \boldsymbol{n_{i+q+1}} < 0.5 \quad (9)$$

Where *q* is the number of networks separating the correlated packages. A lower limit of 0.2 was used to avoid selecting from those ~1% of networks that are least similar to the rest of the set.

(c) The networks comprising the thinner uncorrelated sequence (white deposits on Figure 21C) are drawn such that the cosine similarity between successive networks falls within 0.5 to 0.9 range:

$$0.5 < \boldsymbol{n_i} \bullet \boldsymbol{n_{i+1}} < 0.9 \quad (10)$$

The upper limit was chosen to avoid a sequence of similar networks that would resemble the correlated pattern whereas an approximate lower limit was employed to ensure that the networks comprising these thin sequences are not entirely dissimilar; the experiment data shows that even during the avulsion episodes there is a good amount of overlap (Figure 22B).

***Results***

The rules described above can now be used to generate stratigraphic arrangements that we refer to as guided stacking sequences. Figure 21C depicts a guided stacking scenario in which thicker packages of 60 to 70 networks stacked in a correlated order, are separated by thinner sequences of ~15 less correlated networks. The sequence reflects the basic aspects discussed above: channel clustering and lateral migration (colored packages), and flow spread during avulsion intervals (white packages). The intent was not to mimic the dynamics of the experiment but rather the style. For example, in the experiment, episodes of flow reconfiguration that we interpret as avulsions occurred somewhat irregularly (Figure 22B). The longer duration between the last two avulsions is likely a particularity of the experiment, namely the delta extension translates in a reduction in aggradation rate given that sediment is fed at constant rate but spreads over an increasingly larger surface (Lorenzo-Trueba et al., 2009). Since the avulsion time is proportional to the aggradation rate (Mohrig et al., 2000; Jerolmack and Mohrig, 2007) it follows that, everything else being equal, the avulsion time increases with the shoreline extension. In our simplified construction, however, we assumed a constant aggradation rate, a reasonable assumption if the sediment flux is more or less constant, and the sea level rise offsets the delta growth such that the shoreline remains quasi-stationary.

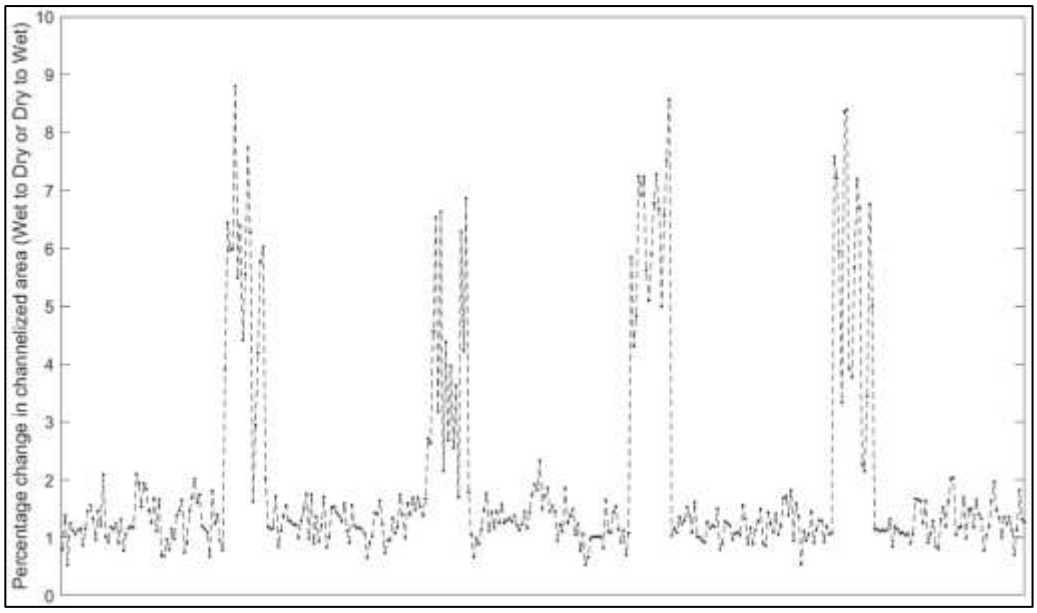


**Figure 23. Change in channelized surface (wet to dry or dry to wet) between successive network stacking realizations based on the controlled stacking scenario depicted in Figure 21C.**

The changes in the experiment are documented at 1-minute intervals whereas no time interval is associated with the deposition between successive surfaces in the simulation. Nonetheless, we can compare the outcomes relatively. Figure 23 shows that the changes in channelized areas between successive networks are comparable to the changes observed in the experiment (Figure 22B). Specifically, within the correlated packages the percentage change is quasi-random yet within a relatively narrow range while within the thinner intervals the percentage of change varies within a broader range from values that overlap those within correlated packages to values that are several times larger, which is also what the experiment reflects. It is important to note that this is an emergent outcome stemming from the rules described above.

***Implications***

Object based models have an essential practical advantage over forward numerical models: they can be relatively easy conditioned to fit existing data. This is essential in oil exploration where the main goal is to describe the spatial connectivity of the objects with high hydraulic conductivity, such as channel facies. Quantifying the connectivity of deposits for fluid extraction purposes is statistically complex (see review by Renard and Allard, 2013) and implies some knowledge about the granular properties of the deposits. In the stratigraphic construction introduced here, the deposits are only defined qualitatively, as coarse or fine (i.e., channel or non-channel). Thus, an assessment of connectivity at granular scale is outside the scope. We provide instead an evaluation of the channel fill arrangements as a crude way of assessing the spatial continuity of the coarse deposits for the three types of sequences showed in Figures 21A-C.

The spatial channel fill clustering patterns that emerge from the guided stacking method described above are markedly different from either a random sequence or from an entirely correlated one. Visually, this is apparent by contrasting Figure 21C against Figure 21A or 21B, respectively. To quantify these differences in a more formal way we tracked the position of a single channel. For this purpose we look at a transect taken at a short distance downstream from the apex, where only two channels are present and focused only on one of the channels. Figure 24A illustrates schematically the location of the channel under correlated, random, and guided stacking scenarios. Figure 24B shows the lateral migration of the channel between successive networks, normalized by the average channel width ($\hat{W}$) and sorted in ascending order. The lateral channel shift, whether to the left or right, is measured as an absolute value, $|\Delta x|$. For the correlated sequence the mean

channel shift value is 0.15 $\hat{W}$. More importantly, the largest shifts are smaller than 1 $\hat{W}$ meaning that in this hypothetical arrangement the channels fill is connected throughout the entire sequence. By contrast, the random sequence has a mean $|\Delta x|$ of 2.15 $\hat{W}$, with most values exceeding 1 $\hat{W}$ which reflect that channel fill deposits are scattered and largely unconnected. The mean channel shift for the guided sequence is 0.62 $\hat{W}$ with approximately 80% of the shifts less than 1 $\hat{W}$, reflecting a clustering tendency. The standard deviations ($\sigma$) of channel shifts for the three kinds of sequences have similar relative magnitudes. For the random sequence $\sigma = 1.90$, approximately one order of

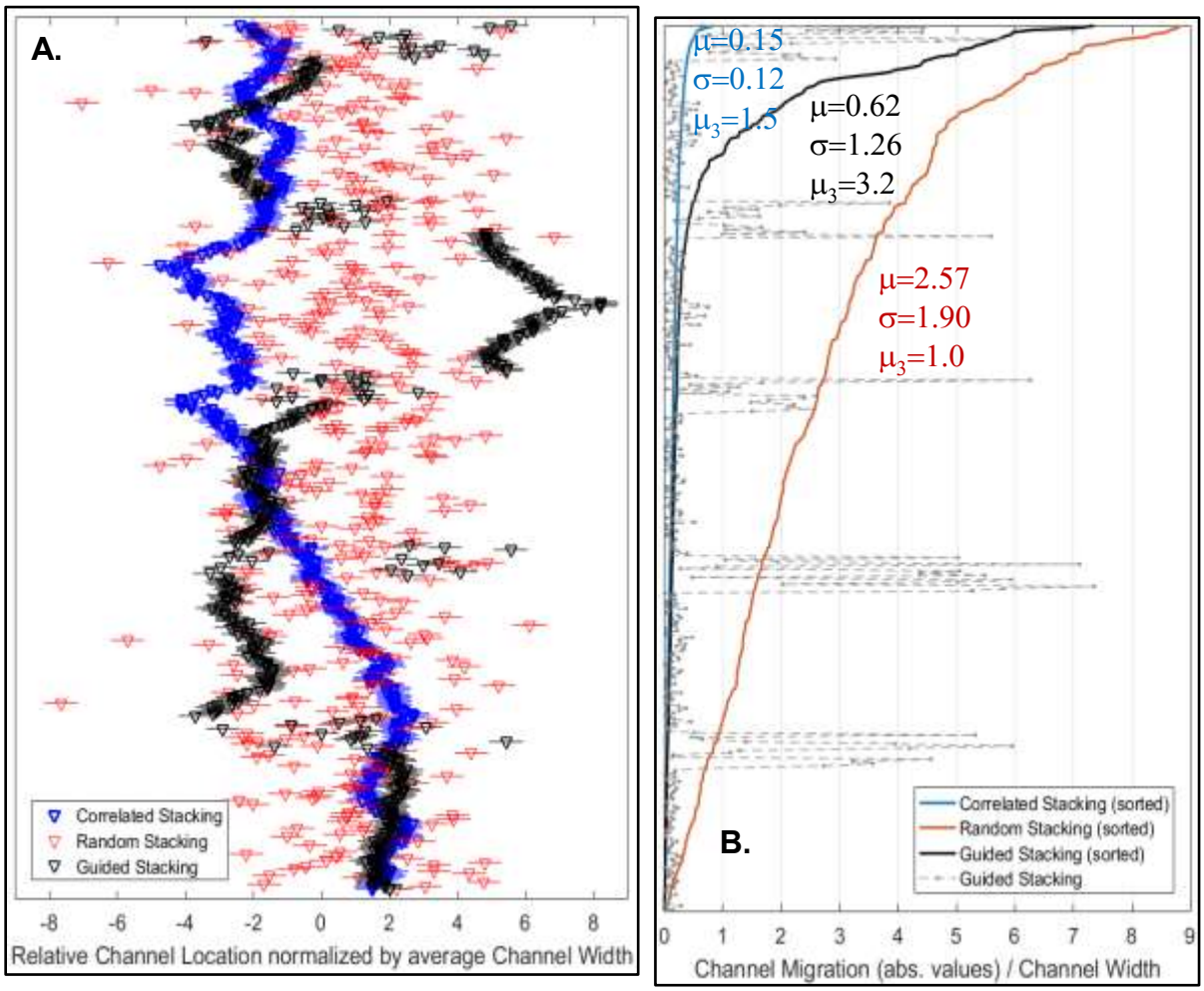


**Figure 24. A: Position of a single upstream channel under the random (red), correlated (blue), and guided (black) stacking scenarios. For clarity, the positions are shown schematically with no vertical units and the horizontal units given as channel widths, relative to an average central position. B: Lateral channel shift normalized by the average channel width and computed as an absolute value, $|\Delta x|$, whether the shift is to the left or right. The values are sorted in ascending order to highlight the distribution of $|\Delta x|$ for the three stacking scenarios. The dashed black line represents the unsorted $|\Delta x|$ for the guided stacking scenario.**

magnitude larger than the value for the correlated sequence ($\sigma$ = 0.12) while the value for the guided stacking sequence falls somewhere in between ($\sigma$ = 1.26). The skewness ($\mu_3$) of channel shifts, however, is largest for the guided staking sequence ($\mu_3$ = 3.5) reflecting a mix of smaller shifts within the clustered sets and larger values for the thinner sets in between. By contrast, for the perfectly correlated staking scenario $\mu_3$ = 1.5, whereas for a random stacking arrangement $\mu_3$ = 1.0, the expected value for the half-normal distribution.

### 4.5 Discussion

The challenge of reproducing detailed deltaic stratigraphy is twofold. First, capturing the stratigraphic details at channel resolution is in itself a challenging endeavor. Secondly, situated at the transition between terrestrial and marine domain, modeling deltaic networks poses some specific challenges. Avulsion, bifurcation, bank cohesion, or complex flow-vegetation interactions are difficult to frame analytically due to their stochastic nature and/or lack of adequate descriptive relationships. Nonetheless, advances in numerical modeling of water and sediment routing and a better understanding of channel bifurcation dynamics (e.g., Edmonds and Slingerland, 2010; Fagherazzi et al., 2015) led to complex simulations of delta evolution. A deterministic approach can offer a good level of detail at channel scale and can be used to predict the morphological evolution on a practical, short term engineering scale. At greater stratigraphic scale, however, the deposit preservation is a function of sediment reworking associated with complex channel migration patterns. It is also a function of factors operating at basin scale such as the hydrologic regime, climate, or sea level variation whose collective effect can be captured in a detailed model only to the extent to which their variation is known. Episodes of erosion or reconfiguration of the entire deltaic domain driven by major regional avulsions add unique challenges to a forward modeling approach lending support to a different and more direct alternative.

The technique of stacking topographic realizations is not common. Object based models typically assume that the background space is either empty or occupied by one facies (e.g., floodplain deposits) into which the objects are inserted (e.g., Deutsch and Tran, 2002). Webb (1994) used stacking of topographic surfaces derived from a random walk model for braided rivers as a way to render deposition. Instead of a database and stacking rules, in Webb's model realizations were stacked then translated (glided) relative to one another, laterally and channel-wise, to obtain a partial overlap of the channel trajectories as a way reduce vertical topographic differences.

The model presented here relies on a number of simplifying assumptions. The intent was to introduce the model in a simple manner, as a proof of concept. Complexity can be added at various scales of individual channel, delta surface, and basin.

At channel scale, we employed a simple channel shape linked through a power coefficient to the discharge. We argued above that the details of the channel shape with possible inclusion of bars or width variation are not crucial for generating the long term stratigraphic architecture as the dynamic of fluvial channels erases channel boundaries through lateral erosion and aggradation. When lateral migration rates dominates over aggradation rates, the amalgamation of composite channel deposits resulting from the channel dynamic obliterates he details of individual shapes of channel deposits (Figure 20). The channel-levee profile, however, does not have to follow a unique template. The fact that the building elements of the model consists of networks of centerlines offers significant flexibility during conversion to 3D surfaces. If desired, the cross-section shapes can be readily modified, globally or locally. Also, sediment texture can be added to the model. One simple possibility is to associate a sand proportion to the channel fill deposits, a proportion that can be varied upstream to downstream to reflect a decrease in net to gross ratio.

We also used simplifications at the scale of the deltaic domain assuming network configurations of only a few channels originating at the same place. These assumptions, however, are not a necessity. The method can be applied to more complex networks with variable number of channels. It would, however, require a much larger database. Generating networks via the algorithm discussed above is computationally intensive in large part due the routine used to address the channel confluences as the networks grow. Keeping the network configuration relatively simple (i.e., few bifurcations), a set of $10^4$ networks was generated in less than 24 hours using an average PC with a modest 2.8 GHz processor. With the ever increasing computational speed, a supercomputer can perhaps create a much larger database (i.e., *O9*) in a matter of weeks. Also, image training and image processing techniques can potentially be used to generate additional look alike networks from individual realizations in order to expand the database.

At basin scale we assumed that the depositional domain (i.e., the subaerial delta) did not move significantly spatially. This is possible if the seaward delta migration (progradation) is countered by the sea level rise and/or subsidence, such that the shoreline remains quasi-stationary. More generally, deltas extend seaward (prograde) if the sea level remains constant or if the deposition rate exceeds the rate of sea level rise.

Alternatively, the delta shoreline may retreat (transgression) if the sea level rise exceeds the rate at which the sediment is delivered to the delta front. Limited progradation or retreat of the shoreline can be captured in the model, by extending or shortening the networks, respectively.

We have also assumed a constant aggradation rate. However, this need not be the case. Aggradation rate can be varied and erosion can be incorporated as well. Figures 22C and 22D depict the same network stack under constant and varied aggradation rate, respectively. In the upper part of Figure 22D the aggradation rate decreases linearly towards zero and becomes negative (i.e., erosion) at the top of the sequence, that is, the sequence ends with a short incisional phase.

While complexity at many levels can be added to the model it would undoubtedly require a significant effort at the front end, to building a large database of networks. However, once the database is in place the simulations are straightforward and fast, a clear advantage over the numerical models. Numerous scenarios exploring plausible internal stratigraphic arrangements can be generated using a matrix oriented coding environment such as Python or Matlab. The flexibility in crafting the evolution parameters and the staking rules to generate numerous outcomes offers a strong exploration platform and has practical relevance for hydrocarbon exploration. Importantly, the model can be directly conditioned against available data (e.g., outcrops, well logs, seismic transects). At each level or location where data is available, the stacking algorithm can be adapted to select only from those networks that honor the data.

### 4.6 Conclusions

The model discussed here illustrates how 3D stratigraphic modeling at channel solving resolution can be accomplished without directly modeling the dynamic evolution of a deltaic system, resorting instead on vertical stacking of topographic representations. The approach relies on a database of distributary networks that, stochastically, are topologically similar to the field deltas. In this geometric construct, the superposition of topographic surfaces replaces the dynamic evolution of the system, mimicking a gradual progression.

Field and experiment observations show that prolonged episodes of incremental lateral channel shifts are separated by episodes of channel network reconfiguration driven by major regional avulsion, indicating that the stacking order should, likewise, consist of thicker sets of similar surfaces separated by thinner intervals of less correlated surfaces.

A simple set of rules for sampling and stacking successive networks can accomplish this task yielding results that compare favorably against the experimental observation.

In developing the technique it became apparent that while $10^4$ networks appear sufficient for the simple proof of concept presented here, a set that is several orders of magnitude larger is needed in order to include more complex domain shapes and networks arrangements. On the plus side, modeling itself is relatively fast and straightforward. The approach can be employed as a flexible tool to quickly render and visualize long term deltaic stratigraphic arrangements and explore various scenarios of long term evolution. Dynamic experiments and/or field data can be used to inform and refine the stacking strategy. The model can be directly conditioned to fit available subsurface data by selecting only those networks that fit the existing data at particular locations.

# Chapter 5. Conclusions and Future Directions

## 5.1 Conclusions

The rule-based models for generating distributary networks (Chapter 2) and for building stratigraphic sequences (Chapter 4) are essentially stochastic models. The rules, that were intentionally kept as simple as possible, do not explicitly reflect the physical process but instead rely on stochastic distributions to reproduce the topologic and stratigraphic observation. As discussed in Chapter 2, the ability of rule-based model to capture the diversity of natural distributary networks is due in part to implicit links between the physical process and rules and in part the direct constraint of certain geometric properties of deltaic networks. In Chapter 4 we discussed some of the challenges and limitations with process-based forward numerical models of deltaic networks or stratigraphy. However, the difficulties posed by a deterministic approach are not in themselves arguments in favor of the stochastic constructions. Better arguments rest on the probabilistic nature of the processes characterizing the origination and dynamic of the deltaic channels. Below we discuss what are perhaps the three most important individual processes acting in deltaic region: lateral channel migration, bifurcation at the mouth bar, and avulsion.

The lateral channel migration is a universal and ubiquitous alluvial process. The bank retreat theory for meander migration, initially presented by Ikeda et al. (1981), has been refined and used to simulate the dynamic of meandering streams in many subsequent models (e.g., Howard 1996; Sun et al., 1996). Under steady state conditions and homogeneous materials sinuous channels emerge from minor perturbations. Even under such simple conditions the dynamic of the meanders and the occasional cutoffs is irregular and non-periodic. Models also assume a single value for the bank erodibility term, $E$, which controls the rate of migration. However, the bank composition vegetation are not homogenous. Consequently, the bank erodibility term can vary substantially altering the migration rates and adding randomness to the channel planform (Posner and Duan, 2012). Furthermore, deltaic channels tend to be characterized by finer sediment and highly cohesive vegetated banks. As a result, as discussed in Chapter 3, deltaic channels are less mobile, compared to meandering rivers defined by coarser bedload and therefore less likely to follow the dynamics predicted by the bank retreat theory.

A second process to consider is the channel bifurcation at the mouth bar, an essential autogenic process that defines the expansion of a delta, in terms of area and number of channels. While the complexity of physical mechanisms governing flow and sediment

dynamic leading to channel bifurcation has been investigated in detail (e.g., Edmonds and Slingerland, 2007, Fagherazzi et al., 2015), the formation of new channels and their geometry is far from predictable. Factors such as cohesion play an important role in controlling the trajectory of the new channels or whether both channels remain active (Edmonds and Slingerland, 2009). Also, long term, the bifurcation sequence is not predictable. In fact, a recent study by Salter et al. (2020) finds that, long term, the occurrence of bifurcation is aperiodic and chaotic.

The third process that does not follow a systematic and predictable pattern is avulsion, also an autogenic process that operates on larger spatial and temporal scales. Avulsions tend to reconfigure the flow and sediment distribution, spreading the delta growth over a broader area, sometimes through creation of new active lobes. Large, regional avulsions in particular result in relocation of a main stem channel and, in turn, relocation of the dominant active area and formation of new minor channels. Frequency of avulsion is a function of multiple factors such as differential aggradation rates between channel and adjacent floodplain, reduction of slope due to channel lengthening, or bank erodibility. While, on average, avulsion frequency is linked to the aggradation rate and avulsion location linked to the transition in the backwater zone (e.g., Nittrouer et al 2012; Lamb et al 2012; Chatanantavet et al, 2012) generally speaking, predicting either the location or occurrence of avulsion cannot be well constrained analytically. Many stratigraphic models typically treat avulsion as a stochastic process assuming, that the spatial and/or temporal relocation of the flow is, at least in part, random (Allen, 1998; Bridge and Leeder, 1979; Allen, 1979; Bryant et al, 1995; Heller and Paola, 1996; Mohrig et al., 2000).

In conclusion, although we have an increasingly sophisticated understanding of the physics governing each of the processes discussed above (at least under steady conditions) long term and under varied conditions the juxtaposition of these processes results an unsystematic channel dynamics and distribution. If we also consider other sources of perturbation, such as variability of the of the inputs (flow regime, sediment type and flux), heterogeneities of the deltaic areal (e.g., sediment cohesion, vegetation density and patterns, uneven compaction) characteristics of the receiving basin (shape, depth, wave and/or tidal regime) a fuller picture behind the reasons for the observed unsystematic arrangement of the deltaic channels emerges and we start to see the value of probabilistic approaches towards modeling distributary networks.

## 5.2 Future Directions

The three lines of research pursued here were presented under generic, simplified assumptions. Each of these lines of research can be expanded to include more specificity and make the models more sophisticated to suit a particular geologic contexts.

In **Chapter 2**, capturing a broad spectrum of river dominated deltas was intentional with the rules for generating distributary networks kept as simple as possible. The next effort should perhaps focus on better understanding the controls on the geometry of deltaic channels, and modify the rules to render various delta styles. For example, several studies (Edmonds and Slingerland, 2009; Caldwell et al., 2014; Burpee et al., 2015) show that, within the spectrum of river dominated deltas, there are morphological differences driven by the sediment size and cohesion. Deltas with a relative abundance of sand tend to have more active distributaries and smoother shoreline shapes, whereas the mud dominated deltas show fewer, longer distributaries and more irregular shorelines (Burpee et al., 2015). Accordingly, the model presented in Chapter 2 could be adapted to reflect these trends. One may think that using different values for the bifurcation probability would be suffice, with a higher probability resulting in more channels while a lower bifurcation probability would reflect the opposite trends. However, since the model can run indefinitely it already has the ability to generate a prescribed number of channels, simply as a function of when the execution stops. To differentiate between sandy deltas and muddy deltas we need to explore the model parameter space more methodically and determine how one type of delta versus another can be predictably generated.

**Chapter 3** explores the dynamic patterns that operate in the deltaic region assessing the relative dominance of continuous channel migration versus episodes of flow reconfiguration and channel relocation through avulsion. By contrasting two distinct experiment we documented important channel dynamic trends and found that lateral migration rates depend on sediment flux and grain size, reinforcing a correlation that was discussed by others based on experiment (Wickert et al., 2013) or field (Constantine et al., 2014) data. However, to better understand how avulsions may operate in the deltaic region further exploration is needed. The avulsions documented in the second experiment discussed in Chapter 3 are not episodes of sudden flow relocation. Rather the flow spreads into numerous anastomosed channels that seem to disintegrate and recombine over a broad area before the flow coalesce into major, quasi-stable routes. Field data (Smith et al., 1989; Berendsen and Stouthamer, 2000; Stouthamer and Berendsen, 2001)

suggest that this is not just a particularity of the experiment which raises important questions:

a) What is the typical duration of these flow relocation episodes relative to the duration of extended periods of stability?

b) What defines the dynamic of the flow during these episodes?

c) What are the aggradation patterns, specifically do these episodes contribute a larger fraction of sediment to the delta surface by filling in topographic lows?

d) What determine the position of the new stable channels that emerge?

**Chapter 4** introduces a novel method for modeling deltaic stratigraphy, top-set dominated deltas in particular, using a database of distributary networks that are converted into topographic surfaces. Sorting out the questions listed above would also help improving the stratigraphic model by guiding the stacking of the topographic surfaces in a more informed, process linked way.

We introduced the stratigraphic model in the most generic form, as proof of concept and, as acknowledged, we employed a number of simplifying assumptions of which a quasi-stationary deltaic domain is perhaps the most important one. We assumed that the deltaic plain does not move significantly (i.e., no significant progradation or regression). Relaxing this assumption provides an opportunity to explore deltaic stratigraphy at basin scale. Long term, the collective effect of sediment supply, subsidence, and sea level fluctuations causes the delta plain to shift considerably, in a cross-shore direction or laterally, generating complex stratigraphic packages. This complexity has been captured in both laterally averaged cross-shore models 2D models (e.g., Hoogendoorn et al., 2008) as well as 3D models (e.g., Falivene et al., 2019). While such mass-balance models capture the large scale architecture of the stratigraphic packages, capturing the details of the internal stratigraphy at channel-scale resolution remains a challenge. One way to meet this challenge is through a more sophisticated version of stacking model proposed here. This would entail a much larger database to allow for the selection of networks reflective of a particular environment and network configuration (i.e., delta style). It would also entail refined rules to guide the stacking of the surfaces in a way that captures the channel dynamic aspects mentioned above.

In summary, a refined stratigraphic model for long term evolution would connect all potential future directions highlighted above and would take the research introduced here to a new level.

## References


Allen, J. R. L. (1965). A review of the origin and characteristics of recent alluvial sediments. *Sedimentology*, *5*(2), 89–191. https://doi.org/10.1111/j.1365-3091.1965.tb01561.x

Allen, J. R. L. (1978). Studies in fluviatile sedimentation: an exploratory quantitative model for the architecture of avulsion-controlled alluvial suites. *Sedimentary Geology*, *21*(2), 129–147. https://doi.org/10.1016/0037-0738(78)90002-7

Allen, J. R. L. (1979). Studies in fluviatile sedimentation: An elementary geometrical model for the connectedness of avulsion-related channel sand bodies. *Sedimentary Geology*, *24*(3–4), 253–267. https://doi.org/10.1016/0037-0738(79)90072-1

Allen, J. R. L. (1983). Studies in fluviatile sedimentation: Bars, bar-complexes and sandstone sheets (low-sinuosity braided streams) in the brownstones (L. Devonian), welsh borders. *Sedimentary Geology*, *33*(4), 237–293. http://doi.org/10.1016/0037-0738(83)90076-3

Andrén, H. (1994), Development of the Laitaure delta, Swedish Lapland: A study of growth, distributary forms, and processes, Ph.D. thesis, 188 pp., Inst. of Earth Sci. Phys. Geogr., Uppsala Univ., Uppsala, Sweden.

Arche, A., & López-Gómez, J. (2005). Sudden changes in fluvial style across the Permian-Triassic boundary in the eastern Iberian Ranges, Spain: Analysis of possible causes. *Palaeogeography, Palaeoclimatology, Palaeoecology*, *229*(1–2), 104–126. https://doi.org/10.1016/j.palaeo.2005.06.033

Ashton, A. D., Hutton, E. W. H., Kettner, A. J., Xing, F., Kallumadikal, J., Nienhuis, J., & Giosan, L. (2013). Progress in coupling models of coastline and fluvial dynamics. *Computers & Geosciences*, *53*, 21–29. https://doi.org/10.1016/j.cageo.2012.04.004

Berendsen, H. J. A., & Stouthamer, E. (2000). Late Weichselian and Holocene palaeogeography of the Rhine-Meuse delta, the Netherlands. *Palaeo*, *161*(3–4), 311–335. https://doi.org/10.1016/S0031-0182(00)00073-0

Blackburn, S., Pelling, M., & Marques, C. (2019). *Megacities and the Coast: Global Context and Scope for Transformation*. *Coasts and Estuaries: The Future*. Elsevier Inc. https://doi.org/10.1016/B978-0-12-814003-1.00038-1

Bridge, J. S. (1984). Large-scale facies sequences in alluvial overbank environments. *Journal of Sedimentary Petrology*, *54*(2), 583–588. https://doi.org/10.1306/212F8477-2B24-11D7-8648000102C1865D

Bridge, J. S. (1985). Paleochannel patterns inferred from alluvial deposits: a critical evaluation. *Journal of Sedimentary Petrology*, *55*(4), 579–589. https://doi.org/10.1306/212F8738-2B24-11D7-8648000102C1865D

Bridge, J. S. (1993). Description and interpretation of fluvial deposits: a critical perspective. *Sedimentology*, *40*(4), 801–810. http://doi.org/10.1111/j.1365-3091.1993.tb01361.x

Bridge, J. S., & Leeder, M. R. (1979). A simulation model of alluvial stratigraphy. *Sedimentology*, *26*(5), 617–644. https://doi.org/10.1111/j.1365-3091.1979.tb00935.x

Bridge, J.S. & Mackey, S.D. (1993). A revised alluvial stratigraphy model. In: Alluvial Sedimentation (Eds M. Marzo and C. Puidefabregas), *IAS Spec. Pub*., 17, 319–337.

Bridge, J.S. (2008). Numerical Modelling of Alluvial Deposits: Recent Developments. *IAS Spec. Pub.*, 40. doi:10.1002/9781444303131.ch4

Bristow C.S., (1999). Crevasse splays from the rapidly aggrading sand-bed braided Niobrara River, Nebraska: effect of base-level rise. *Sedimentology 46,*1029–47

Broussard, M.L. (ed.) (1975). Deltas, Models for Exploration. Houston Geological Society, Houston, TX, 555 pp.

Bryant, M., Falk, P., & Paola, C. (1995). Experimental study of avulsion frequency and rate of deposition. *Geology*, *23*(4), 365–368. https://doi.org/10.1130/0091-7613(1995)023<0365:ESOAFA>2.3.CO;2

Burpee, A. P., Slingerland, R. L., Edmonds, D. A., Parsons, D., Best, J., Cederberg, J., Royce, J. (2015). Grain-size controls on the morphology and internal geometry of river-dominated deltas. *Journal of Sedimentary Research*, *85*(6), 699–714. https://doi.org/10.2110/jsr.2015.39

Caldwell, R. L., & Edmonds, D. A. (2014). The effects of sediment properties on deltaic processes and morphologies: A numerical modeling study. *Journal of Geophysical Research: Earth Surface*, *119*, 961–982. https://doi.org/10.1002/2013JF002965

Caldwell, R. L., Edmonds, D. A., Baumgardner, S., Paola, C., & Roy, S. (2019). A global delta dataset and the environmental variables that predict delta formation on marine coastlines. *Earth Surface Dynamics*, *7*, 773–787.

Camporeale, C., Perona, P., Porporato, A., & Ridolfi, L. (2005). On the long-term behavior of meandering rivers. *Water Resources Research*, *41*(12), 1–13. http://doi.org/10.1029/2005WR004109

Catuneanu, O. (2019). Model-independent sequence stratigraphy. *Earth-Science Reviews*, *188*, 312–388. https://doi.org/10.1016/j.earscirev.2018.09.017

Chadwick, A. J., Lamb, M. P., Moodie, A. J., Parker, G., & Nittrouer, J. A. (2019). Origin of a Preferential Avulsion Node on Lowland River Deltas. *Geophysical Research Letters, 46*(8), 4267–4277. https://doi.org/10.1029/2019GL082491

Chamberlin, E. P., & Hajek, E. A. (2015). Interpreting Paleo-Avulsion Dynamics from Multistory Sand Bodies. *Journal of Sedimentary Research*, *85*(2), 82–94. https://doi.org/10.2110/jsr.2015.09

Chamberlin, E. P., & Hajek, E. A. (2019). Using bar preservation to constrain reworking in channel-dominated fluvial stratigraphy. *Geology*, *47*(6), 531–534. https://doi.org/10.1130/G46046.1

Chatanantavet, P., Lamb, M. P., & Nittrouer, J. A. (2012). Backwater controls of avulsion location on deltas. *Geophysical Research Letters*, *39*(1), 1–6. http://doi.org/10.1029/2011GL050197

Coffey, T. S., & Shaw, J. B. (2017). Congruent Bifurcation Angles in River Delta and Tributary Channel Networks. *Geophysical Research Letters*, *44*(22), 11,427-11,436. https://doi.org/10.1002/2017GL074873

Constantine, J. A., Dunne, T., Ahmed, J., Legleiter, C., & Lazarus, E. D. (2014). Sediment supply as a driver of river meandering and floodplain evolution in the Amazon Basin. *Nature Geoscience*, *7*(12), 899–903. http://doi.org/10.1038/ngeo2282

Coulthard, T. J., & Van De Wiel, M. J. (2012). Modelling river history and evolution. *Philosophical Transactions of the Royal Society A: Mathematical, Physical and Engineering Sciences*, *370*(1966), 2123–2142. https://doi.org/10.1098/rsta.2011.0597

Coulthard, T. J., Neal, J. C., Bates, P. D., Ramirez, J., de Almeida, G. A. M., & Hancock, G. R. (2013). Integrating the LISFLOOD-FP 2D hydrodynamic model with the CAESAR model: Implications for modelling landscape evolution. *Earth Surface Processes and Landforms*, *38*(15), 1897–1906. https://doi.org/10.1002/esp.3478

Day, J. W., Boesch, D. F., Clairain, E. J., Kemp, G. P., Laska, S. D., Mitsch, W. J., & Whigham, D. F. (2007). Restoration of the Mississippi Delta: Lessons from Hurricanes Katrina and Rita. *Science*, *315*(5819), 1679–1684. https://doi.org/10.1126/science.1137030

Day, J. W., Ramachandran, R., Giosan, L., Syvitski, J., & Paul Kemp, G. (2019). *Delta Winners and Losers in the Anthropocene*. *Coasts and Estuaries: The Future*. Elsevier Inc. https://doi.org/10.1016/B978-0-12-814003-1.00009-5

Dalman, R. A. F., & Weltje, G. J. (2008). Sub-grid parameterisation of fluvio-deltaic processes and architecture in a basin-scale stratigraphic model. *Computers & Geosciences*, *34*(10), 1370–1380. https://doi.org/10.1016/j.cageo.2008.02.005

Deutsch, C. V, & Tran, T. T. (2002). FLUVSIM : a program for object-based stochastic modeling of fluvial depositional systems $. *Computers & Geosciences*, *28*, 525–535.

Edmonds, D. A., & Slingerland, R. L. (2007). Mechanics of river mouth bar formation: Implications for the morphodynamics of delta distributary networks. *Journal of Geophysical Research*, *112*(F2), F02034. https://doi.org/10.1029/2006JF000574

Edmonds, D. A., & Slingerland, R. L. (2009). Significant effect of sediment cohesion on delta morphology. *Nature Geoscience*, *3*(2), 105–109. https://doi.org/10.1038/ngeo730

Edmonds, D. A., Paola, C., Hoyal, D. C. J. D., & Sheets, B. A. (2011). Quantitative metrics that describe river deltas and their channel networks. *Journal of Geophysical Research*, *116*(F4), F04022. https://doi.org/10.1029/2010JF001955

Edmonds, D. A., Shaw, J. B., & Mohrig, D. (2011). Topset-dominated deltas: A new model for river delta stratigraphy. *Geology*, *39*(12), 1175–1178. https://doi.org/10.1130/G32358.1

Edmonds, D. A., Slingerland, R., Best, J., Parsons, D., & Smith, N. (2010). Response of river-dominated delta channel networks to permanent changes in river discharge. *Geophysical Research Letters*, *37*(12). https://doi.org/10.1029/2010GL043269

Fagherazzi, S., Bortoluzzi, A., Dietrich, W.E., Adami, A., Lanzoni, S., Marani, M., Rinaldo, A., (1999). Tidal networks: 1. Automatic network extraction and preliminary scaling features from digital terrain maps, Water Resour. Res., v. 35(12), 3891–3904

Fagherazzi, S., Edmonds, D. A., Nardin, W., Leonardi, N., Canestrelli, A., Falcini, F., Slingerland, R. L. (2015). Dynamics of river mouth deposits. *Review of Geophysics*, *69*(37), 849–849. https://doi.org/10.1029/88EO01108

Falivene, O., Frascati, A., Pittaluga, M. B., & Martin, J. (2019). Three-dimensional reduced-complexity simulation of fluvio-deltaic clastic stratigraphy. *Journal of Sedimentary Research*, *89*(January), 46–65.

Ferguson, R. I. (1976). Disturbed periodic model for river meanders. *Earth Surface Processes*, *1*, 337–347.

Fernandes, A. M., Törnqvist, T. E., Straub, K. M., & Mohrig, D. (2016). Connecting the backwater hydraulics of coastal rivers to fluviodeltaic sedimentology and stratigraphy. *Geology*, *44*(12), 979–982. http://doi.org/10.1130/G37965.1

Frascati, A., & Lanzoni, S. (2013). A mathematical model for meandering rivers with varying width. *Journal of Geophysical Research: Earth Surface*, *118*(3), 1641–1657. http://doi.org/10.1002/jgrf.20084

Friend, P.F., (1983). Towards the field classification of alluvial architecture or sequence. In Collinson, J.D., and Lewin, J. (Eds), *Modern and Ancient Fluvial Systems*: International Association of Sedimentologists, Special Publication 6, 345–354.

Furbish, D. J. O. N. (1991). Spatial autoregressive structure in meander evolution. *GSA Bullentin*, (12). https://doi.org/10.1130/0016-7606(1991)103<1576

Ganti, V., Chadwick, A. J., Hassenruck-Gudipati, H. J., Fuller, B. M., & Lamb, M. P. (2016). Experimental river delta size set by multiple floods and backwater hydrodynamics. *Science Advances*, *2*(5), e1501768. http://doi.org/10.1126/sciadv.1501768

Geleynse, N., Storms, J. E. A., Stive, M. J. F., Jagers, H. R. A., & Walstra, D. J. R. (2010). Modeling of a mixed-load fluvio-deltaic system. *Geophysical Research Letters*, *37*(5). https://doi.org/10.1029/2009GL042000

Geleynse, N., Storms, J. E. A., Walstra, D. J. R., Jagers, H. R. A., Wang, Z. B., & Stive, M. J. F. (2011). Controls on river delta formation; insights from numerical modelling. *Earth and Planetary Science Letters*, *302*(1–2), 217–226. https://doi.org/10.1016/j.epsl.2010.12.013

Geleynse, N., Voller, V. R., Paola, C., & Ganti, V. (2012). Characterization of river delta shorelines. *Geophysical Research Letters*, *39*(17). https://doi.org/10.1029/2012GL052845

Giosan, L., Syvitski, J., Constantinescu, S., & Day, J. (2014). Climate change: Protect the world's deltas. *Nature*, *516*(729), 31–33. https://doi.org/10.1038/516031a

Granjeon, D. (2014). 3D forward modeling of the impact of sediment transport and base-level cycles on continental margins and incised valleys. In Martinius, A.W., Ravnas, R., Howell, J.A., Steel, R.J., and Wonham, J.P., eds., From Depositional Systems to Sedimentary Successions on the Norwegian Continental Margin, First Edition: IAS Spec. Pub. 46, p. 453–472.

Hajek, E. A., & Straub, K. M. (2017). Autogenic Sedimentation in Clastic Stratigraphy. *Annual Review of Earth and Planetary Sciences*, *45*(1), 681–709. https://doi.org/10.1146/annurev-earth-063016-015935

Hajek, E. A., & Wolinsky, M. A. (2012). Simplified process modeling of river avulsion and alluvial architecture: Connecting models and field data. *Sedimentary Geology*, *257-260*, 1–30. http://doi.org/10.1016/j.sedgeo.2011.09.005

Hajek, E. A., Heller, P. L., & Schur, E. L. (2012). Field test of autogenic control on alluvial stratigraphy (Ferris Formation, Upper Cretaceous-Paleogene, Wyoming). *Bulletin of the Geological Society of America*, *124*(11–12), 1898–1912. https://doi.org/10.1130/B30526.1

Hajek, E. A., Heller, P. L., & Sheets, B. A. (2010). Significance of channel-belt clustering in alluvial basins. *Geology*, *38*(6), 535–538. https://doi.org/10.1130/G30783.1

Hampson, G. J., Royhan Gani, M., Sahoo, H., Rittersbacher, A., Irfan, N., Ranson, A., Bracken, B. (2012). Controls on large-scale patterns of fluvial sandbody distribution in alluvial to coastal plain strata: Upper Cretaceous Blackhawk Formation, Wasatch Plateau, Central Utah, USA. *Sedimentology*, *59*(7), 2226–2258. https://doi.org/10.1111/j.1365-3091.2012.01342.x

Harris, A. D., Covault, J. A., Madof, A. S., Sun, T. A. O., Sylvester, Z., & Granjeon, D. (2016). Three-dimensional numerical modeling of eustatic control on continental-margin sand distribution. *Journal of Sedimentary Research*, *86*, 1434–1443. https://doi.org/http://dx.doi.org/10.2110/jsr.2016.85

Hayes, B. (2006). Up a Lazy River. *American Scientist*, *94*(6), 490. https://doi.org/10.1511/2006.62.490

Heller, P. L., & Paola, C. (1996). Downstream changes in alluvial architecture: An exploration of controls on channel-stacking patterns. *Journal of Sedimentary Research* 66(2), 297–306.

Hillen, M. M., Geleynse, N., & Storms, J. E. A. (2014). Morphodynamic modelling of wave reworking of an alluvial delta and application of results in the standard reservoir modelling workflow. *IAS Spec.l Pub.*, *46*, 167–186.

Hofmann, M. H., Wroblewski, A., & Boyd, R. (2011). Mechanisms Controlling the Clustering of Fluvial Channels and the Compensational Stacking of Cluster Belts. *Journal of Sedimentary Research*, *81*(9), 670–685. https://doi.org/10.2110/jsr.2011.54

Hoogendoorn, R. M., Overeem, I., & Storms, J. E. a. (2008). Process-response modelling of fluvio-deltaic stratigraphy. *Computers & Geosciences*, *34*(10), 1394–1416. https://doi.org/10.1016/j.cageo.2008.02.006

Horton, R.E.: Erosional development of streams and their drainage basins; hydrophysical approach to quantitative geomorphology. *Bull. Geol. Soc. Amer.* 56, 275-370 (1945).

Howard, A., & Knutson, T. R. (1984). Sufficient Conditions for River Meandering: A Simulation Approach. *Water Resources Research*, *20*, 1659–1667. https://doi.org/0043-1397/84/004W-1017

Howard, A.D. (1996). Modelling channel evolution and floodplain morphology. In: Anderson, M.G, Walling D.E., Bates P.D. (Eds.), *Floodplain Processes*, pp 15–62.

Hoyal, D. C. J. D., & Sheets, B. A. (2009). Morphodynamic evolution of experimental cohesive deltas. *Journal of Geophysical Research*, *114*(F2), F02009. https://doi.org/10.1029/2007JF000882

Hudson, P. F., & Kessel, R. H. (2000). Channel migration and meander-bend curvature in the lower Mississippi River prior to major human modification. *Geology*, *28*(6), 531–534. http://doi.org/10.1130/0091-7613 (2000)

Hudson, P. F., & Kessel, R. H. (2000). Channel migration and meander-bend curvature in the lower Mississippi River prior to major human modification. *Geology*, *28*(6), 531–534. https://doi.org/10.1130/0091-7613(2000)28<531:cmamci>2.0.co;2

Ikeda, S., Parker, G., & Sawai, K. (1981). Bend theory of river meanders. Part 1. Linear development. *Journal of Fluid Mechanics*, *112*(1), 363. https://doi.org/10.1017/S0022112081000451

Jerolmack, D. J. (2009). Conceptual framework for assessing the response of delta channel networks to Holocene sea level rise. *Quaternary Science Reviews*, *28*(17-18), 1786–1800. http://doi.org/10.1016/j.quascirev.2009.02.015

Jerolmack, D. J., & Mohrig, D. (2007). Conditions for branching in depositional rivers. *Geology*, *35*(5), 463. https://doi.org/10.1130/G23308A.1

Jerolmack, D. J., & Paola, C. (2007). Complexity in a cellular model of river avulsion. *Geomorphology*, *91*(3–4), 259–270. https://doi.org/10.1016/j.geomorph.2007.04.022

Jerolmack, D. J., & Swenson, J. B. (2007). Scaling relationships and evolution of distributary networks on wave-influenced deltas. *Geophysical Research Letters*, *34*(23), n/a-n/a. https://doi.org/10.1029/2007GL031823

Jobe, Z. R., Howes, N. C., & Auchter, N. C. (2016). Comparing submarine and fluvial channel kinematics: Implications for stratigraphic architecture. *Geology*, *44*(11), 931–934. https://doi.org/10.1130/G38158.1

Jones, T.A., & Larue, D.K. (1997). Object-based modeling and deepwater depositional systems. In: Pawlowsky- Glahn, V. (Ed.), *Proceedings of IAMG'97*, Vol. 1, pp. 438–443

Julien, P. Y., & Wargadalam, J. (1995). Alluvial Channel Geometry: Theory and Applications. *Journal of Hydraulic Engineering*, *121*(4), 312–325.

Karssenberg, D., & Bridge, J. S. (2008). A three-dimensional numerical model of sediment transport, erosion and deposition within a network of channel belts, floodplain and hill slope: extrinsic and intrinsic controls on floodplain dynamics and alluvial architecture. *Sedimentology*, *55*(6), 1717–1745. https://doi.org/10.1111/j.1365-3091.2008.00965.x

Kim, W., Mohrig, D., Twilley, R., Paola, C., & Parker, G. (2009). Is it feasible to build new land in the Mississippi River delta? *Eos*, *90*(42), 373–374. https://doi.org/10.1029/2009EO420001

Kim, W., Paola, C., Voller, V. R., & Swenson, J. B. (2006). Experimental Measurement of the Relative Importance of Controls on Shoreline Migration. *Journal of Sedimentary Research*, *76*(2), 270–283. https://doi.org/10.2110/jsr.2006.019

Kirchner, J. (1993). Statistical inevitability of Horton's laws and the apparent randomness of stream channel networks. *Geology*, *21*.

Kleinhans, M. G., Jagers, H. R. A., Mosselman, E., & Sloff, C. J. (2008). Bifurcation dynamics and avulsion duration in meandering rivers by one-dimensional and three-dimensional models. *Water Resources Research*, *44*(8). https://doi.org/10.1029/2007WR005912

Konsoer, K., Zinger, J., & Parker, G. (2013). Bankfull hydraulic geometry of submarine channels created by turbidity currents: Relations between bankfull channel characteristics and formative flow discharge. *Journal of Geophysical Research: Earth Surface*, *118*(1), 216–228. https://doi.org/10.1029/2012JF002422

Kraus M. J., (1996). Avulsion Deposits in Lower Eocene Alluvial Rocks, Bighorn Basin, Wyoming. *SEPM Journal of Sedimentary Research*, *Vol. 66*(June). https://doi.org/10.1306/d4268347-2b26-11d7-8648000102c1865d

Lamb, M. P., Nittrouer, J. A., Mohrig, D., & Shaw, J. (2012). Backwater and river plume controls on scour upstream of river mouths: Implications for fluvio-deltaic morphodynamics. *Journal of Geophysical Research*, *117*(F1), F01002. http://doi.org/10.1029/2011JF002079

Langbein, W. B. and Leopold, L. B. (1966): River meanders: theory of minimum variance, *USGS Professional Paper, 422-H*.

Lazarus, E. D., & Constantine, J. A. (2013). Generic theory for channel sinuosity. *Proceedings of the National Academy of Sciences of the United States of America*, *110*(21), 8447–8452. https://doi.org/10.1073/pnas.1214074110

Lee, J.-S., & Julien, P. Y. (2006). Downstream Hydraulic Geometry of Alluvial Channels. *Journal of Hydraulic Engineering*, *132*(12), 1347–1352.

Leeder, M.R. (1978). A quantitative stratigraphic model for alluvium, with special reference to channel deposit density and interconnectedness. In: Miall, A.D. (Ed.), Fluvial Sedimentology. Memoir, *Canadian Society Petroleum Geologists*, pp. 587–596.

Liang, M., & Voller, V. R. (2011). Fixed and Deforming Grid Solutions of Solidification in an Undercooled Melt: A Benchmark Problem. *Numerical Heat Transfer, Part B: Fundamentals*, *60*(1), 1–17. https://doi.org/10.1080/10407790.2011.582404

Liang, M., Geleynse, N., Edmonds, D. A., & Passalacqua, P. (2015). A reduced-complexity model for river delta formation – Part 2: Assessment of the flow routing scheme. *Earth Surface Dynamics*, *3*(1), 87–104. https://doi.org/10.5194/esurf-3-87-2015

Liang, M., Dyk, C. Van, & Passalacqua, P. (2016). Journal of Geophysical Research : Earth Surface Quantifying the patterns and dynamics of river deltas under conditions of steady forcing and relative sea level rise. *Journal of Geophysical Research : Earth Surface*, 465–496. https://doi.org/10.1002/2015JF003653.Received

Liang, M., Voller, V. R., & Paola, C. (2014). A reduced-complexity model for river delta formation – Part 1: Modeling deltas with channel dynamics. *Earth Surface Dynamics Discussions*, *2*(2), 823–869. https://doi.org/10.5194/esurfd-2-823-2014

Limaye, A. B. S., & Lamb, M. P. (2014). Numerical simulations of bedrock valley evolution by meandering rivers with variable bank material. *Journal of Geophysical Research*, *119*, 927–950. https://doi.org/10.1002/2013JF002997

Limaye, A. B., Lazarus, E. D., Li, Y., & Schwenk, J. (2021). River sinuosity describes a continuum between randomness and ordered growth. Geology, 49, 1–5. https://doi.org/10.1130/G49153.1/5393369/g49153.pdf

Lorenzo-Trueba, J., Voller, V. R., Muto, T., Kim, W., Paola, C., & Swenson, J. B. (2009). A similarity solution for a dual moving boundary problem associated with a coastal-plain depositional system. *Journal of Fluid Mechanics*, *628*, 427. https://doi.org/10.1017/S0022112009006715

Mack, G. H., & Leeder, M. R. (1998). Channel shifting of the Rio Grande, southern Rio Grande rift: Implications for alluvial stratigraphic models. *Sedimentary Geology*, *117*(3–4), 207–219. https://doi.org/10.1016/S0037-0738(98)00015-3

Mackey, S. D., & Bridge, J. S. (1995). Three-dimensional model of alluvial stratigraphy: theory and application. *Journal of Sedimentary Research B: Stratigraphy & Global Studies*, (B65(1)), 7–31. http://doi.org/10.1306/d42681d5-2b26-11d7-8648000102c1865d

Mariethoz, G., Comunian, A., Irarrazaval, I., & Renard, P. (2014). Analog-based meandering channel simulation. *Water Resources Research*, 836–854. https://doi.org/10.1002/2013WR013730.Received

Marzo, M., Nijman, W., & Puigdefàbregas, C. (1988). Architecture of the Castissent fluvial sheet sandstones, Eocene, South Pyrenees, Spain. *Sedimentology*, *35*(5), 719–738. http://doi.org/10.1111/j.1365-3091.1988.tb01247.x

Miall, A. D. (1985). Architectural-element analysis: A new method of facies analysis applied to fluvial deposits. *Earth Science Reviews*, *22*(4), 261–308. http://doi.org/10.1016/0012-8252(85)90001-7

Michael, H. A., Li, H., Boucher, A., Sun, T., Caers, J., & Gorelick, S. M. (2010). Combining geologic-process models and geostatistics for conditional simulation of 3-D subsurface heterogeneity. *Water Resources Research*, *46*(5), 1–20. https://doi.org/10.1029/2009wr008414

Milliman, J.D. and Farnsworth, K.L., (2011). River Discharge to the Coastal Ocean: A global synthesis. Cambridge University Press

Mohrig, D., Heller, P. L., Paola, C., & Lyons, W. J. (2000). Interpreting avulsion process from ancient alluvial sequences : Guadalope-Matarranya system (northern Spain) and Wasatch Formation (western Colorado). *GSA Bullentin*, *112*, 1787–1803. https://doi.org/10.1130/0016-7606

Morozova, G. S., & Smith, N. D. (2000). Holocene avulsion styles and sedimentation patterns of the Saskatchewan River, Cumberland Marshes, Canada. *Sedimentary Geology*, *130*(1-2), 81–105. http://doi.org/10.1016/S0037-0738(99)00106-2

Motta, D., Abad, J. D., Langendoen, E. J., & Garcia, M. H. (2012). A simplified 2D model for meander migration with physically-based bank evolution. *Geomorphology*, *163-164*, 10–25. http://doi.org/10.1016/j.geomorph.2011.06.036

Nienhuis, J. H., Ashton, A. D., Edmonds, D. A., Hoitink, A. J. F., Kettner, A. J., Rowland, J. C., & Törnqvist, T. E. (2020). Global-scale human impact on delta morphology has led to net land area gain. *Nature*, *577*(7791), 514–518. https://doi.org/10.1038/s41586-019-1905-9

Newman, M.E.J. (2010): Networks: An Introduction. Oxford University Press, pp720.

Nicholas, A. P. (2013). Modelling the continuum of river channel patterns. *Earth Surface Processes and Landforms*, *38*(10), 1187–1196. https://doi.org/10.1002/esp.3431

Nittrouer, J. A., Shaw, J., Lamb, M. P., & Mohrig, D. (2012). Spatial and temporal trends for water-flow velocity and bed-material sediment transport in the lower Mississippi River. *Bulletin of the Geological Society of America*, *124*(3-4), 400–414. http://doi.org/10.1130/B30497.1

Olariu, C., & Bhattacharya, J. P. (2006). Terminal Distributary Channels and Delta Front Architecture of River-Dominated Delta Systems. *Journal of Sedimentary Research*, *76*(2), 212–233. https://doi.org/10.2110/jsr.2006.026

Omre, H. (1992). Heterogeneity models. In: Skjæveland, S.M., Kleppe, J. (Eds.), SPOR Monograph: Recent Advances in Improved Oil Recovery Methods for North Sea Sandstone Reservoirs, Norway. Norwegian Petroleum Directorate, Stavanger, pp. 141–153

Overeem, I., Kroonenberg, S. B., Veldkamp, A., Groenesteijn, K., Rusakov, G. V., & Svitoch, A. A. (2003). Small-scale stratigraphy in a large ramp delta: recent and Holocene sedimentation in the Volga delta, Caspian Sea. *Sedimentary Geology*, *159*(3–4), 133–157. https://doi.org/10.1016/S0037-0738(02)00256-7

Overeem, I., Syvitski, J. P. M., & Hutton, E. W. H. (2011). Three-Dimensional Numerical Modeling of Deltas. *River Deltas-Concepts, Models, and Examples*, (83), 11–30. https://doi.org/10.2110/pec.05.83.0011

Paola, C. (2000). Quantitative models of sedimentary basin. *Sedimentology*, *47*.

Paola, C., Twilley, R. R., Edmonds, D. A., Kim, W., Mohrig, D., Parker, G.,Voller, V. R. (2011). Natural Processes in Delta Restoration: Application to the Mississippi Delta. *Annual Review of Marine Science*, *3*(1), 67–91. https://doi.org/10.1146/annurev-marine-120709-142856

Parker, G., Muto, T., Akamatsu, Y., Dietrich, W. E., & Wesley Lauer, J. (2008). Unravelling the conundrum of river response to rising sea-level from laboratory to field. Part II. The Fly-Strickland River system, Papua New Guinea. *Sedimentology*, *55*(6), 1657–1686. https://doi.org/10.1111/j.1365-3091.2008.00962.x

Posner, A. J., & Duan, J. G. (2012). Simulating river meandering processes using stochastic bank erosion coefficient. *Geomorphology*, *163–164*, 26–36. https://doi.org/10.1016/j.geomorph.2011.05.025

Postma, G., (1995). Causes of architectural variations in deltas. *In Oti, M.N., and Postma, G., eds., Geology of Deltas*: Rotterdam, Balkema, p. 3–16.

Pyrcz, M. J., Boisvert, J. B., & Deutsch, C. V. (2009). ALLUVSIM: A program for event-based stochastic modeling of fluvial depositional systems. *Computers & Geosciences*, *35*(8), 1671–1685. https://doi.org/10.1016/j.cageo.2008.09.012

Reitz, M. D., Jerolmack, D. J., & Swenson, J. B. (2010). Flooding and flow path selection on alluvial fans and deltas. *Geophysical Research Letters*, *37*(6), n/a-n/a. https://doi.org/10.1029/2009GL041985

Renard, P., & Allard, D. (2013). Connectivity metrics for subsurface flow and transport. *Advances in Water Resources*, *51*, 168–196. https://doi.org/10.1016/j.advwatres.2011.12.001

Rinaldo, A., Fagherazzi, S., Lanzoni, S., Marani, M., (1999). Tidal networks 2: watershed delineation and comparative network morphology. *Water Resources Research, 35(12),* 3905–3917

Ritchie, B. D., Gawthorpe, R. L., & Hardy, S. (2004). Three-Dimensional Numerical Modeling of Deltaic Depositional Sequences 1: Influence of the Rate and Magnitude of Sea-Level Change. *Journal of Sedimentary Research*, *74*(2), 203–220. https://doi.org/10.1306/091303740203

Ritchie, B. D., Hardy, S., & Gawthorpe, R. L. (1999). Three-dimensional numerical modeling of coarse-grained clastic deposition in sedimentary basins. *Journal of Geophysical Research*, *104*(B8), 17759. https://doi.org/10.1029/1999JB900170

Rodríguez-Iturbe, I. & Rinaldo, A.: Fractal river basins: chance and self-organization. Cambridge University. Press, pp. 564.

Salter, G., Voller, V. R., & Paola, C. (2020). Chaos in a simple model of a delta network. *Proceedings of the National Academy of Sciences*, *117*(44), 27179–27187. https://doi.org/10.1073/pnas.2010416117

Savitzky, A. & Golay, M.J.E. (1964). Smoothing and differentiation of data by simplified least squares procedures. *Anal. Chem., 36* 1627–1639.

Scheliing, H. von. (1951). Most frequent particle paths in a plane. *Transactions American Geophysical Union*, 32, 222-226.

Schuurman, F., Shimizu, Y., Iwasaki, T., & Kleinhans, M. G. (2016). Dynamic meandering in response to upstream perturbations and floodplain formation. *Geomorphology*, *253*, 94–109. https://doi.org/10.1016/j.geomorph.2015.05.039

Seybold, H. J., Molnar, P., Akca, D., Doumi, M., Tavares, M. C., Shinbrot, T., Herrmann, H. J. (2010). Topography of inland deltas : Observations, modeling, and experiments. *Geophysical Research Letters*, *37*, 1–5. https://doi.org/10.1029/2009GL041605

Seybold, H. J., Molnar, P., Singer, H. M., Andrade, J. S., Herrmann, H. J., & Kinzelbach, W. (2009). Simulation of birdfoot delta formation with application to the Mississippi Delta. *Journal of Geophysical Research*, *114*(F3), F03012. https://doi.org/10.1029/2009JF001248

Seybold, H., Andrade, J. S., & Herrmann, H. J. (2007). Modeling river delta formation. *Proceedings of the National Academy of Sciences of the United States of America*, *104*(43), 16804–16809. https://doi.org/10.1073/pnas.0705265104

Shaw, J. B., & Mohrig, D. (2013). The importance of erosion in distributary channel network growth, Wax Lake Delta, Louisiana, USA. *Geology*, *42*(1), 31–34. https://doi.org/10.1130/G34751.1

Sheets, B. A., Paola, C., & Kelberer, J. M. (2007). Creation and preservation of channel-form sand bodies in an experimental alluvial system. *In Sedimentary Processes, Environments and Basins, edited by G. Nichols*, pp. 555–567, Blackwell, Malden, Mass.

Slingerland, R., & Smith, N. D. (2004). River Avulsions and Their Deposits. *Annual Review of Earth and Planetary Sciences*, *32*(1), 257–285. http://doi.org/10.1146/annurev.earth.32.101802.120201

Smith, N. D., Cross, T. A., Dufficy, J. P., & Clough, S. R. (1989). Anatomy of an avulsion. *Sedimentology*, *36*(1), 1–23. https://doi.org/10.1111/j.1365-3091.1989.tb00817.x

Stouthamer, E., & Berendsen, H. J. A. (2001). Avulsion frequency, avulsion duration, and intervulsion period of holocene channel belts in the rhine-meuse delta, the Netherlands. *Journal of Sedimentary Research*, *71*(4), 589–598.

Stouthamer, E., & Berendsen, H. J. A. (2007). Avulsion: The relative roles of autogenic and allogenic processes. *Sedimentary Geology*, *198*(3-4), 309–325. http://doi.org/10.1016/j.sedgeo.2007.01.017

Straub, K. M., Paola, C., Mohrig, D., Wolinsky, M. A., & George, T. (2009). Compensational Stacking of Channelized Sedimentary Deposits. *Journal of Sedimentary Research*, *79*(9), 673–688. https://doi.org/10.2110/jsr.2009.070

Sun, T., Meakin, P., Jossang, T., & Schwarz, K. (1996). A simulation model for meandering rivers. *Water Resources Research*, *32*(9), 2937–2954.

Sun, T., Paola, C., Parker, G., & Meakin, P. (2002). Fluvial fan deltas: Linking channel processes with large-scale morphodynamics. *Water Resources Research*, *38*(8), 26-1-26–10. https://doi.org/10.1029/2001WR000284

Surkan, A., & Van Kan, J. (1969). Constrained Random Walk Meander Generation. *Water Resources Research*, *5*(6), 1343–1352.

Swenson, J. B. (2005). Fluviodeltaic response to sea level perturbations: Amplitude and timing of shoreline translation and coastal onlap. *Journal of Geophysical Research*, *110*(F3), F03007. https://doi.org/10.1029/2004JF000208

Sylvester, Z., Durkin, P., & Covault, J. A. (2019). High curvatures drive river meandering. *Geology*, *47*(3), 1–4. http://doi.org/10.1130/G45608.1

Sylvester, Z., Pirmez, C., & Cantelli, A. (2011). A model of submarine channel-levee evolution based on channel trajectories: Implications for stratigraphic architecture. *Marine and Petroleum Geology*, *28*(3), 716–727. http://doi.org/10.1016/j.marpetgeo.2010.05.012

Syvitski, J. P. M. (2006). The morphodynamics of deltas and their distributary channels. *Proceedings IAHR*.

Syvitski, J. P. M., & Saito, Y. (2007). Morphodynamics of deltas under the influence of humans. *Global and Planetary Change*, *57*(3–4), 261–282. https://doi.org/10.1016/j.gloplacha.2006.12.001

Syvitski, J. P. M., Kettner, A. J., Overeem, I., Hutton, E. W. H., Hannon, M. T., Brakenridge, G. R., Nicholls, R. J. (2009). Sinking deltas due to human activities. *Nature Geoscience*, *2*(10), 681–686. https://doi.org/10.1038/ngeo629

Syvitski, J. P. M., Overeem, I., Brakenridge, G. R., & Hannon, M. (2012). Floods, floodplains, delta plains - A satellite imaging approach. *Sedimentary Geology*, *267–268*, 1–14. https://doi.org/10.1016/j.sedgeo.2012.05.014

Thakur, T. R. and Scheidegger, A. E. (1968): A test of the statistical theory of meander formation, *Water Resources Research*, 4, 317-329.

Thakur, T. R. and Scheidegger, A. E. (1970): Chain model of river meanders, *Water Resources Research, 12*, 25-47.

Törnqvist, T. E., & Bridge, J. S. (2002). Spatial variation of overbank aggradation rate and its influence on avulsion frequency. *Sedimentology*, *49*(5), 891–905. https://doi.org/10.1046/j.1365-3091.2002.00478.x

van de Lageweg, W. I., Schuurman, F., Cohen, K. M., van Dijk, W. M., Shimizu, Y., & Kleinhans, M. G. (2016). Preservation of meandering river channels in uniformly aggrading channel belts. *Sedimentology*, *63*(3), 586–608. https://doi.org/10.1111/sed.12229

van de Lageweg, W. I., van Dijk, W. M., & Kleinhans, M. G. (2013). Channel belt architecture formed by a meandering river. *Sedimentology*, *60*(3), 840–859. https://doi.org/10.1111/j.1365-3091.2012.01365.x

Wang, Y., Straub, K. M., & Hajek, E. A. (2011). Scale-dependent compensational stacking: An estimate of autogenic time scales in channelized sedimentary deposits. *Geology*, *39*(9), 811–814. https://doi.org/10.1130/G32068.1

Webb, E. K. (1994). Simulating the three-dimensional distribution of sediment units in braided-stream deposits. *Journal of Sedimentary Research*, *B64*(2), 219–231.

Wickert, A. D., Martin, J. M., Tal, M., Kim, W., Sheets, B., & Paola, C. (2013). River channel lateral mobility: metrics, time scales, and controls. *Journal of Geophysical Research: Earth Surface*, *118*(2), 396–412. https://doi.org/10.1029/2012JF002386

Wolinsky, M. A. A unifying framework for shoreline migration: 1. Multiscale shoreline evolution on sedimentary coasts. *Journal of Geophysical Research* 114, F01008 (2009).

Woodroffe, C. D., Nicholls, R. J., Saito, Y., Chen, Z., & Goodbred, S. L. (2007). Landscape Variability and the Response of Asian Megadeltas to Environmental Change. *Global Change and Integrated Coastal Management*, 277–314. https://doi.org/10.1007/1-4020-3628-0_10

Zolezzi, G., & Seminara, G. (2001). Downstream and upstream influence in river meandering. Part 1. General theory and application to overdeepening. *Journal of Fluid Mechanics*, *438*(September 2015), 183–211.